AD-A039 374 NAVAL POSTGRADUATE SCHOOL MONTEREY CALIF F/G 20/1
FREQUENCY-TIME CORRELATION OF SURFACE SCATTERED UNDERWATER SOUN--ETC(U)
DEC 76 M F LOOMIS

UNCLASSIFIED NL

1 OF 2
AD A039 374

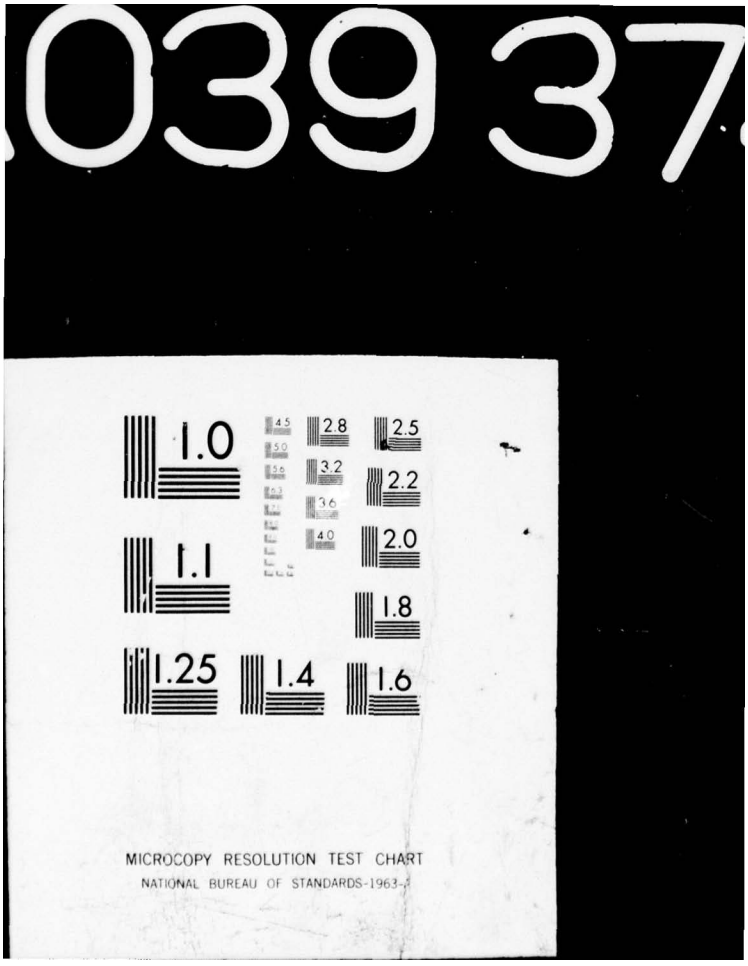
039 37
1.0
1.1
1.25
1.4
1.6
1.8
2.0
2.2
2.5
2.8
3.2
3.6
4.0
4.5
5.0
5.6
6.3
MICROCOPY RESOLUTION TEST CHART
NATIONAL BUREAU OF STANDARDS-1963-A

NAVAL POSTGRADUATE SCHOOL
Monterey, California

THESIS

FREQUENCY-TIME CORRELATION OF

SURFACE SCATTERED UNDERWATER SOUND

by

Michael Francis Loomis

December 1976

Thesis Advisor: H. Medwin

Approved for public release; distribution unlimited.

UNCLASSIFIED

SECURITY CLASSIFICATION OF THIS PAGE (When Data Entered)

REPORT DOCUMENTATION PAGE		READ INSTRUCTIONS BEFORE COMPLETING FORM
1. REPORT NUMBER	2. GOVT ACCESSION NO.	3. RECIPIENT'S CATALOG NUMBER
4. TITLE (and Subtitle) Frequency-Time Correlation of Surface Scattered Underwater Sound,		5. TYPE OF REPORT & PERIOD COVERED Master's Thesis; December 1976
		6. PERFORMING ORG. REPORT NUMBER
7. AUTHOR(s) Michael Francis Loomis		8. CONTRACT OR GRANT NUMBER(s)
9. PERFORMING ORGANIZATION NAME AND ADDRESS Naval Postgraduate School Monterey, California 93940		10. PROGRAM ELEMENT, PROJECT, TASK AREA & WORK UNIT NUMBERS
11. CONTROLLING OFFICE NAME AND ADDRESS Naval Postgraduate School Monterey, California 93940		12. REPORT DATE December 1976
		13. NUMBER OF PAGES 90
14. MONITORING AGENCY NAME & ADDRESS(if different from Controlling Office) 104p.		15. SECURITY CLASS. (of this report) Unclassified
		15a. DECLASSIFICATION/DOWNGRADING SCHEDULE

16. DISTRIBUTION STATEMENT (of this Report)

Approved for public release; distribution unlimited.

17. DISTRIBUTION STATEMENT (of the abstract entered in Block 20, if different from Report)

18. SUPPLEMENTARY NOTES

19. KEY WORDS (Continue on reverse side if necessary and identify by block number)

Scattered Sound
Acoustic Signal Processing
Frequency Variation

20. ABSTRACT (Continue on reverse side if necessary and identify by block number)

The wind driven surface of a large anechoic tank was used to study forward scattered underwater sound. A 10 kHz sawtooth signal was used to drive an omnidirectional source to insonify the rough surface. Direct and reflected path sound signals to a point hydrophone were separated by appropriate gating and the reflected path signal was analyzed for up to 2 minutes at 10 and 20 msec. intervals, using digital FFT spectral analysis. Graphs

over

DD FORM 1 JAN 73 1473 (Page 1)

EDITION OF 1 NOV 65 IS OBSOLETE
S/N 0102-014-6601

UNCLASSIFIED

SECURITY CLASSIFICATION OF THIS PAGE (When Data Entered)

251 450

AB

of sound pressure level vs. time for every 10 kHz from 30 kHz to 120 kHz (Surface roughnesses between 1.1 and 10.5) are shown. Correlation of the scattered sound pressure with frequency was analyzed. Evidence is presented to support the hypothesis that for large roughnesses, the instantaneous sound amplitudes are harmonic functions of sound frequency; that is, there is a consistent frequency separation between instantaneous amplitude maxima at one frequency and minima at another frequency.

Frequency-Time Correlation of Surface Scattered Underwater Sound

by

Michael Francis Loomis
Lieutenant Commander, United States Navy
B.S., St. Procopius College, 1959

Submitted in partial fulfillment of the requirements for the degree of

MASTER OF SCIENCE IN ENGINEERING ACOUSTICS

from the

NAVAL POSTGRADUATE SCHOOL
December 1976

Author Michael F. Loomis

Approved by: _____
Thesis Advisor

_____
Second Reader

_____
Chairman, Department of Physic and Chemistry

_____
Dean of Science and Engineering

ABSTRACT

The wind driven surface of a large anechoic tank was used to study forward scattered underwater sound. A 10 kHz saw-tooth signal was used to drive an omnidirectional source to insonify the rough surface. Direct and reflected path sound signals to a point hydrophone were separated by appropriate gating and the reflected path signal was analyzed for up to 2 minutes at 10 and 20 msec. intervals, using digital FFT spectral analysis. Graphs of sound pressure level vs. time for every 10 kHz from 30 kHz to 120 kHz (Surface roughnesses between 1.1 and 10.5) are shown. Correlation of the scattered sound pressure with frequency was analyzed. Evidence is presented to support the hypothesis that, for large roughnesses, the instantaneous scattered sound amplitudes are harmonic functions of sound frequency; that is, there is a consistent frequency separation between instantaneous amplitude maxima at one frequency and minima at another frequency.

TABLE OF CONTENTS

LIST OF FIGURES

ACKNOWLEDGEMENTS

The author wishes to express his sincere appreciation to the following for assistance during this research:

Dr. Herman Medwin provided invaluable guidance and constructive criticism in pursuing this research. Of particular note was his ability to recommend new courses of action when the effort was foundering or leading into non-productive areas.

Mrs. Elena Bohannan performed all computer program editing and modifications and provided invaluable assistance in every phase of data processing and graphic production.

The manager and staff of the ASW Systems Project Office, ASW-12, and the Office of Naval Research (Code 486) have maintained continuing interest and support for this research.

I. INTRODUCTION

For a number of years, acousticians have studied the fluctuations of underwater acoustic signals when scattered from a statistically rough interface, typically either the surface or bottom. This effect has been described as "building and fading" of the signal; an analogy has frequently been drawn between this effect and the twinkling of stars. The mechanism of this scattering has been the object of many theories; References 1 through 5 refer to the basic developments in this area. The theoretical developments have common shortcomings: in order to solve the integral equation governing the scattered sound field, it is necessary to make many assumptions involving the boundary conditions, the value of the normal derivative on the surface, the spatial statistics of the insonified area; most analyses deal with high or low frequency limits; shadowing and multiple scattering is usually ignored in all but the most complex and sophisticated treatments. These comments concerning the shortcomings of strictly theoretical approaches to the scattering problem have been made in order that the need for supplemental experimental research be noted. A mixture of theoretical insight and controlled experimental procedure is sometimes more fruitful than purely theoretical studies with arbitrary assumptions. Such is the philosophy adopted for this research.

A. OBJECTIVES

The objective of this research is to investigate the effects that variation of frequency has on the sound scattered from a statistically rough, fluctuating, wind driven water surface, and to determine if a predictable relationship exists between the intensities of various harmonics of a given sound source when scattered from such a surface. The basic concepts of this experimental effort are:

1. Insonification of the fluctuating surface with many frequencies simultaneously.

2. Isolation of surface reflected sound from other paths through the use of gated signals.

B. INTERMEDIATE GOALS

The following intermediate goals are presented as logical steps in attainment of the objective described above:

1. Perform preliminary studies of the wind driven surface, and monofrequency sound scattered from such a surface.

2. Develop the electronic circuitry to transmit a wide range of frequencies simultaneously, receive and process these signals.

3. Develop and test an acoustic source capable of transmitting over a wide range of frequencies, with the stipulation that frequencies of interest be far enough above the 'noise' to permit meaningful signal processing.

4. Analyze the processed data to see if the stated objective can be met.

II. RESEARCH FACILITIES

A. OCEAN ACOUSTIC WAVE FACILITY (OAWF)

The Ocean Acoustic Wave Facility is a combination of a wind generated wave tunnel and an anechoic acoustic tank. The wind tunnel is approximately 17 meters long, 1.2 meters wide and 1.2 meters deep. By varying the number of fans and/or the distance between the water surface and the top of the tunnel, a wide range of ocean surfaces can be obtained. Figures 1 and 2 (from Tourville) show the essential features of the OAWF.

The wave generation tunnel empties into a water filled tank with dimensions of 3 meters on each side. The wind generated waves are dissipated on a constructed beach to prevent reflected waves from interfering with wind generated waves. The tank is constructed of 4x4 redwood posts, placed with corners facing outward. The use of redwood provides sound absorption, as shown in Reference 8; however, scattering of sound from these surfaces did present some experimental difficulties, as pointed out in a later section. Equipment was positioned within the tanks by use of movable racks as shown in Figure 3. The OAWF models the real ocean on a scale on the order of 150 to 1 up to sea state 3.

B. DATA ACQUISITION AND PROCESSING CAPABILITIES

Data acquisition and processing were accomplished by utilizing a digital computer system composed of three primary components each of which is interfaced to provide high speed

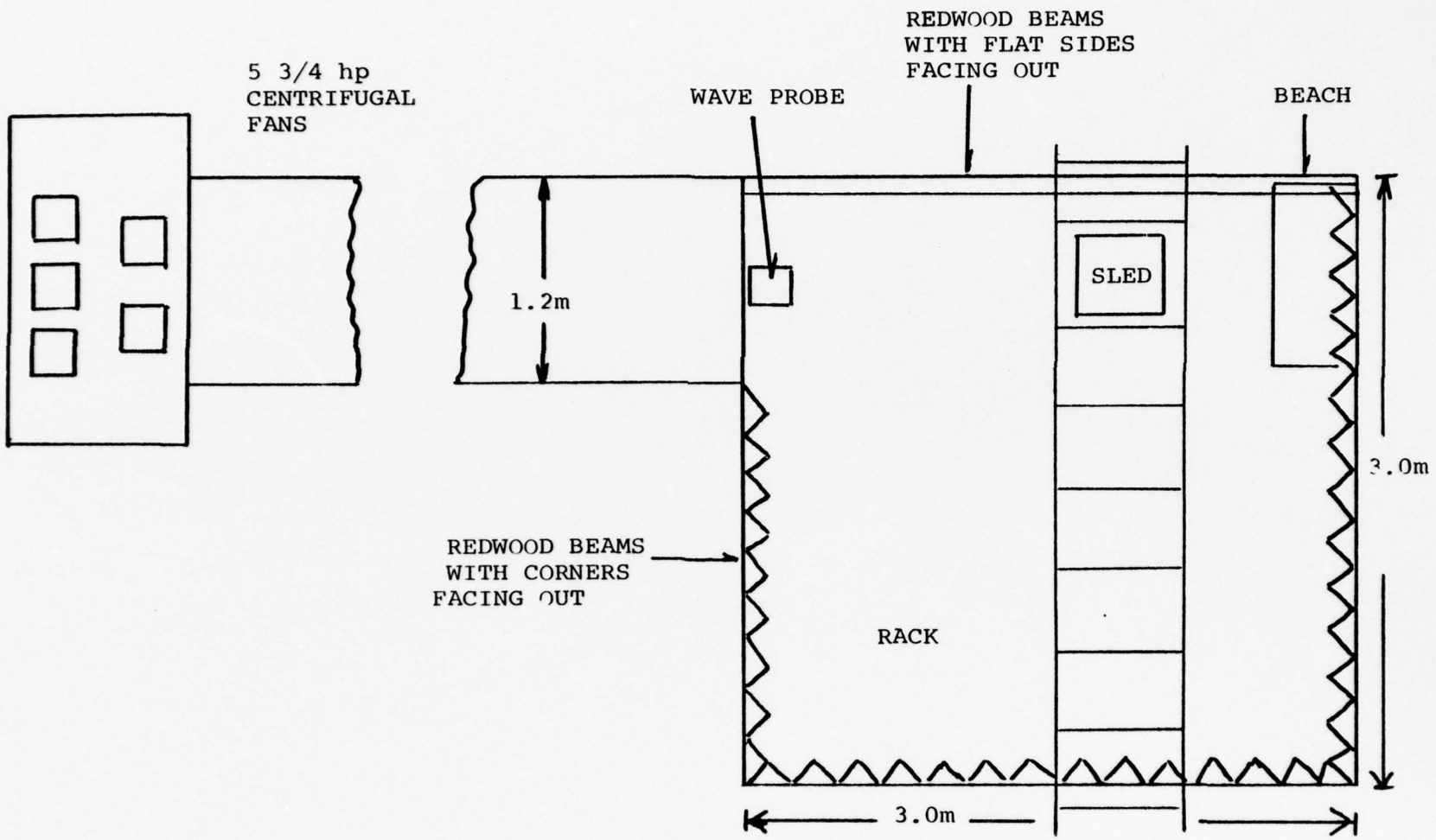

FIGURE 1. TOP VIEW of OAWF

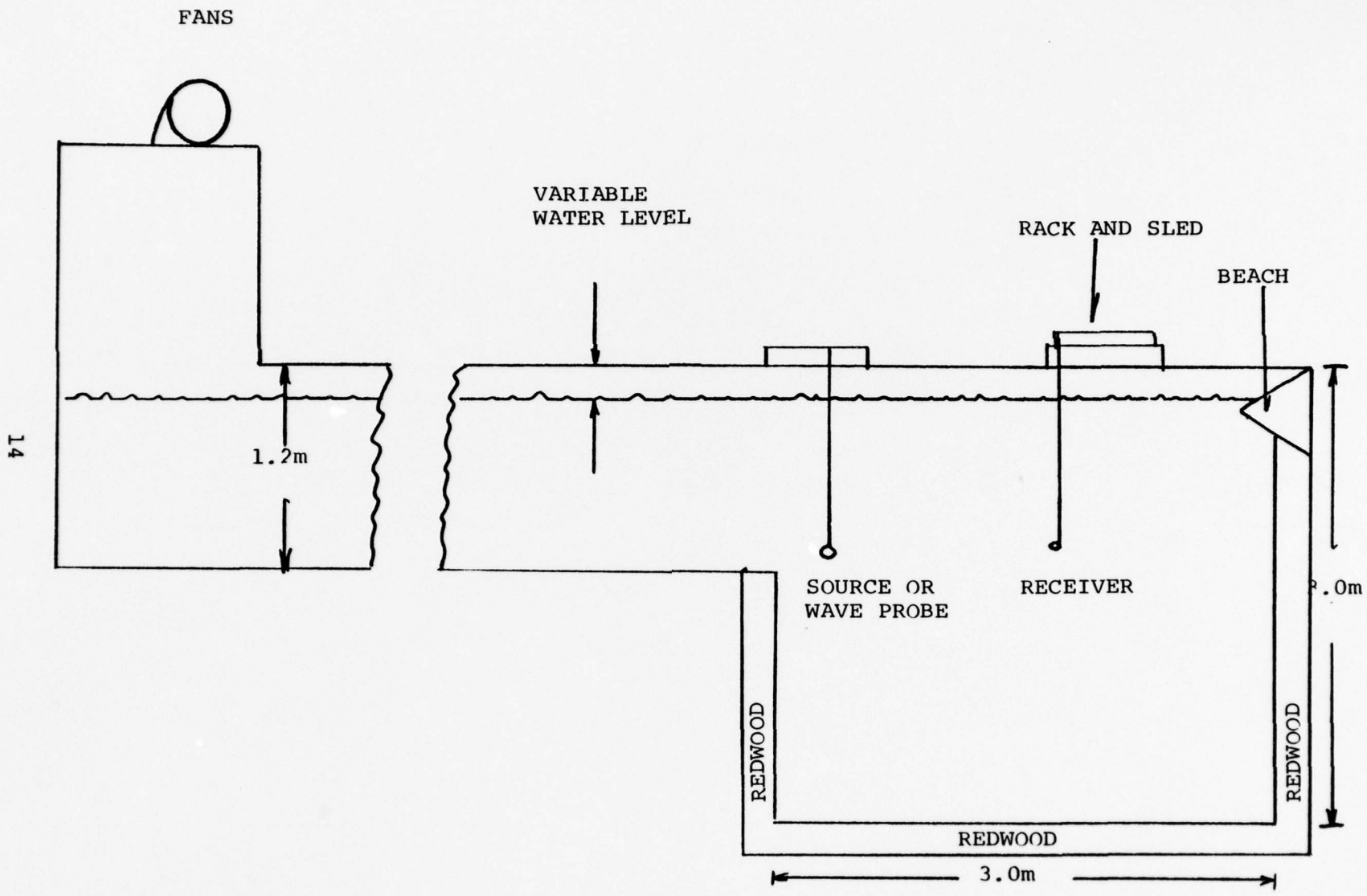

Figure 2. Side View of OAWF

analog to digital conversion, digital processing, and data printout and recording. The design was developed by the Special Projects Section of the Naval Air Development Center in conjunction with Pinkerton Computer Consultants, Inc., of Warminster, Pennsylvania. The three components are pictured in Figure 4 and described below.

1. Interdata Model 70 Computer

This minicomputer is a digital design that is FORTRAN programmable with a 64 thousand byte memory. In addition to actual core memory, data that have been stored on digital cassettes can be read into the computer for processing.

2. Phoenix Analog to Digital Converters, Model ADC 712

Two ADC 712 analog to digital converters may be used separately or simultaneously. Each converter is a high speed device capable of encoding $\pm$ 10 volt input signals in digital form and providing an accuracy of 0.005 volts in 20 volts. The maximum sampling rate is 320,000 samples per second; this rate was routinely used.

3. Texas Instruments Silent Electronic Data Terminal Model 733

The TI 733 consists of a keyboard used as a programming input/output control device, a printer, and a playback/record section used in conjunction with digital cassettes. The overall system facilitates rapid, accurate processing of any desired type of analog electrical signal and was used mainly for statistical and frequency domain analysis using standard FFT algorithms. Further descriptions are contained in References 6 and 7.

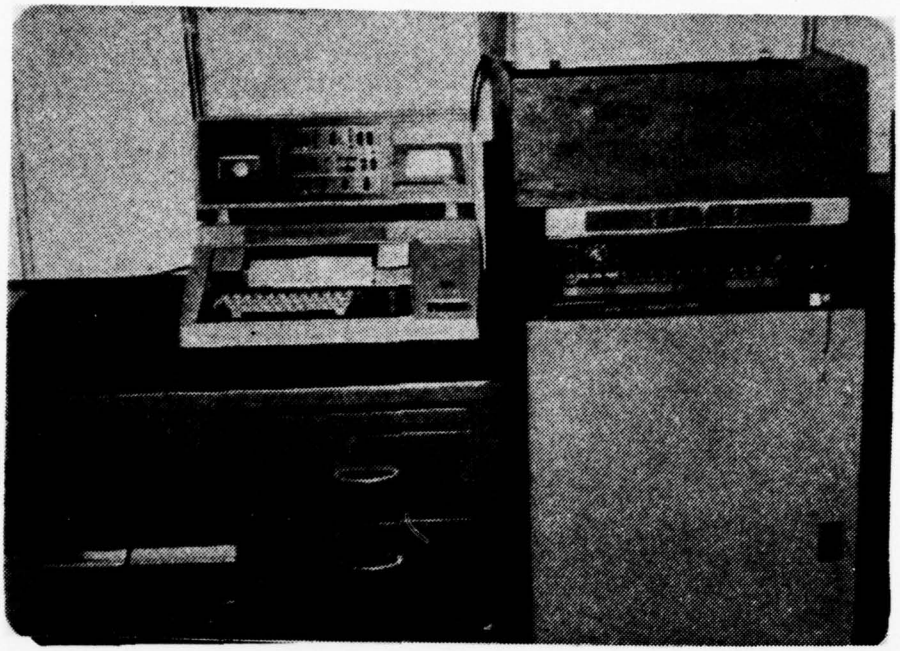

Figure 3. Computer System

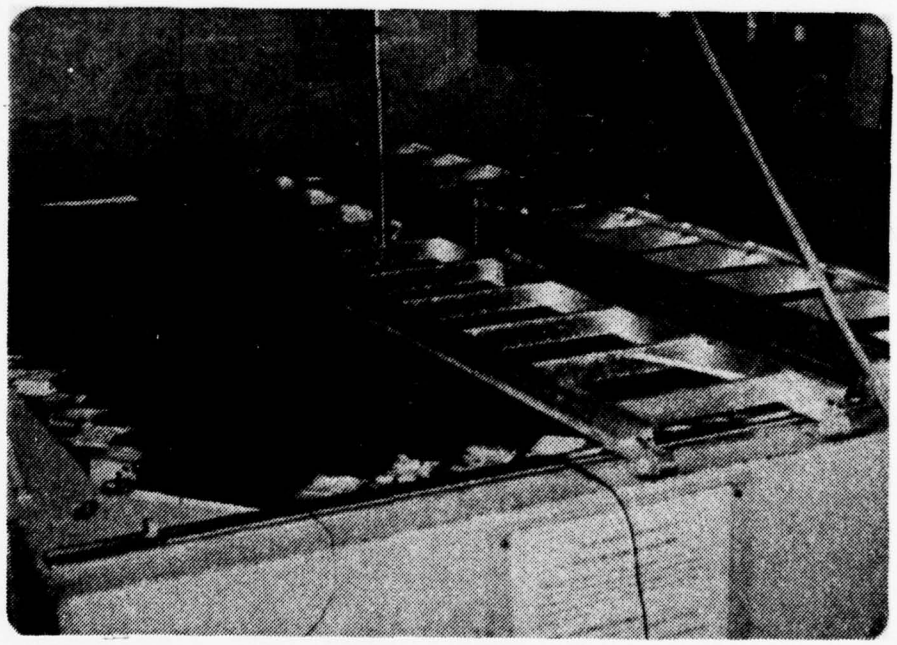

Figure 4. View of OAWF

4. IBM-360 Interface

In addition to the digital system just described, another processing capability consisted of the TI 733 terminal and taped digital data interfaced via phone link to the IBM-360/67 CP/CMS system. This capability was used to provide data rearrangement, card punch capability and graphical output (with the aid of a CAL-COMP plotter).

C. STANDARD EQUIPMENT LIST

Much of the equipment used was standard off the shelf scientific measurement equipment; a list of standard equipment referred to throughout the text is given below:

Abbreviation	Full Description
Scope	Tectronix Model 545B 4-channel oscilloscope
HP 465A Amp	Hewlett-Packard Voltage Amplifier Model 465A
HP 466A Amp	Hewlett-Packard Voltage Amplifier Model 466A
HP 467A Amp	Hewlett-Packard Power Amplifier Model 467A
HP 218	Hewlett-Packard Model 218 Digital Delay Generator
HP 219	Hewlett-Packard Model 219 Dual Pulse Unit
PAR 113 Amp	Princeton Applied Research Amplifier Model 113
KH 3322 Filter	Krohn-Hite Model 3322 Freq. Filter
KH 3342 Filter	Krohn-Hite Model 3342 Freq. Filter
KH 3350 Filter	Krohn-Hite Model 3350 Freq. Filter
Freq. Counter	Hewlett-Packard 5223L Electronic Frequency Counter

DMM	Fluke Model 8000A Digital Multi Meter
GR-1192B	General Radio Electronic Frequency and Period Counter
GR-1217C	General Radio Model 1217C Unit Pulse Generator
GR-1396	General Radio Model 1396A Tone Burst Generator
Impedance Bridge	General Radio Model 1650A Impedance Bridge
Wavetek 114	Wavetek Model 114 Function Generator
Wavetek 136	Wavetek Model 136 Function Generator
Wavetek 144	Wavetek Model 144 Function Generator

Sound sources, receivers, wave probes and other miscellaneous equipment will be described in the text, as necessary.

III. EXPERIMENTAL PROCEDURES

The experimental procedures followed in the course of this research can be grouped into four general categories: (1) Calibration of the Surface Wave Probe and determination of wave spectra, wave heights and surface roughnesses; (2) Continuous wave sound scatter measurements; (3) Sound Source testing and selection; (4) Surface Reflected Pulsed Sound Wave analysis.

A. WAVE PROBE CALIBRATION, WAVE SPECTRA AND WAVE HEIGHT MEASUREMENTS

In two previous works [Refs. 6 and 7], wave height frequency spectra of wind generated water waves were determined. Confirmation of these previous studies was considered to be an excellent starting point of this current research and would afford valuable insight into the use of the specialized measuring equipment and into the use and programming of the digital minicomputer. It was intended to extend these investigations over those previously performed by studying waves generated by all combinations of fans and also to develop a program to give actual RMS values of wave height.

1. Wave Probe Calibration

The wave height probe is a linear capacitative probe developed by Stanford University and consists basically of a thin wire whose total capacitance is determined by the water depth to which the probe is immersed. The probe is connected

to the impedance bridge and the remainder of the circuitry as shown in Figure 5. The impedance bridge used had a convenient feature which provided a 1 kHz output signal modulated by the value of the input capacitance. As the probe depth is varied the final signal (which is pure D.C. for a smooth surface) provides a linear output proportional to the probe depth. The probe was mounted on a rigid frame, but was able to be varied in depth by means of a rotating knob-screw arrangement. A graduated depth scale was attached to the frame with an accuracy of about 0.02 cm. The probe was then calibrated as shown in Figure 6. Initial attempts at calibration were not successful due to lack of repeatability. This was corrected by slight modifications to the filtering network and the final calibration curve was satisfactory.

2. Wave Spectra Measurements

Upon completion of the wave height probe calibration, measurement of wave height spectra was undertaken using the circuitry of Figure 5 as shown previously. The time varying signal proportional to instantaneous wave height was input into one A/D channel of the digital computer for analysis using the SKIP-1C program (all programs used are described briefly in Appendix A). The computer A/D sampling rate was set at 20 Hz; 50 runs of 256 (2^8) samples each were taken at this sample rate. Previous spectral measurements had indicated that most of the spectral components were below 4 Hz so that the Nyquist criterion was satisfied in all cases. Spectral resolution for this particular data gathering

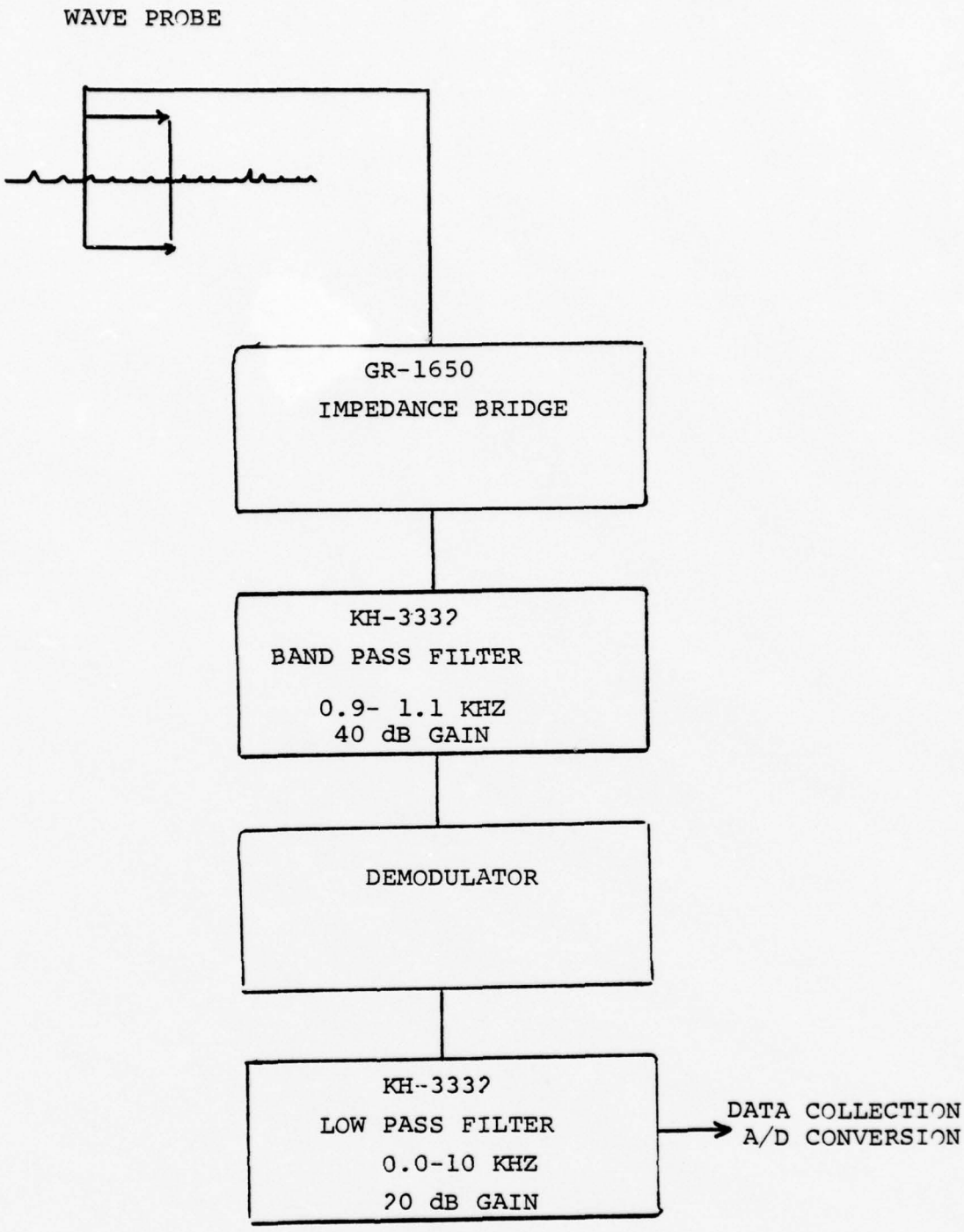

Figure 5. Wave Height Circuitry

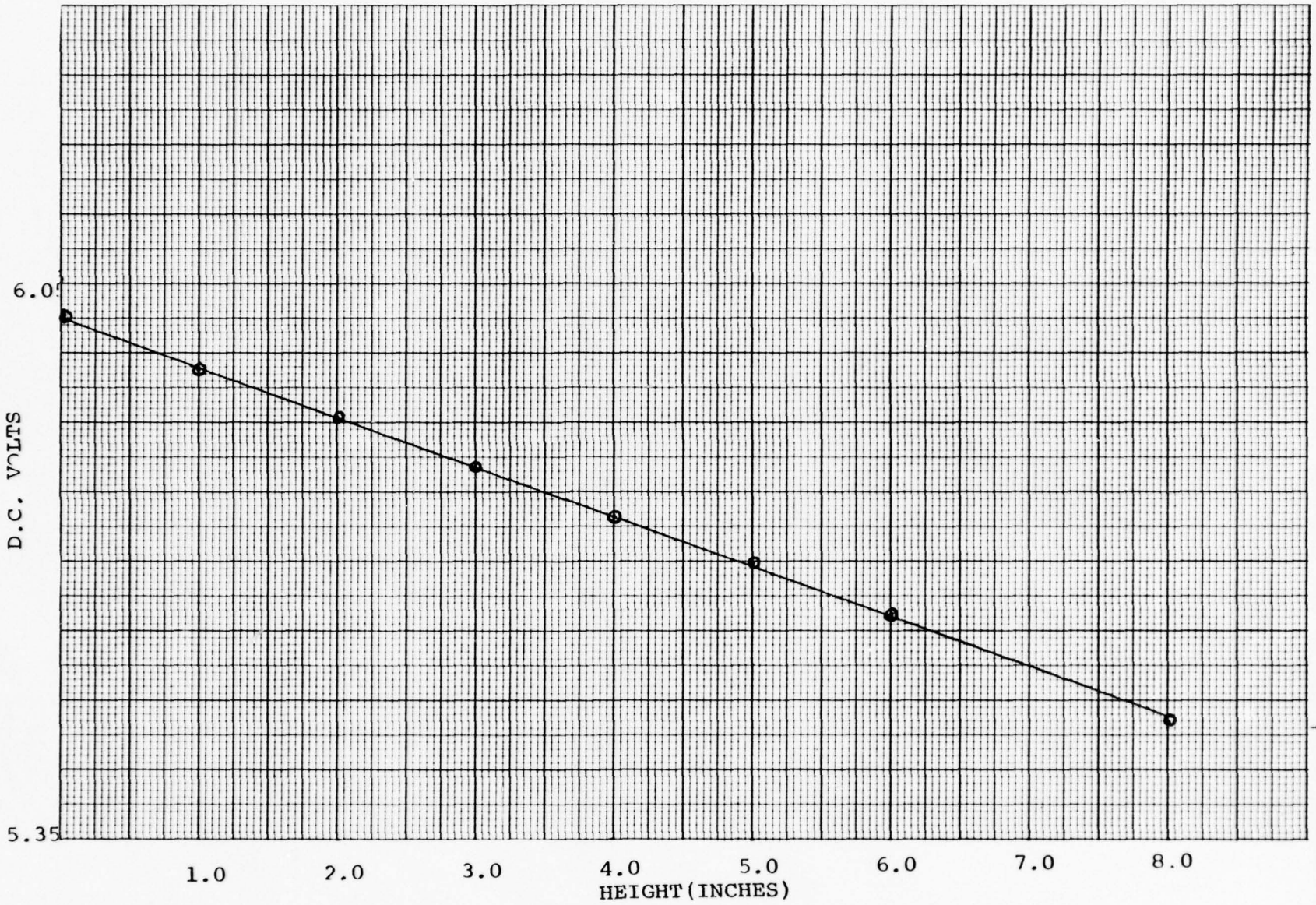

Figure 6. Wave Height Probe Calibration Curve.

arrangement is 0.078 Hz. For each of the 50 data sets, Fast Fourier Transform (FFT) analysis was performed and the output spectral density for each run was computed, normalized and averaged. The output spectral densities of surfaces for all fan combinations of one to five fans were computed and plotted. The graphs of output power spectral densities vs. frequencies are shown in Figure 7. This set of curves shows the expected spectral shifts as the wave heights and wave periods are increased by the use of more fans. The general results were in agreement with Perkins and Tourville, hence further data processing simply for the purpose of curve smoothing was not performed. As a further check on the computer accuracy and program, signals were also input to a PAR Fourier Analyzer and the spectral output vs. frequency were plotted on an XY recorder. Spectra produced by this alternate means were consistent with those analyzed by digital means. A typical example of this alternate spectral curve is shown in Figure 8.

3. Average Wave Height Determination

After the wave height probe calibration curve was obtained, the next task to be undertaken was accurate determination of average wave heights for all fan combinations. This was accomplished by using the circuitry of Figure 5 once again, in conjunction with a computer program entitled CAL 01. This program sampled the wave height output voltage, performed root-mean-square averaging of the total number of A/D data points, and compared this with a reference sin wave

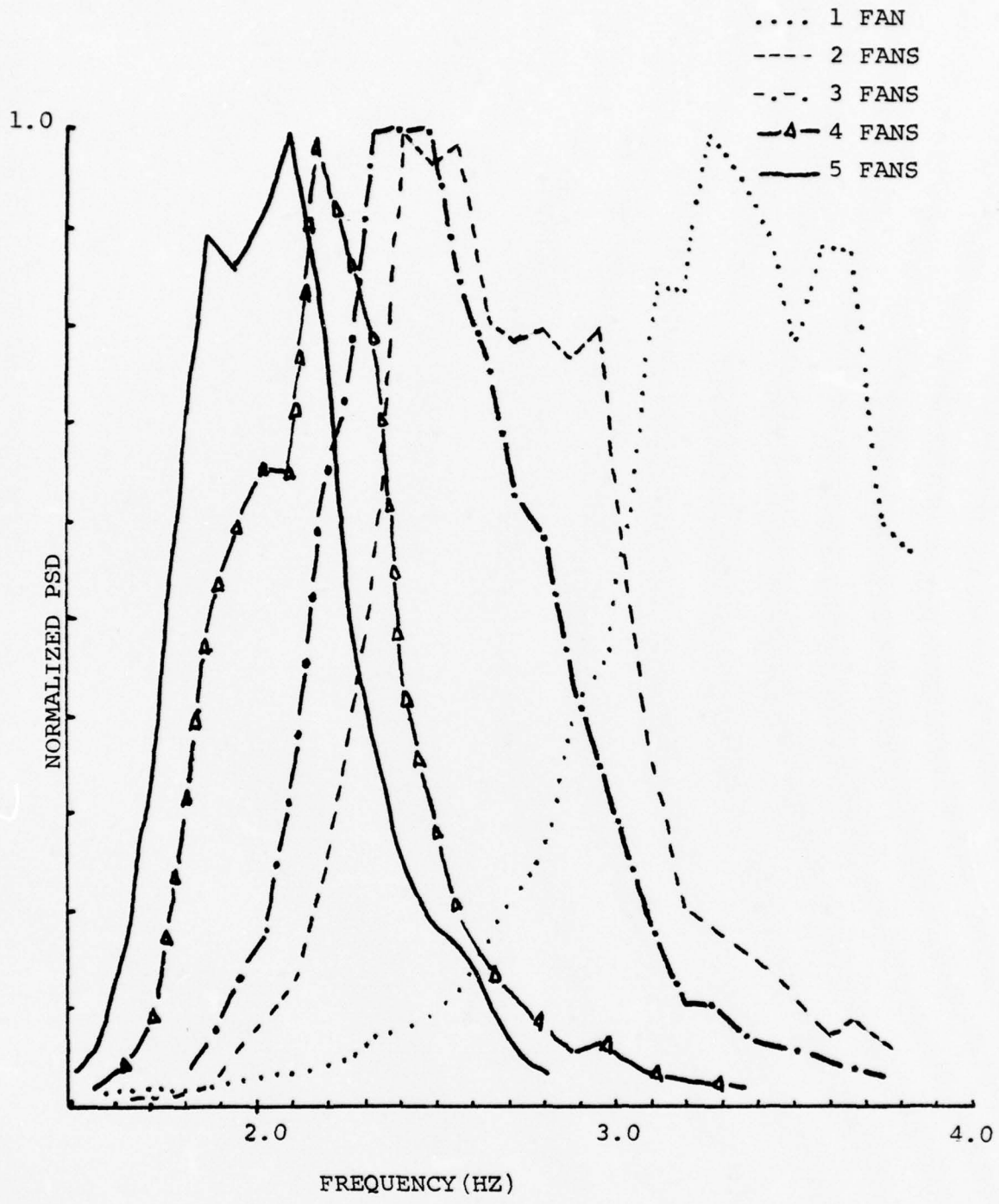

Figure 7. Spectral Density vs Frequency.

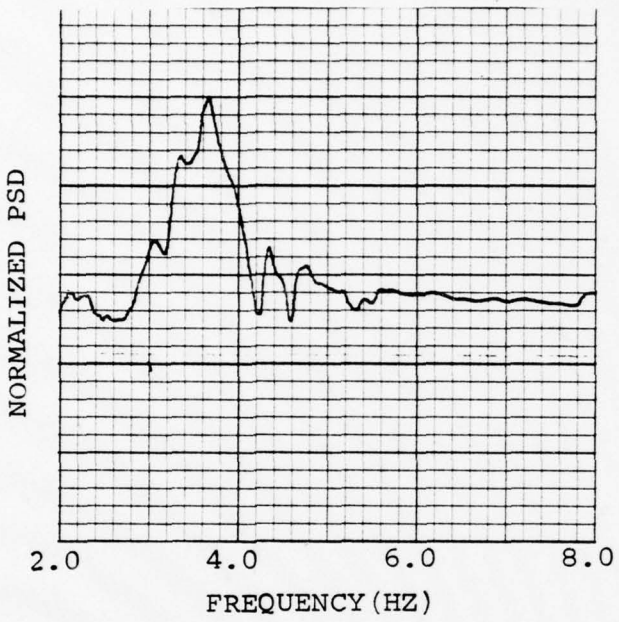

Figure 8. One Fan Wave Spectrum, PAR FOURIER ANALYZER.

voltage set exactly to 1.000 volts. (This comparison eliminated the need for A/D voltage calibration each time the program was used.) This program was extensively tested with signals of known RMS values to ensure accuracy prior to experimentally determining the wave heights. Once the program was known to be working properly, RMS voltage values for all fan combinations were determined, and converted to wave heights using the linear calibration curve. These values are shown in Table I. Once the average wave heights were

Table I

RMS Wave Heights vs. Number of Fans

No. of Fans	AC (RMS) Volts	RMS Wave Height (Cm)
1	0.01475	0.447
2	0.0180	0.546
3	0.0244	0.740
4	0.0343	1.041
5	0.0416	1.262

obtained for each fan combination, it was then a simple matter to compute surface roughness values using the definition:

$$g^{\frac{1}{2}} = \frac{2\pi\sigma}{\lambda} \quad (2 \cos \theta)$$

where $g^{\frac{1}{2}}$ is defined as the roughness parameter, σ is the RMS wave height, λ is the wavelength of the sound source and θ is the angle of incidence. The roughness values were computed using the geometry of Figure 21; values are contained in Table II.

Table II

Roughness Parameters

Freq (kHz)	λ (m)	Roughness $\sqrt{g}$			
		1 Fan	2 Fans	3 Fans	4 Fans
10	0.15	0.37	0.45	0.62	0.86
20	0.075	0.74	0.91	1.23	1.72
30	0.050	1.11	1.36	1.85	2.60
40	0.0375	1.49	1.81	2.46	3.51
50	0.030	1.86	2.27	3.08	4.33
60	0.0250	2.23	2.72	3.69	5.20
70	0.0214	2.60	3.18	4.31	6.06
80	0.01875	2.97	3.63	4.92	6.92
90	0.0166	3.35	4.08	5.54	7.79
100	0.0150	3.72	4.53	6.15	8.7
110	0.0136	4.09	4.99	6.77	9.52
120	0.0125	4.46	5.45	7.38	10.38

B. CONTINUOUS WAVE SOUND SCATTER MEASUREMENTS

It was decided to initially analyze the scattered sound spectra of a continuous 20 kHz source. The source and receiver setup and associated circuitry are shown in Figure 9 and are similar to that of Perkins so that comparison of results could be made. The source used was a 2" ceramic sphere; the receiver was a standard LC-10 hydrophone. The receiver was positioned in a Lloyds' mirror maximum signal

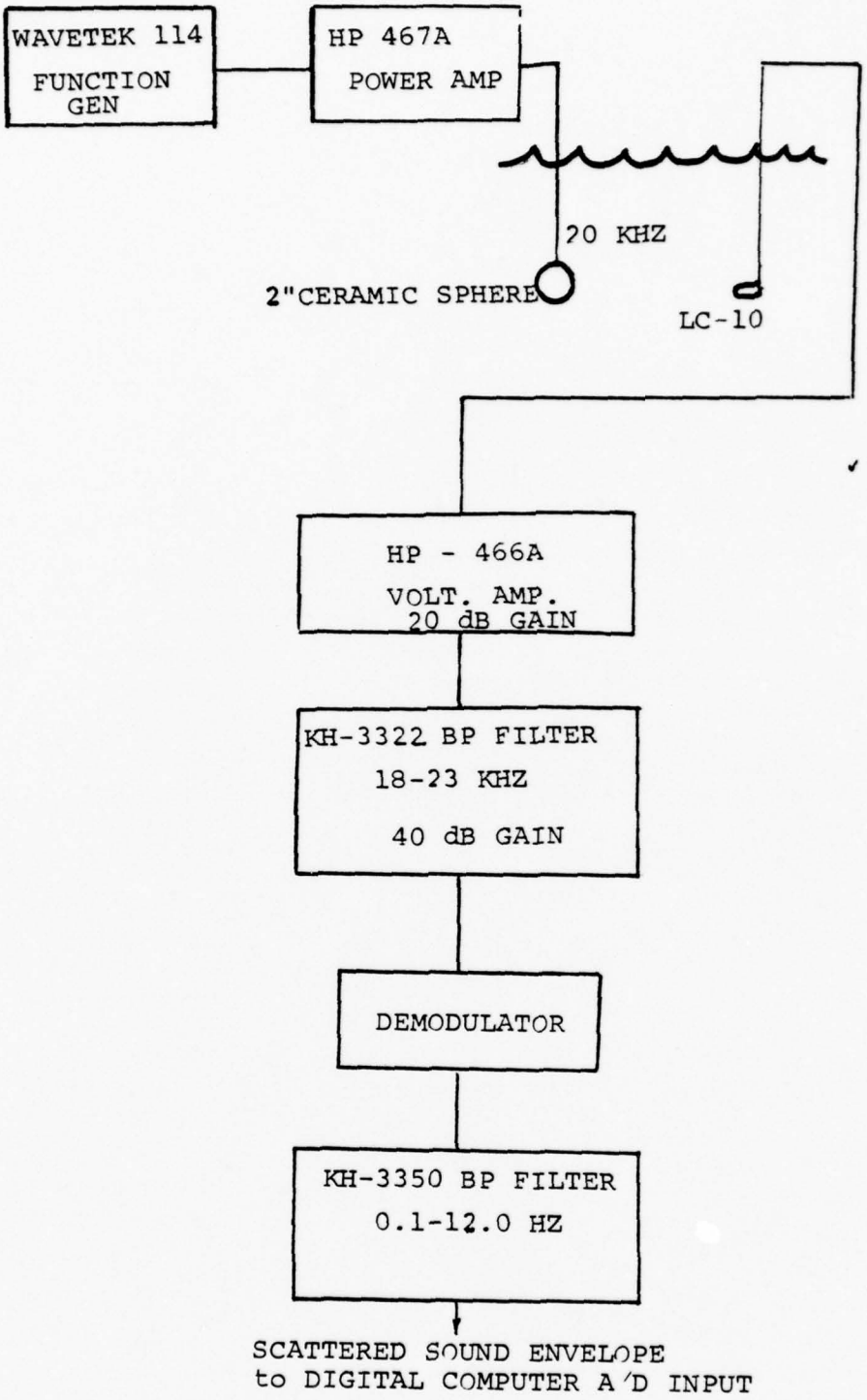

Figure 9.Sound Processing Circuitry

location. The demodulated scattered sound envelope was input into the digital computer and analyzed with the SKIP-1C program. The normalized scattered sound spectral densities for 1 to 5 fans are shown in Figures 10-14. Each spectral density curve is an average of 50 FFT's, each consisting of 256 sample points, sampled at a rate of 128 samples/sec. Once again results were consistent with previous experimenters' results. Oscilloscope photos of typical modulated and demodulated sound signals are shown in Figures 15 and 16.

C. SOUND SOURCE SELECTION AND TESTING

As discussed in the introductory chapter, in order to insonify an area simultaneously with a wide range of frequencies, it was necessary to test various sources to see which could provide the maximum transmitting frequency response in the range of interest, nominally 5 to 160 kHz.

1. Transducer Construction and Testing

A significant number of potential transducers were constructed and tested; for the sake of brevity only a brief description of each will be given along with the reason for rejection.

a. Two-inch ceramic sphere, hollow interior: this transducer was utilized in the initial sound scattering studies at 20 kHz. The transducer did not have a significant output below 20 kHz and significant 'ringing' occurred at 50 kHz which would have made the sphere unsuitable for short separation gated pulses.

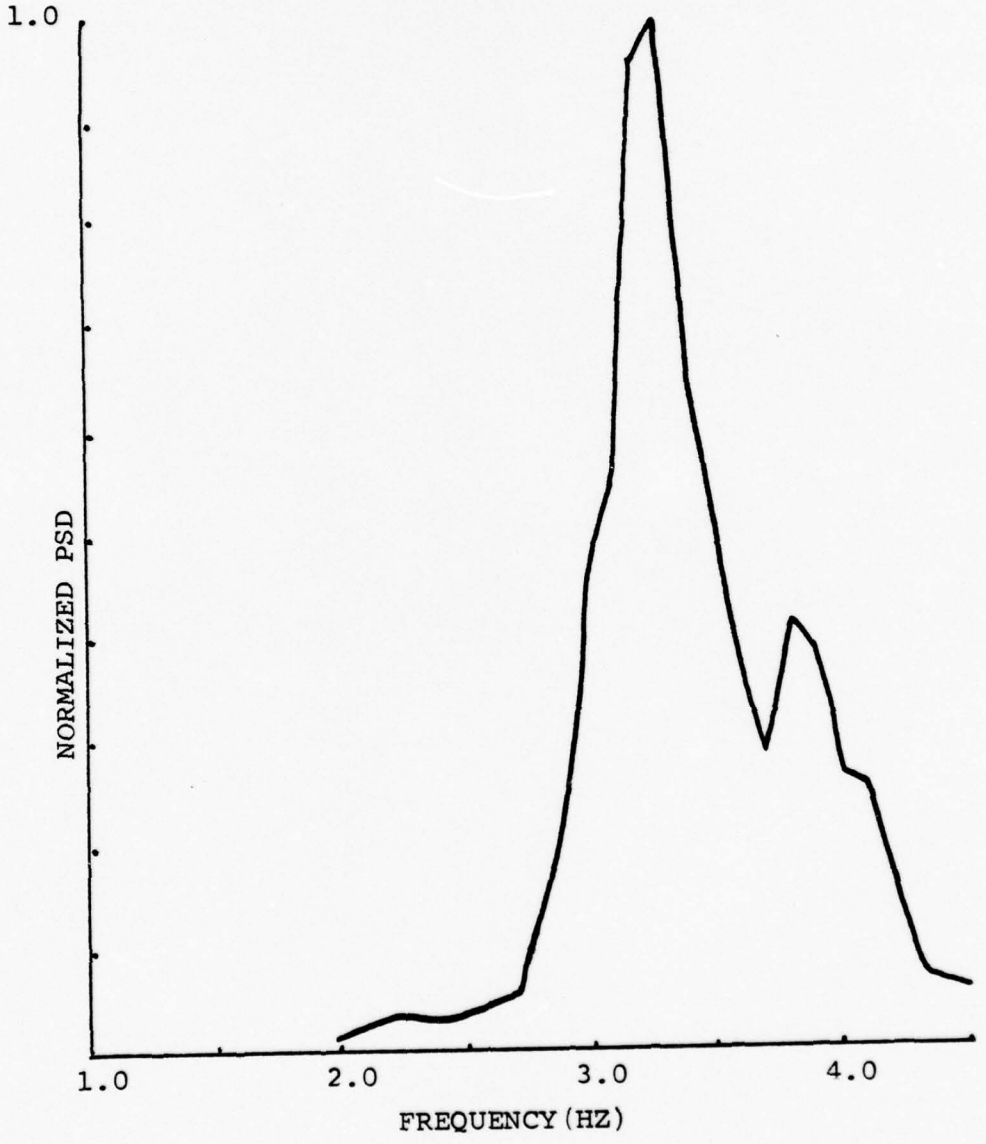

Figure 10. Surface Modulated Sound Spectrum, 1 Fan.

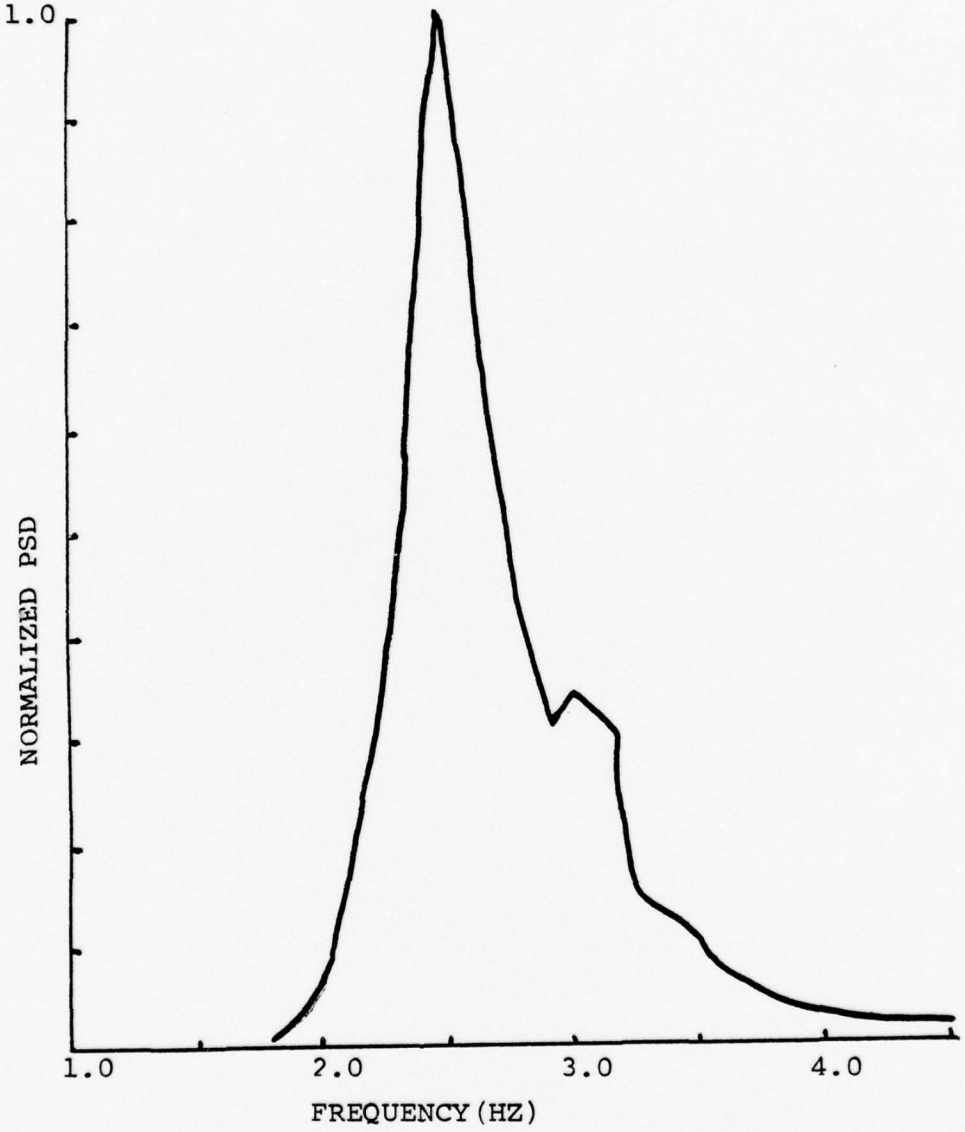

Figure 11. Surface Modulated Sound Spectrum, 7 Fans

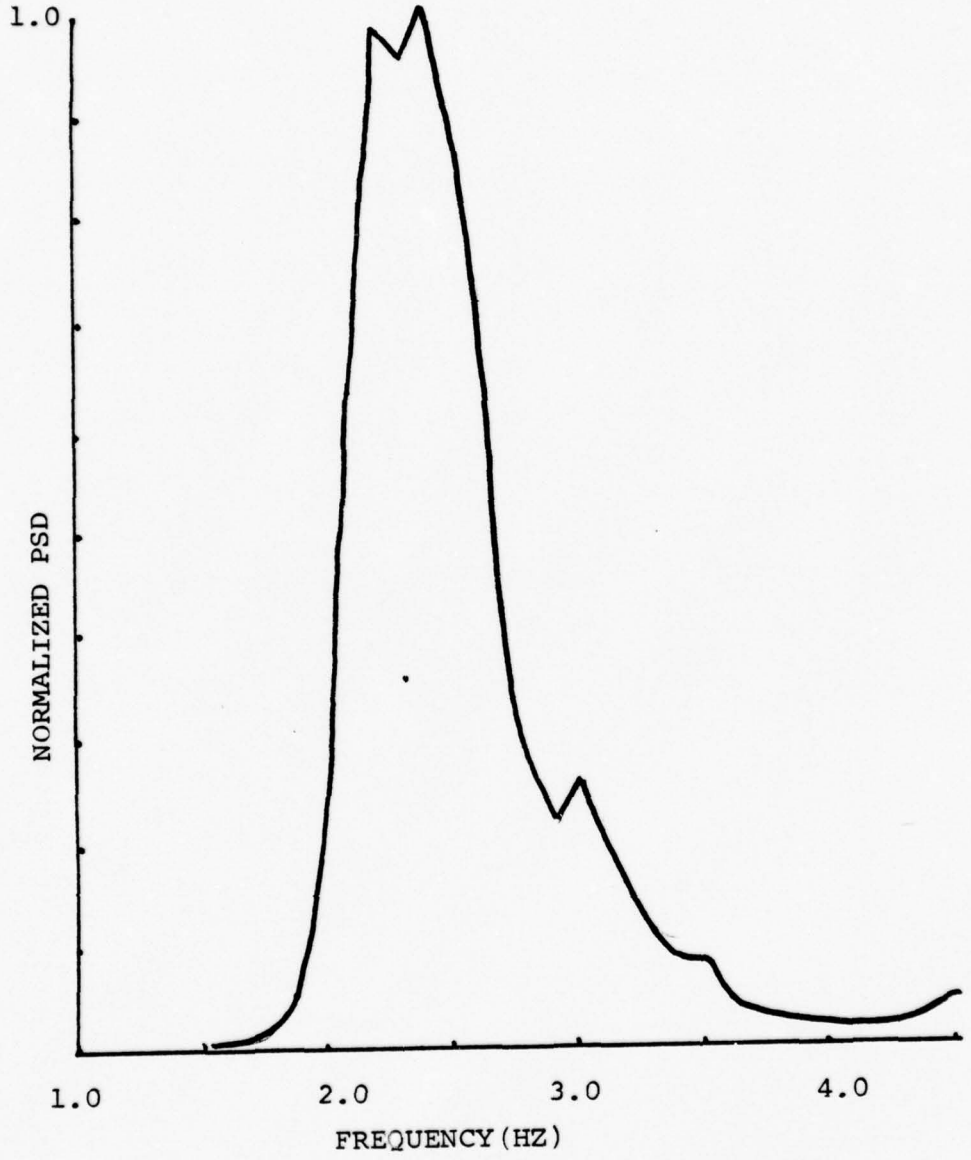

Figure 12. Surface Modulated Sound Spectrum, 3 Fans.

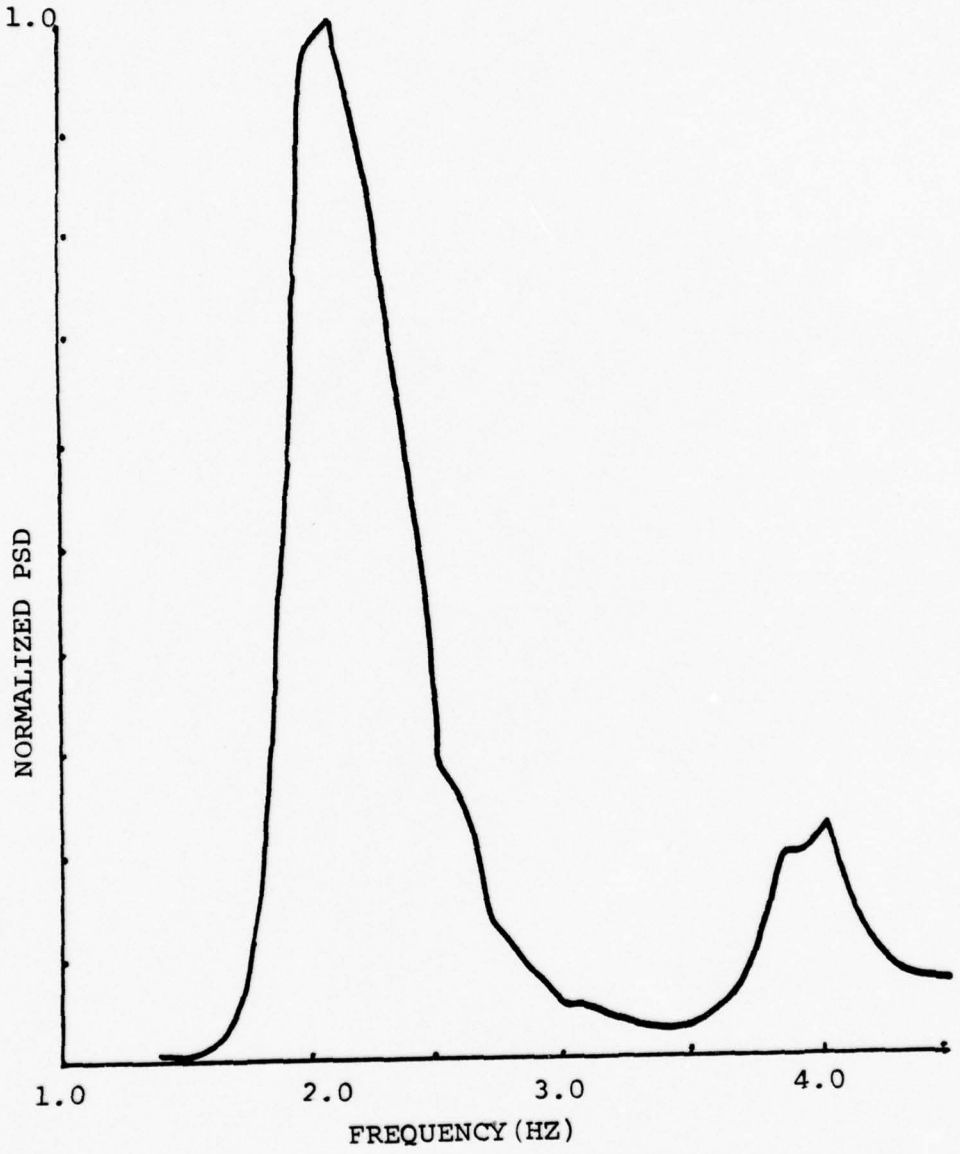

FIGURE 13. Surface Modulated Sound Spectrum, 4 Fans.

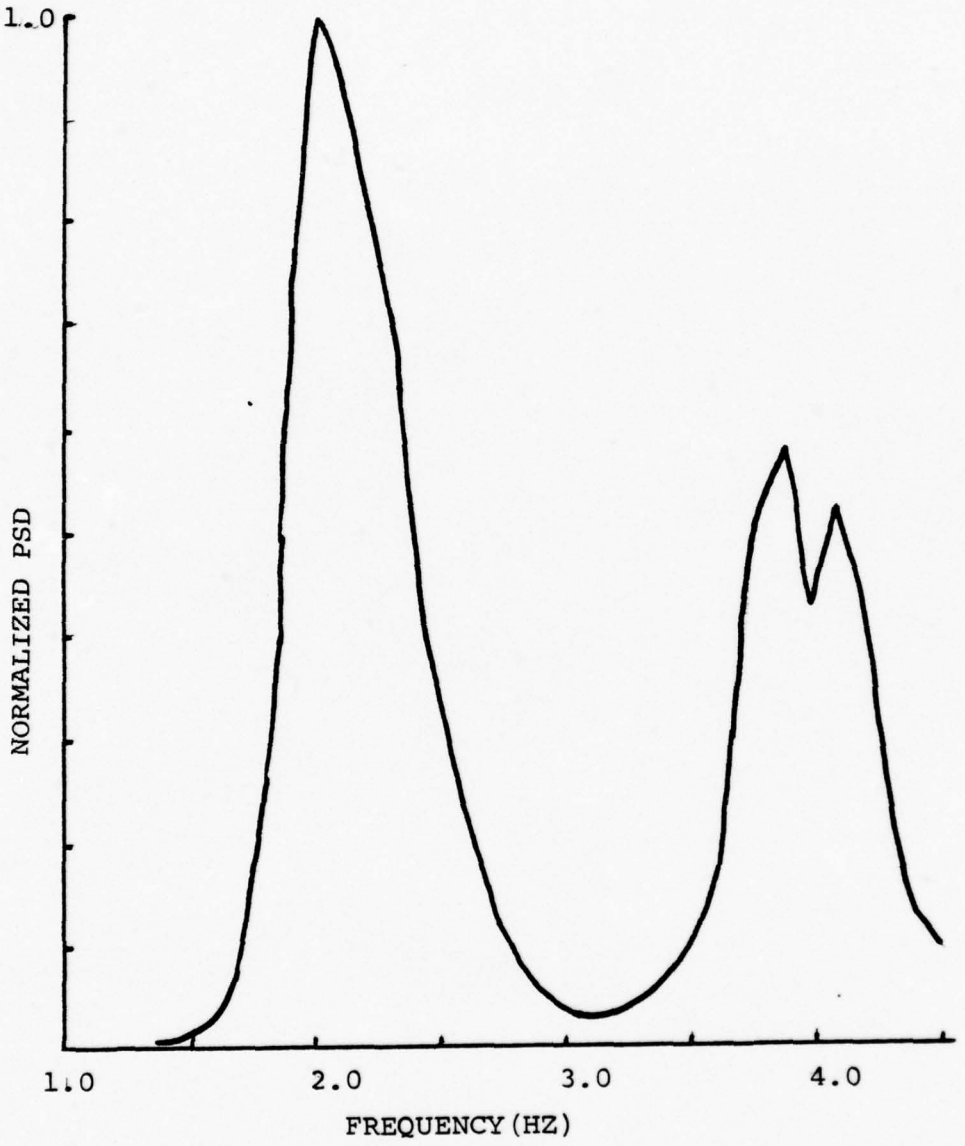

Figure 14. Surface Modulated Sound Spectrum, 5 Fans.

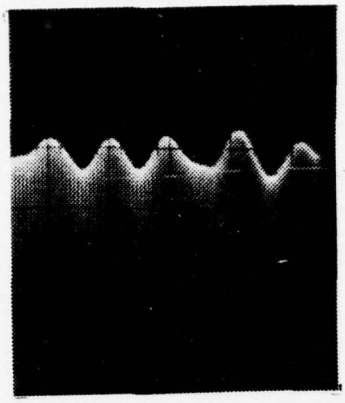

Figure 15. Surface Modulated Sound Signal

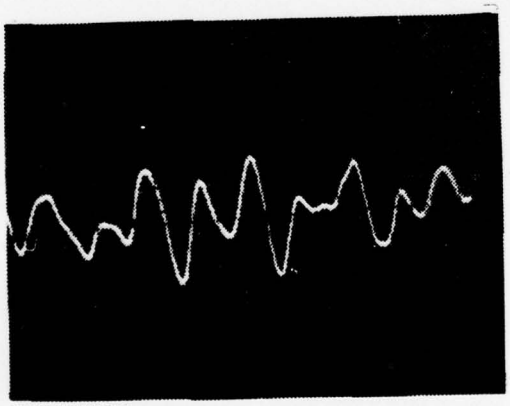

Figure 16. Surface Demodulated Sound Signal. (Figure 16 is not the demodulation of Figure 15,but was taken at a different time and is a typical demodulated signal.)

b. One-inch ceramic sphere, hollow interior: same comments as in a., extensive ringing around 75 kHz.

c. One-inch ceramic sphere, oil filled: same problems as previously discussed. Oil was introduced into the cavity to damp out the ringing phenomenon but it only shifted the resonance values.

d. One-inch ceramic sphere, oil filled with steel wool damping. No major improvement noted here.

e. One-inch ceramic sphere, packed with heavy powdered metal. Same comments as c. apply.

f. Four cylindrical mylar transducers were constructed, 1" and 2" in diameter, 10" and 20" in length respectively. The transducers had an aluminum core, thin mylar covering, with the entire assembly coated with neoprene waterproofing compound. When tested, all four of these transducers exhibited too low a signal level to be useful.

g. LC-10 ceramic hydrophone. This hydrophone exhibited satisfactory signal level over the entire frequency range; due to its small size and relative omnidirectional features, this standard receiving hydrophone was utilized as an acceptable source throughout the remainder of the experiment. Actual characteristics of this transducer will be shown and discussed in subsequent sections.

D. SURFACE REFLECTED PULSED WAVE ANALYSIS

This section will detail the experimental procedure used to analyze the surface reflected sound as a function of

frequency and time. Prior to studying the behavior of sound in the anechoic tank, a study of the sawtooth oscillator was initiated as described below.

1. Wavetek 144 Sawtooth Waveform Analysis

As previously mentioned, a Wavetek 144 function generator was modified to give an asymmetrical sawtooth wave with a slope ratio of 44:1. This asymmetrical output was coupled directly into the A/D input channel of the digital computer. The THCDB program was utilized for Fourier analyses of this input signal. Each entire analysis of the 10 kHz sawtooth waveform consisted of 49 sample blocks, each block consisting of 256 sample points taken at a sample rate of 320 kHz, giving an available frequency resolution of 1250 Hz. The sawtooth waveform was analyzed in both a continuous and gated mode. Examination of the output data (mean spectral density values, and standard deviation vs. 5 kHz frequency increments) revealed an unacceptably high value in the higher frequency ranges. Values of standard deviation in dB re 1 μbar for frequencies over 100 kHz were greater than 3 dB in all cases. In order to make subsequent experiments meaningful, a method had to be found to decrease the standard deviation to less than 1 dB for all frequencies to be examined.

The first study performed was to compare the Wavetek 144 spectral analyses with similar results from other signal generators. As can be seen in Table III, three different models of function generators gave similar results, showing the increased instability of harmonics with frequency.

Table III

Standard Deviation vs. Frequency for Various Function Generators

Frequency	Wavetek-144 Sawtooth	Wavetek-144 Gated Sawtooth	Wavetek-184 Sawtooth	HP-3300A Triangle Wave	Wavetek-144 Triangle Wave
10 kHz	.06 db	.01 db	.01 db	.06 db	.01 db
20	.08	.03	.04		
30	.15	.07	.109	.24	.10
40	.29	.15	.196		
50	.46	.25	.31	2.2	.29
60	.75	.36	.45		
70	1.19	.6	.62	2.5	.06
80	1.6	.9	.83		
90	2.2	1.5	1.0	3.7	1.1
100	3.0	2.5	1.3		
110	6.0	3.8	1.6	6.4	1.9
120	5.0	4.0	1.9		
130	4.3	4.0	2.1	4.3	3.2
140	5.8	4.0	2.0		
150	5.7	7.0	1.2	4.3	5.5
160	7.0	7.5	1.5		

Various methods were tried in order to overcome this difficulty; amplitude variation was investigated but had no significant effect. The ultimate solution to this problem proved to be band pass filtering of the output of the Wavetek prior to analysis. An extensive study of the effects of variation of filter limits was performed; results showed that filtering was effective in reducing the standard deviation of the output signal to within 0.5 dB or less. Further studies of this nature were performed with the direct and reflected sound paths in the wave tank and will be subsequently discussed.

2. Circuit Arrangement for Sound Analysis

The basic circuit arrangement for all future discussions on sound analysis is shown in Figure 17. A brief discussion of the basic function of each component is necessary to understand the processing of the various sound signals. The Wavetek 144 function generator controls the basic repetition frequency of the entire transmissions circuit. The GR 1217 Pulse Generator controls the actual length of the sawtooth waveform, and the positive going portion of its pulse initiates the timing sequence of the HP 218/219. The HP 218/219 Digital Delay Generator, when operated in the 'common' mode has as its output two pulses of variable amplitude and width, each of which can be set to a pre-adjusted time delay in microseconds. This component also has a synchronizing output for use in oscilloscope 'synch' input. The time delayed pulses are used as the timing or gating signals

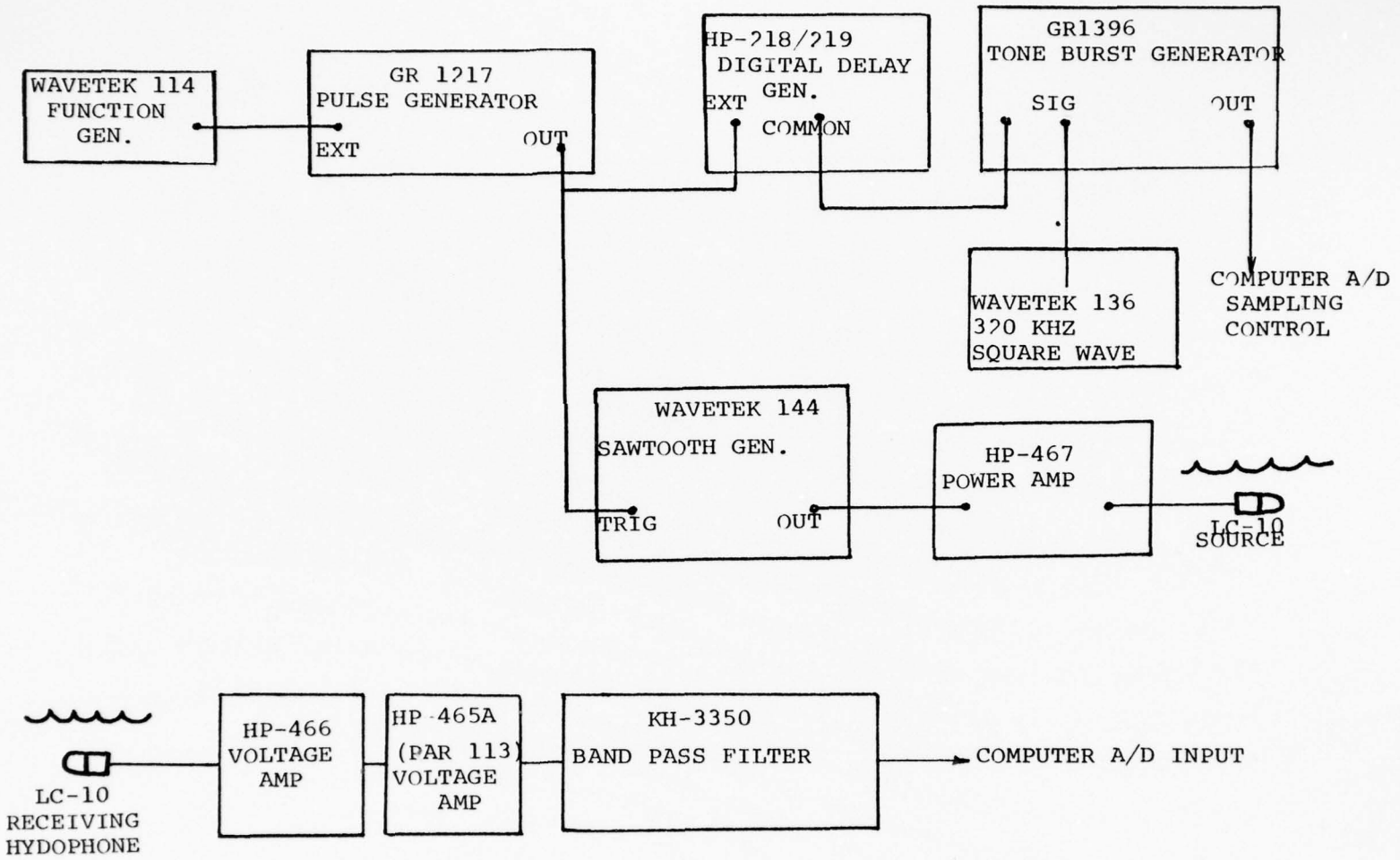

Figure 17. Surface Reflected Pulsed Sound Analysis Circuitry.

for the GR-1394 Tone Burst generator. This component, in turn, allows the passage of the 320 kHz sampling frequency to the computer only as the gating pulses permit.

The GR-1217 also controls the sawtooth waveform going to the LC-10 source. The receiving circuit consists of an LC-10 hydrophone, 80 dB of amplification, and a band-pass filter. The output signal of the filter goes to the A/D input channel for computer analysis. The series of oscilloscope photographs shown in Figures 18-20 present the various waveforms and their interrelation. In examination of these figures, the appearance of the waveforms should be noted. In Figures 19 and 20, the direct path and the surface reflected path can easily be identified; however in both cases, additional scattering is present following the surface reflected wave, consisting of a mixture of acoustic energy scattered from the side and side-surface of the wave tank. It was the presence of this additional scattered wave which determined the minimum separation (about 7 msec.) between successive sound pulses and also determined the maximum length the surface reflected pulse could attain (about 0.6 msec.) without overlap with the scattering.

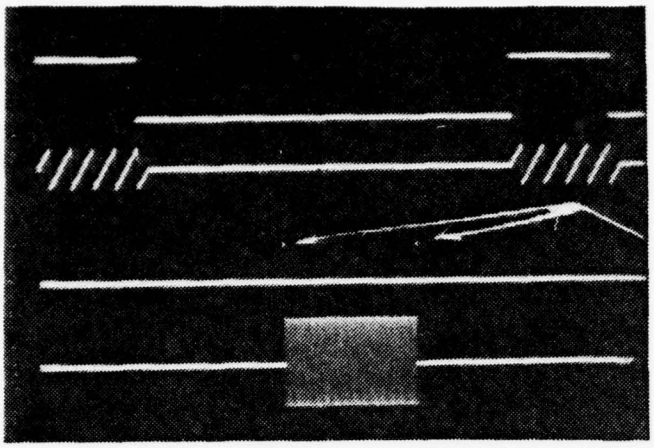

CONTROL PULSE, GR-1217 OUTPUT

WAVETEK 144 GATED 10 KHZ OUT.

HP-218/219 DELAYED PULSES

GATED 320KHZ COMPUTER SAMPLING SIGNAL. GR-1396 OUTPUT.

Figure 18.

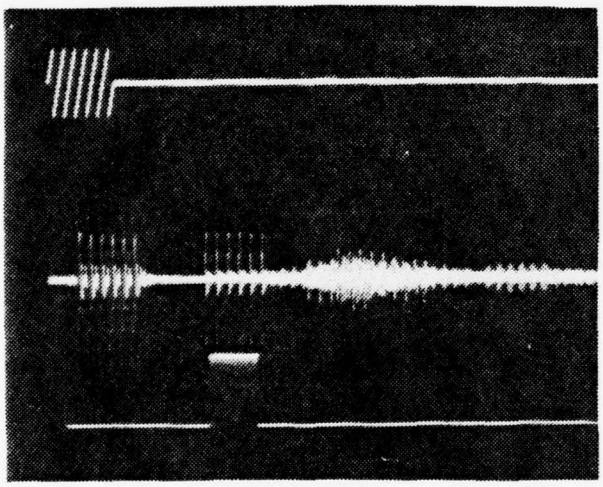

WAVETEK 144 GATED OUTPUT

DIRECT AND REFLECTED SAWTOOTH SOUND SIGNALS, FOLLOWED BY SCATTERING.

COMPUTER SAMPLING SIGNAL LOCATED DIRECTLY BELOW SURFACE REFLECTED SOUND SIGNAL.

Figure 19.

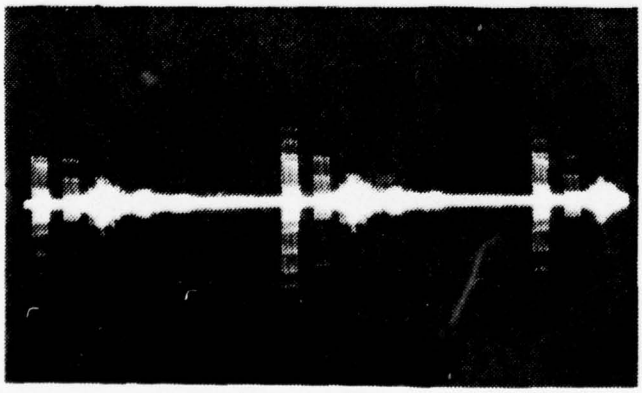

SERIES OF DIRECT, REFLECTED, AND SCATTERED SOUND PULSES SHOWN WITH A 20 MSEC. SEPARATION.

Figure 20.

IV. EXPERIMENTAL RESULTS AND ANALYSIS

A. STATIC ACOUSTIC WAVEFORM INVESTIGATION

Upon completion of the testing and spectral analysis of the direct output of the Wavetek 144 oscillator, testing of the direct path and smooth surface reflected acoustic signals was initiated. Although some variation of geometry was initially utilized, the geometry of Figure 21 was used for all analysis unless otherwise noted. The circuit arrangement of Figure 17, shown in the previous section, applies.

A study of the spectral components of a 10 kHz sawtooth waveform transmitted via the two different paths of interest was conducted. Although filtering of the signal was performed, the old problem of high standard deviation among the components was noted but could not be reduced to acceptable levels; many of the standard deviations were on the order of 2 dB and this was felt to be unacceptable for the supposedly stable direct and reflected path signals. Further study revealed that both the PAR-113 and KH-3550 had voltage limitations on their output, which if exceeded, resulted in clipping of the output. The PAR-113 started to clip at $\pm$ 6 volts and the KH-3550 at an output of $\pm$ 8 volts. By reducing the magnitude of the input signal, the amplified received sound could be kept within these bounds; when the signals were kept within these limits standard deviations were greatly reduced and were acceptable (Table IV). Due to the inherent limitations of the PAR-113, it was replaced by a HP-465 amplifier

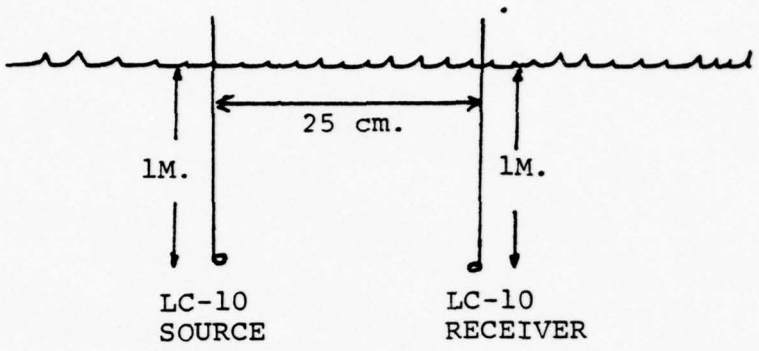

Figure 21. Source and Receiver Geometry.

which had no limitations near the range of voltage values encountered. Particular care had to be taken when analyzing the fluctuating signals of the rough surface to ensure the clipping point of the KH-3550 was not approached. During this phase of testing, the filter limits of 20-130 kHz were found to produce the most stable signals with the least overall standard deviation of the direct and reflected waveforms.

The spectral output of the direct and surface reflected sound paths, as analyzed by the THCDB program are shown in Table IV below. These values are representative for the smooth surface case. Typical noise values, obtained by disconnecting the source, and analyzing the received signal with the THCDB program are also shown. The results of this table are shown graphically in Figure 22. Each mean value and standard deviation were computed over a 50 block average, with each block consisting of 128 sample points sampled at 320 kHz. The slightly higher standard deviation for the reflected path at 120 kHz is thought to be due to a minor surface rippling due to slight air movement over the wave tank. Note that most signal to noise ratios for the reflected wave are on the order of 30 dB or higher.

B. ROUGH SURFACE SOUND SCATTER MEASUREMENT

Surface sound scatter measurements were now attempted for all combinations of 1 to 5 fans. As before, the circuit arrangement of Figure 17 was used. Gated sound pulses were set to a 20 msec. interval between pulses; the A/D sampling

Table IV

Typical Smooth Surface Direct and Reflected Path Sound Levels

Freq. (kHz)	Direct Path Sound Level (dB re 1 μbar)		Reflected Path Sound Level (dB re 1 μbar)		Mean Noise Levels (dB re 1 μbar)
	Mean	Std. Dev.	Mean	Std. Dev.	
30	17.9	0.23	-0.6	0.62	-23
40	23.0	0.11	9.3	0.26	-20
50	23.0	0.07	12.2	0.20	-21
60	19.1	0.16	14.1	0.13	-22
70	16.9	0.13	14.0	0.11	-22
80	21.1	0.10	13.9	0.16	-21
90	17.3	0.12	15.0	0.24	-20
100	26.8	0.18	16.2	0.24	-23
110	27.7	0.09	13.5	0.50	-23
120	21.5	0.14	10.0	1.2	-23

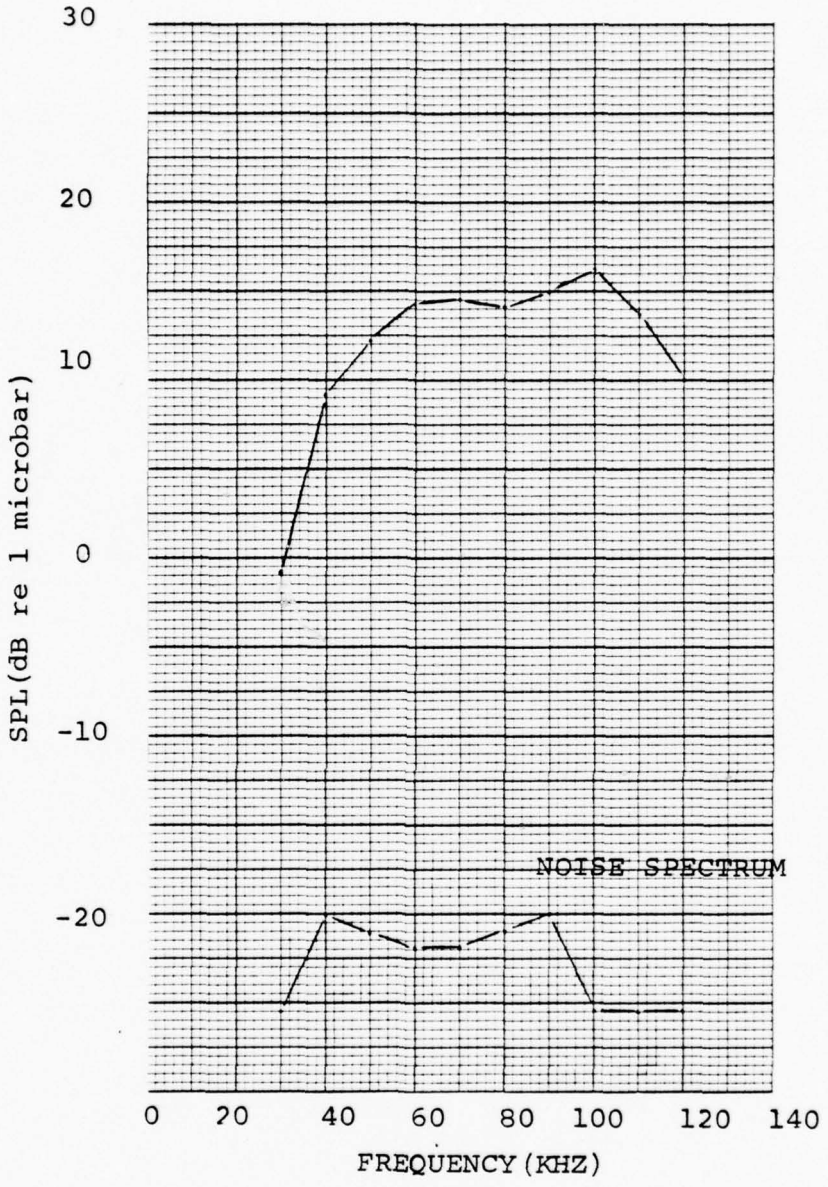

Figure 22. Reflected Waveform Spectrum, Smooth Surface.

pulses were positioned in time to be directly coincident with reception of the surface scattered sound pulses. Each of the 50 blocks consisted of 128 A/D samples taken at a rate of 320 kHz; thus each sample block took 0.4 msec. During this small time interval, it was assumed that the rough wave surface is frozen in space over the sampling period. This assumption is justified based on examination of the wave frequency spectra previously shown where the peak energy is at a period of approximately 300 msec.

The output sound pressure levels vs. frequency for each of the time separated reflected pulses was computed using the THCDB program, and stored on a separate digital tape cassette for each fan combination. This tape was, in turn, processed by another program, SORTF, which sorted the SPL vs. time by frequency. At this point, for each 5 kHz increment of frequency there existed a set of SPL data over 50 points, each point separated by 20 msec. in time, encompassing a total time span of 1 sec. The data of the SORTF program was also stored on digital tape cassettes. Utilizing a phone link with the IBM 360 computer complex, the SORTF data was card punched and subsequently plotted using the IBM 360 plotting routines and the CAL COMP plotter.

1. Initial Results

Typical results from the previously described process are shown in Figures 23 and 24. The particular curves shown are for relatively low surface roughness values. Study of the whole series of curves obtained for the 1-5 fan cases indicated

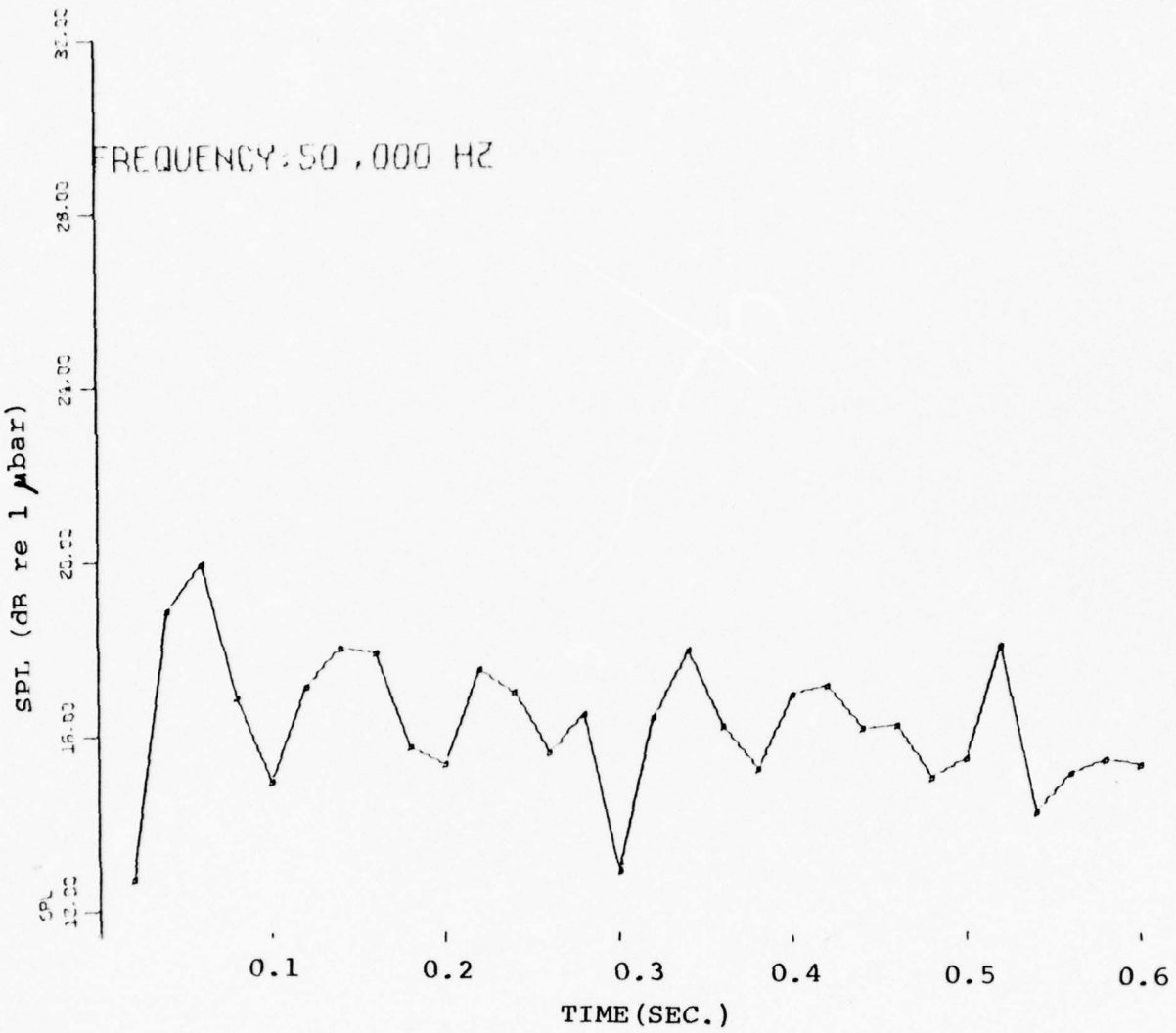

Figure 23. SPL vs. Time, 50 KHZ, 1 Fan.

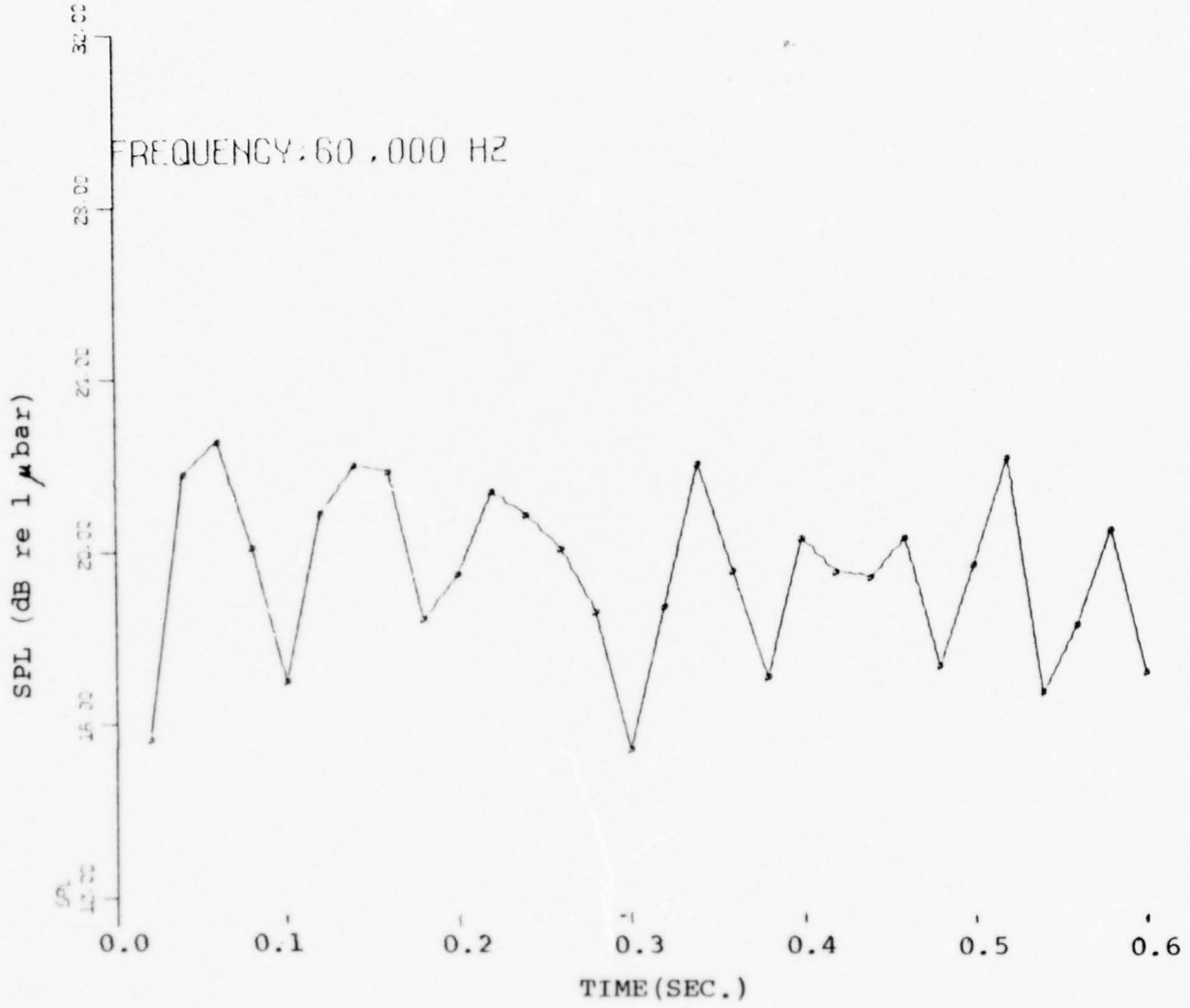

Figure 24. SPL vs. Time,60 KHZ,1 Fan.

the existence of a possible problem. The pseudo periodicity of the SPL curves was on the order of 12-15 Hz; this was approximately three times that expected for the lower roughness values. A complete review of experimental and computational procedures was initiated to seek the answer to this problem. A reexamination of the THCDB program showed that after the A/D data for one sample had been stored, Fourier analysis and all remaining computational processes were being performed prior to the storage of the next A/D data set. In effect, what resulted was a skipping of the timed computer sampling orders until the computational steps were performed, which resulted in timed samples being taken only every 60 to 80 msec. vice the 20 msec. separation which was expected. As a result of this finding, it was decided to modify the existing programs to eliminate the problem.

2. Program Modifications

In order to get data at the precise time desired, a number of program modifications were made as described below:

a. Raw A/D data were taken and stored on a digital cassette using an existing program, PERK1A. In order to ensure the data were being taken at the exact time desired, testing was performed on 10 kHz triangle wave with A/D data being taken with a 5 msec. separation. The resulting A/D data were manually plotted and fitted exactly to the predicted triangle form. The PERK1A program was subsequently modified to be able to take up to 100 data blocks of 128 points each. The modified program was called PRKMOD.

b. The THCDB program was modified to be able to accept input data from a cassette and to be able to compute and store on tape the output spectral analyses of up to 100 blocks in time. The modified program was tested on a static reflected wave from the smooth surface. This was compared with the original program and nearly identical results were obtained; the modified program was labeled THCDB(1).

c. The SORTF program was modified to accept up to 100 data blocks.

3. Final Experimental Data

With the program modifications described above final experimental data taking was commenced. The first set of data taken was for fan combinations of 1 to 5, pulse and sample time separation of 20 msec., for a total duration of 1 sec. of data. The resulting graphs of this data were plotted with the aid of the CAL COMP plotter and a redrawn overlay showing curves for selected fan combinations is given in Figures 25, 25a, 26. The amplitudes shown are relative and placed on each overlay such that the mean values of individual curves are a fixed distance (2") apart; these mean values are shown on the overlays as 'tic marks' on the ordinate axis. It will be noted that the 5 fan combination is missing; during 5 fan data taking, a slow undulation of the direct path sound signal was noted; this undulation was not present in the 1 to 3 fan cases but was also noted in the 4 fan case after about 10 minutes at this fan combination. It is surmised that this variation in the direct path sound was due either to relative motion of the

source/receiver induced by wave slap on the mounting rods or by some type of oscillating current within the wave tank itself. For these reasons, 5 fan data were no longer taken.

The examination of the first data set indicated that the time resolution in the upper frequencies might not be fine enough; consequently an additional set of data with a 10 msec. time separation was taken encompassing a total time of 0.75 seconds. These data were plotted as before and overlays shown in Figures 27, 28, and 29.

It was also felt that the total time display of data might not be long enough to show changes in the SPL which were taking place; therefore a last set of experimental data was taken, utilizing a 20 msec. pulse separation but over nearly 100 points for a total time history on the order of 2 seconds. These data were plotted and overlays shown in Figures 30, 31, and 32.

Analysis of the entire data array is contained in sub-paragraph 5 of this section. Individual plots showing actual sound pressure levels and accurate time scales are available in the Ocean Physics Laboratory, Naval Postgraduate School.

4. Post Experimental Data Processing

After completion of the graphical presentation of the three varied data sets, and after being faced with the somewhat overwhelming mass of this graphical data, it was felt that further data processing might lead to some simplification of analysis. The form that this further processing was to take was that of cross-correlation; a method was desired by which

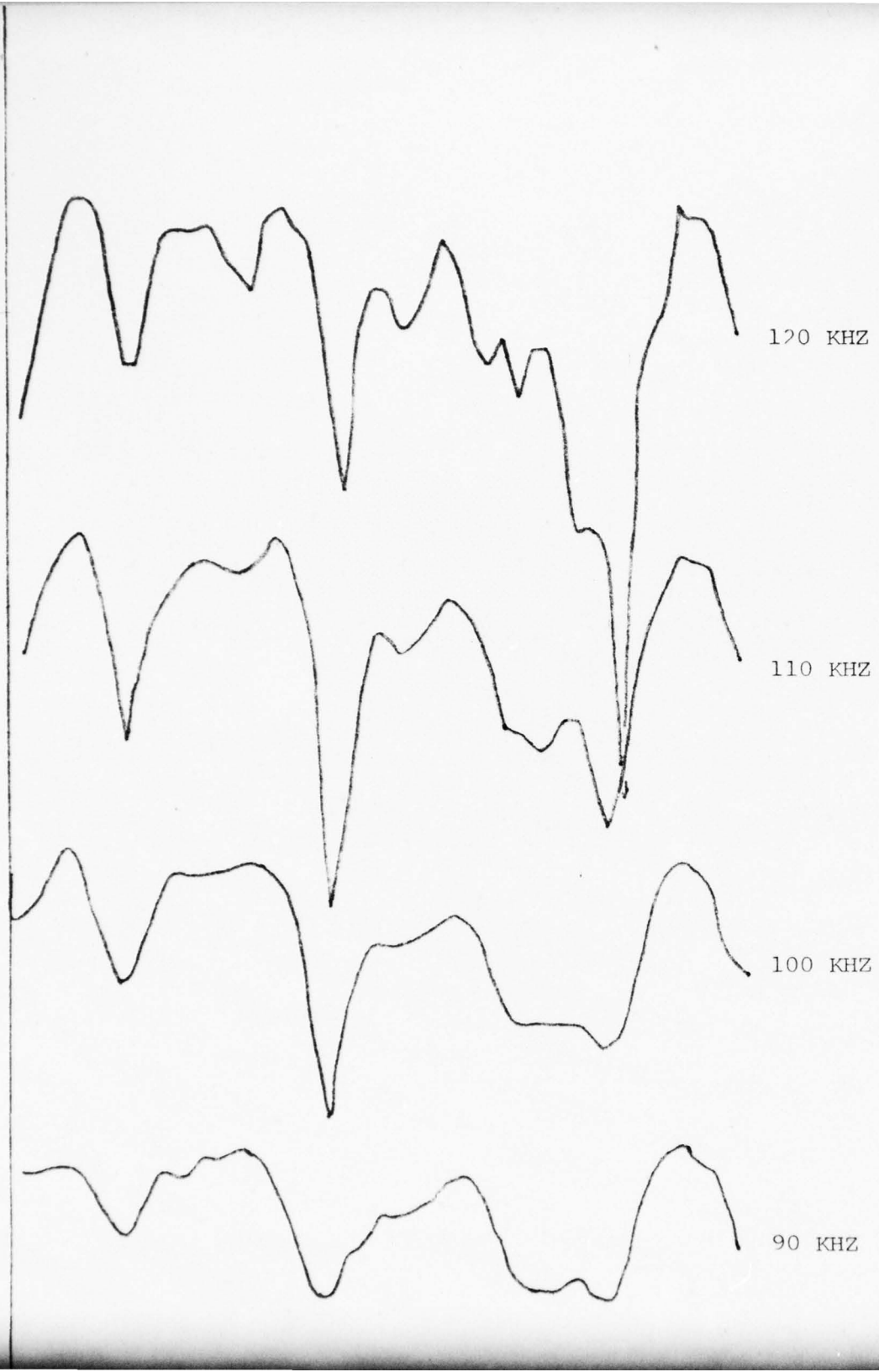
120 KHZ
110 KHZ
100 KHZ
90 KHZ

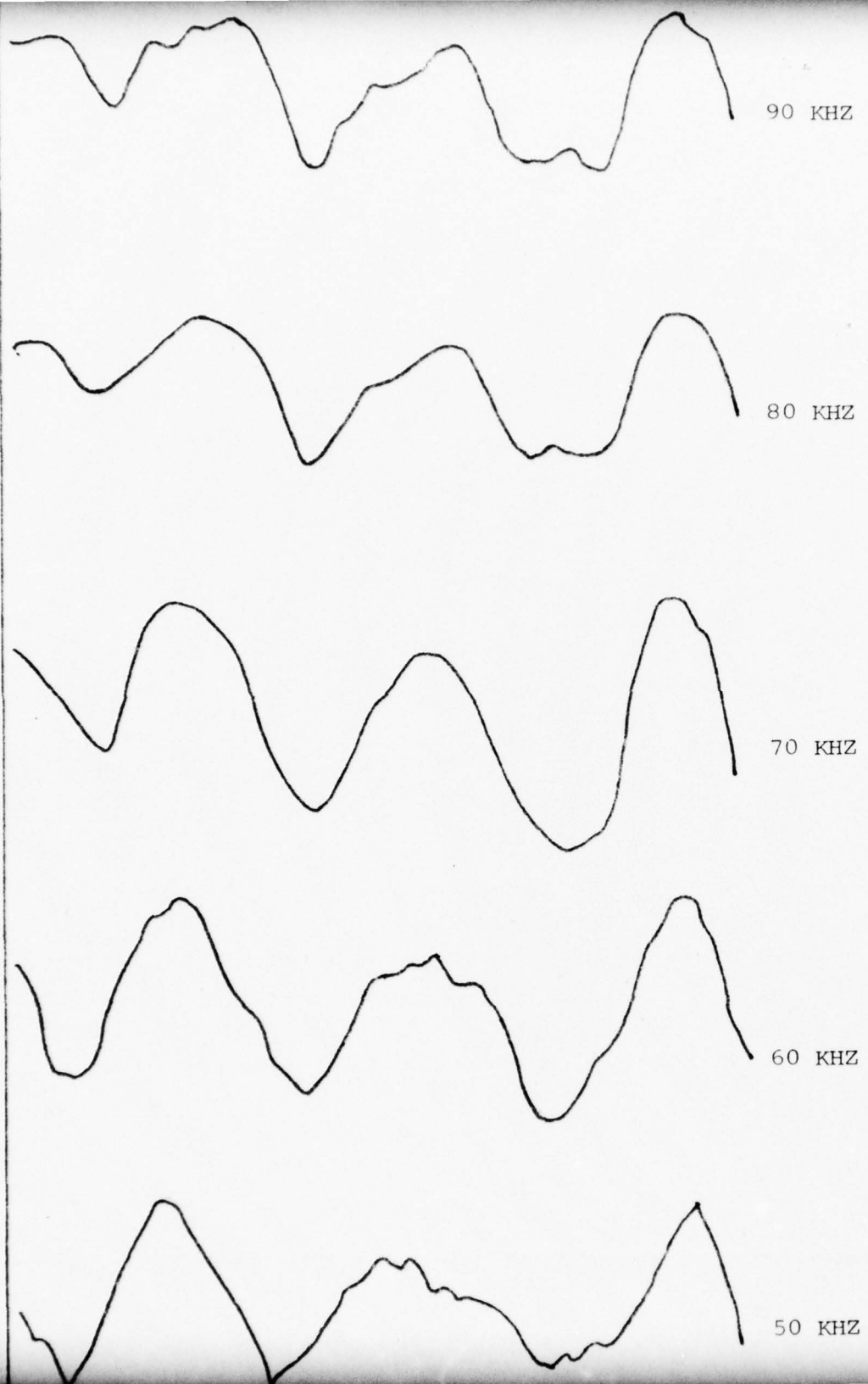
90 KHZ
80 KHZ
70 KHZ
60 KHZ
50 KHZ

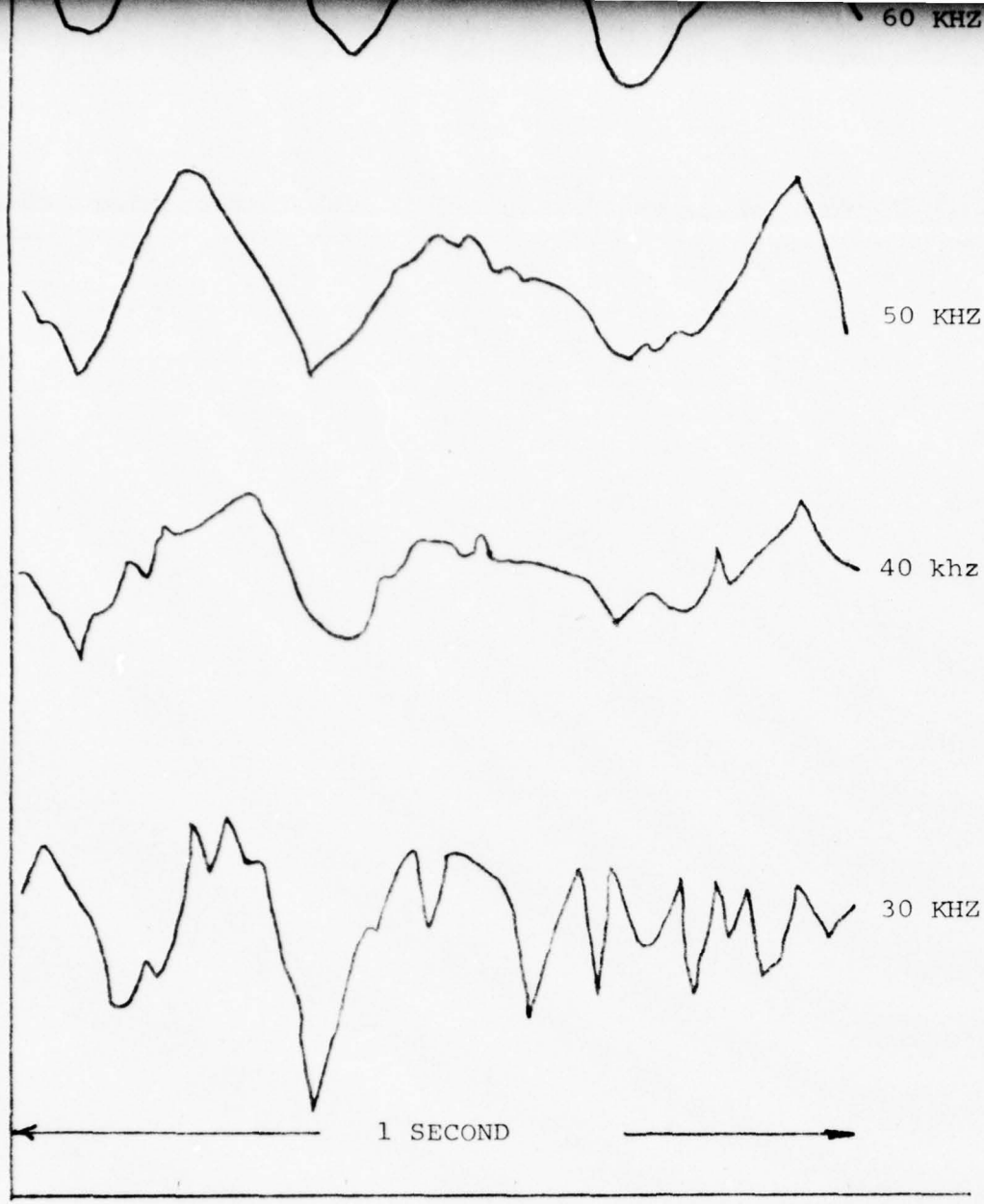

1 FAN
1"= 4 dB(30-70 KHZ)
1"= 8 dB(80-120KHZ)
2" MEAN SEPARATION
BETWEEN CURVES

Figure 25.SPL vs Time OVERLAY,1Fan.

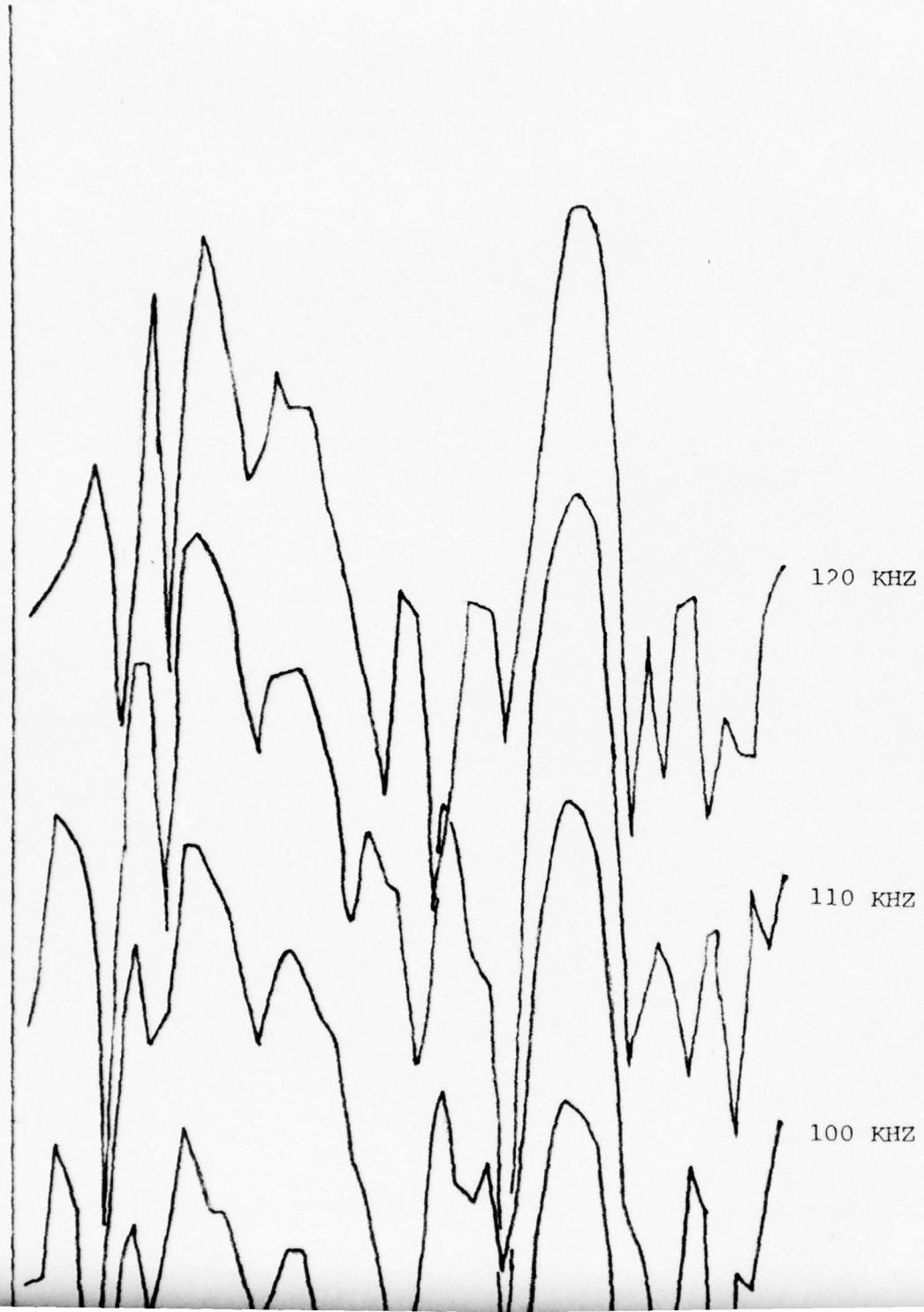
120 KHZ
110 KHZ
100 KHZ

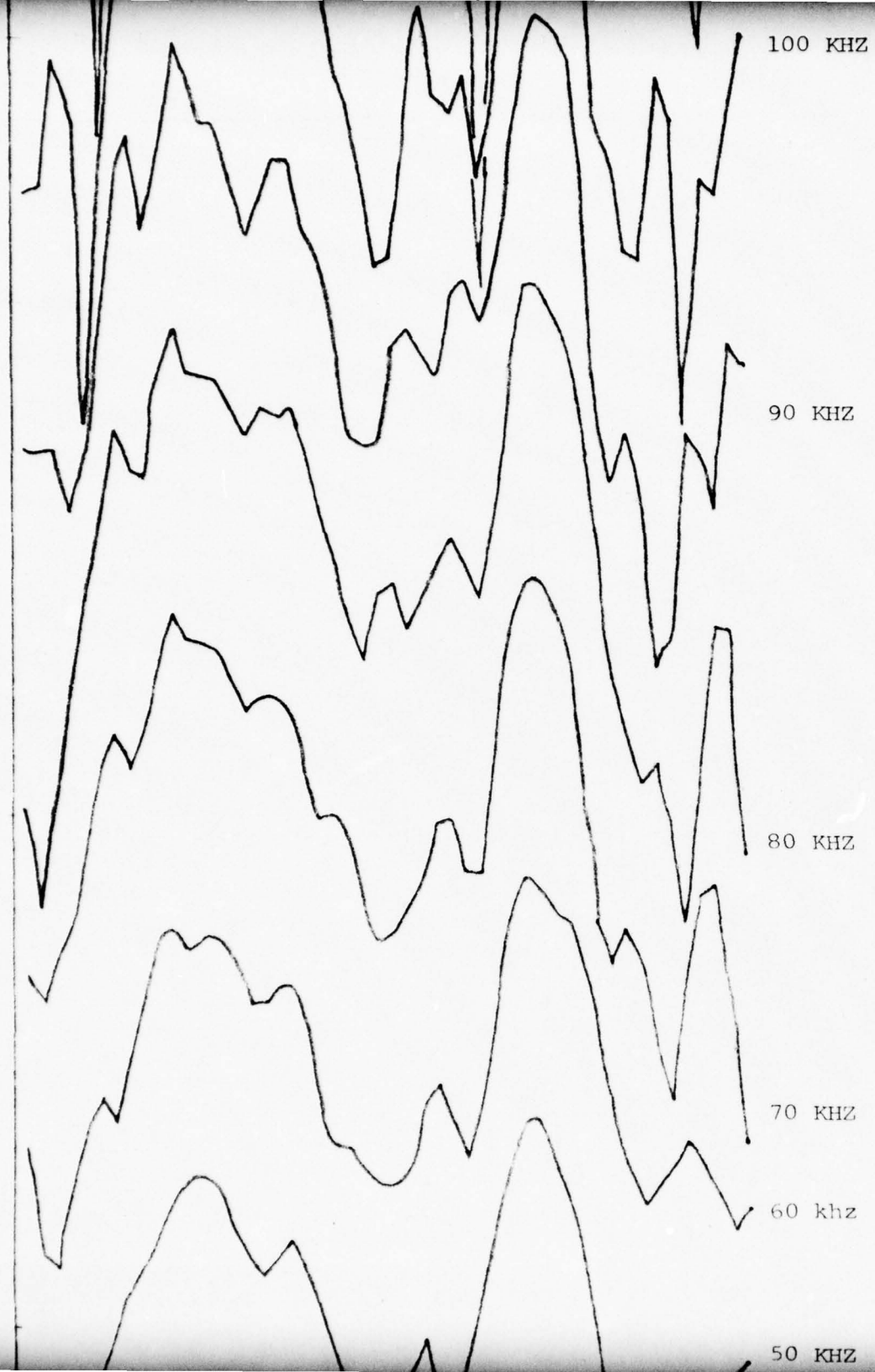
100 KHZ
90 KHZ
80 KHZ
70 KHZ
60 khz
50 KHZ

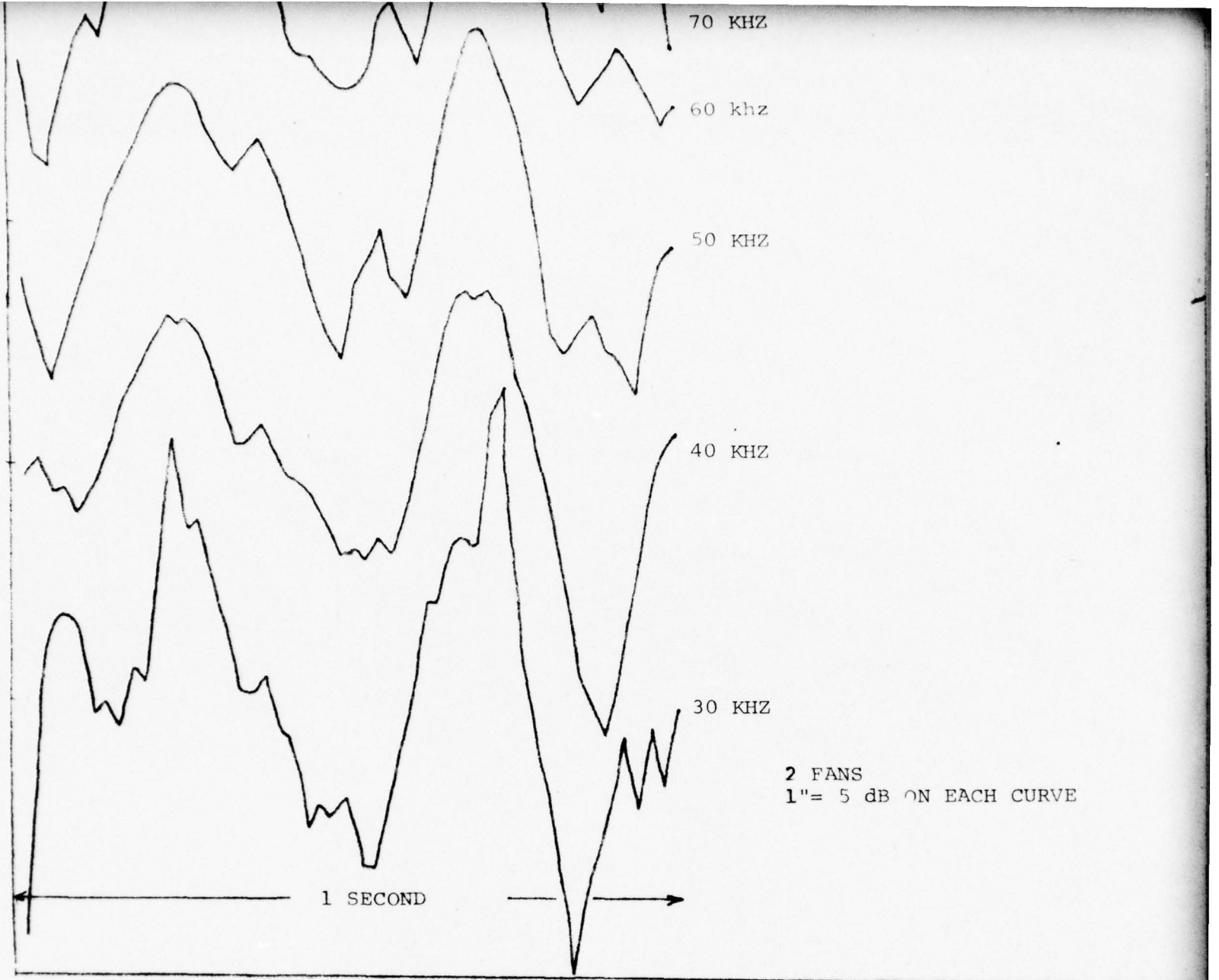

Figure25A. SPL vs Time Overlay, 2 Fans.

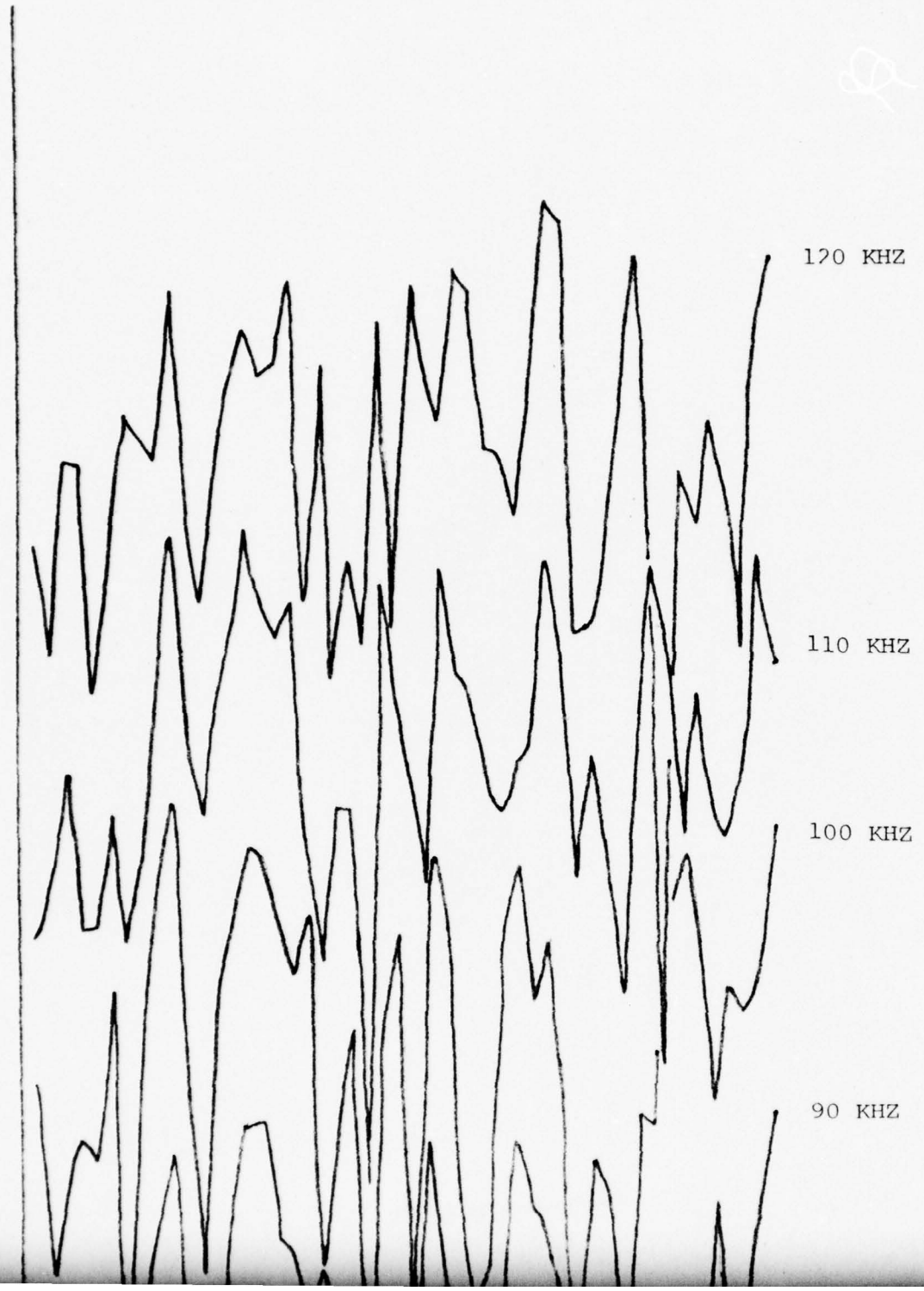
120 KHZ
110 KHZ
100 KHZ
90 KHZ

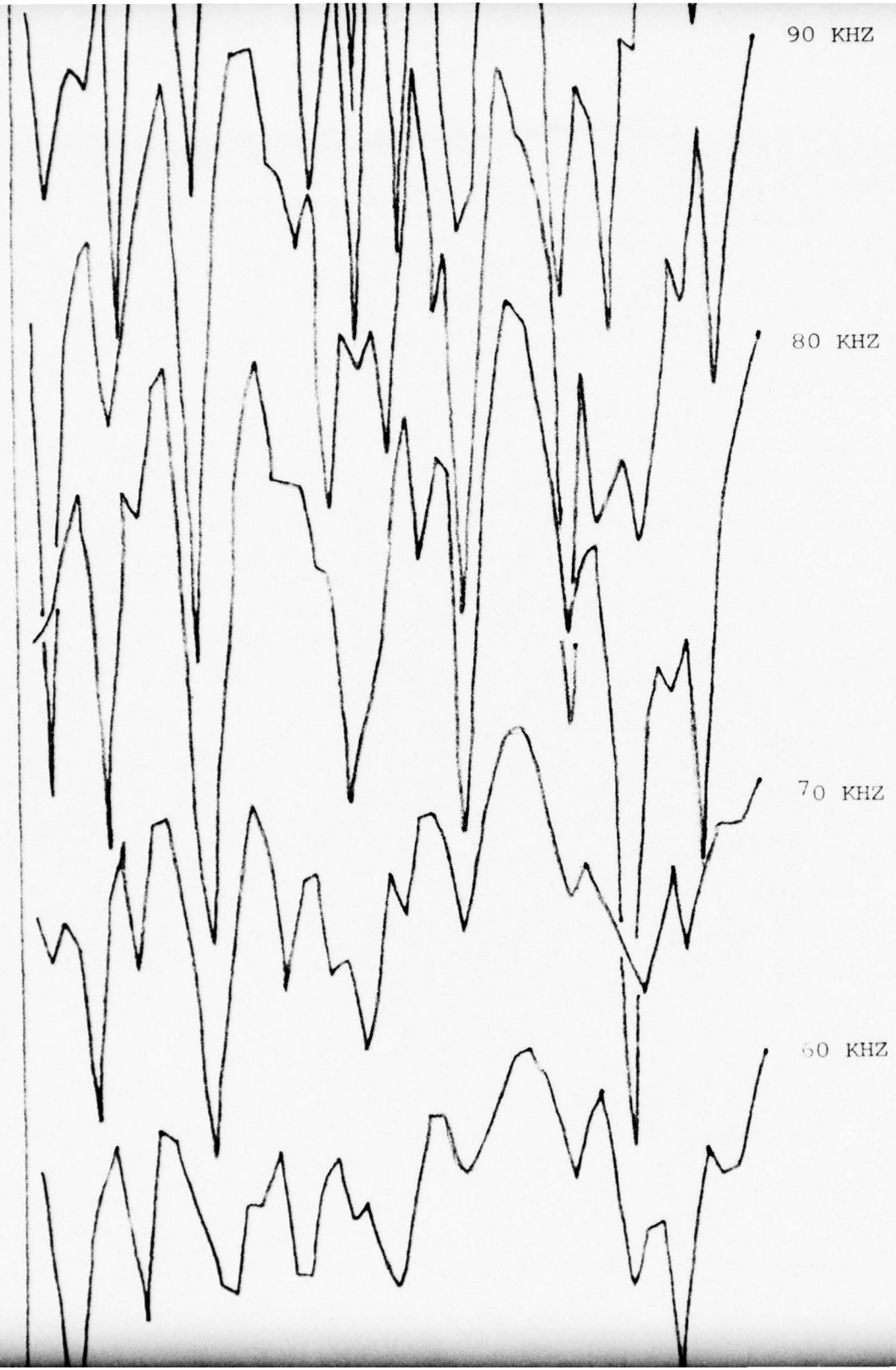
90 KHZ
80 KHZ
70 KHZ
60 KHZ

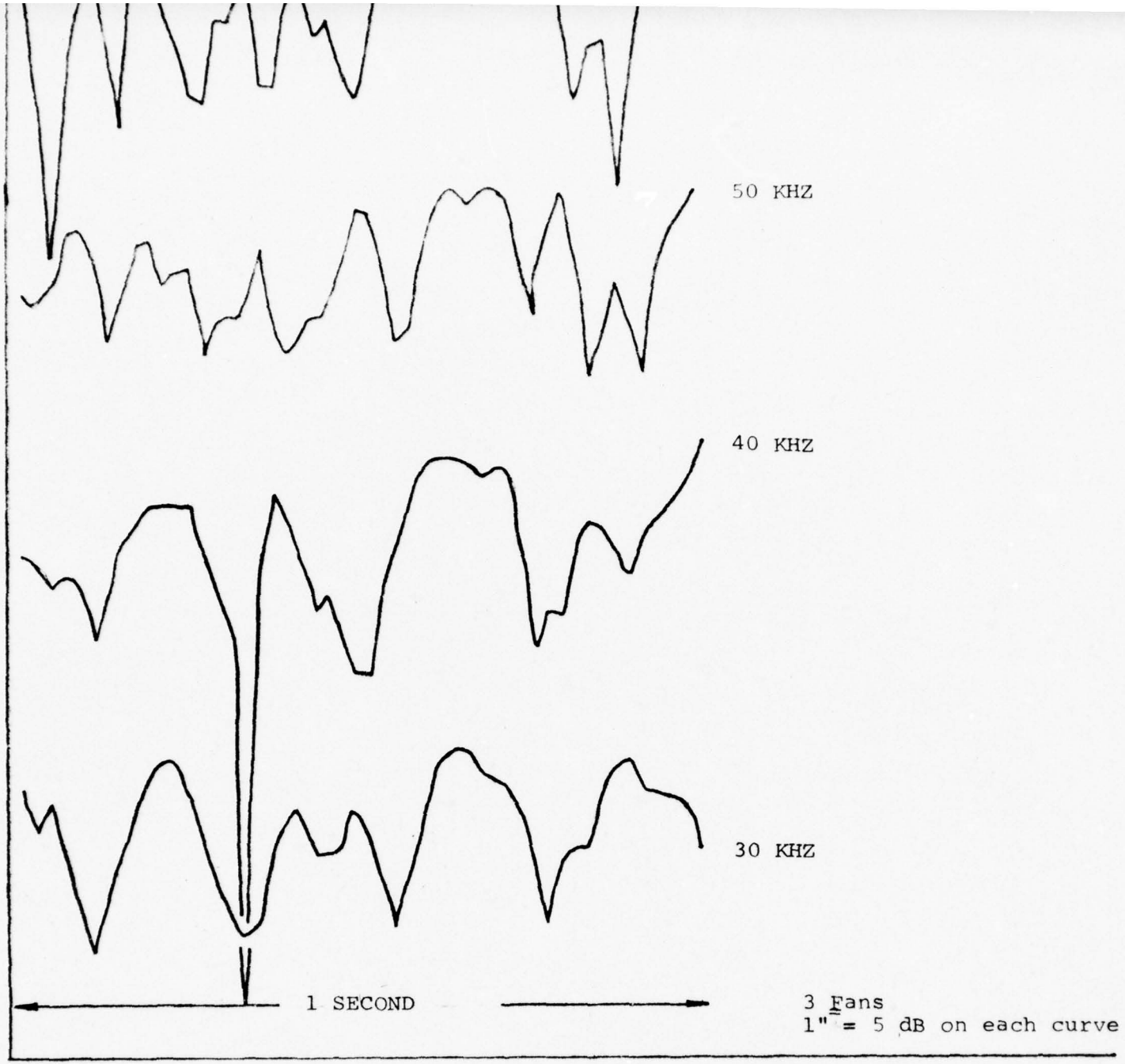

Figure 26. SPL vs Time Overlay, 3 Fans.

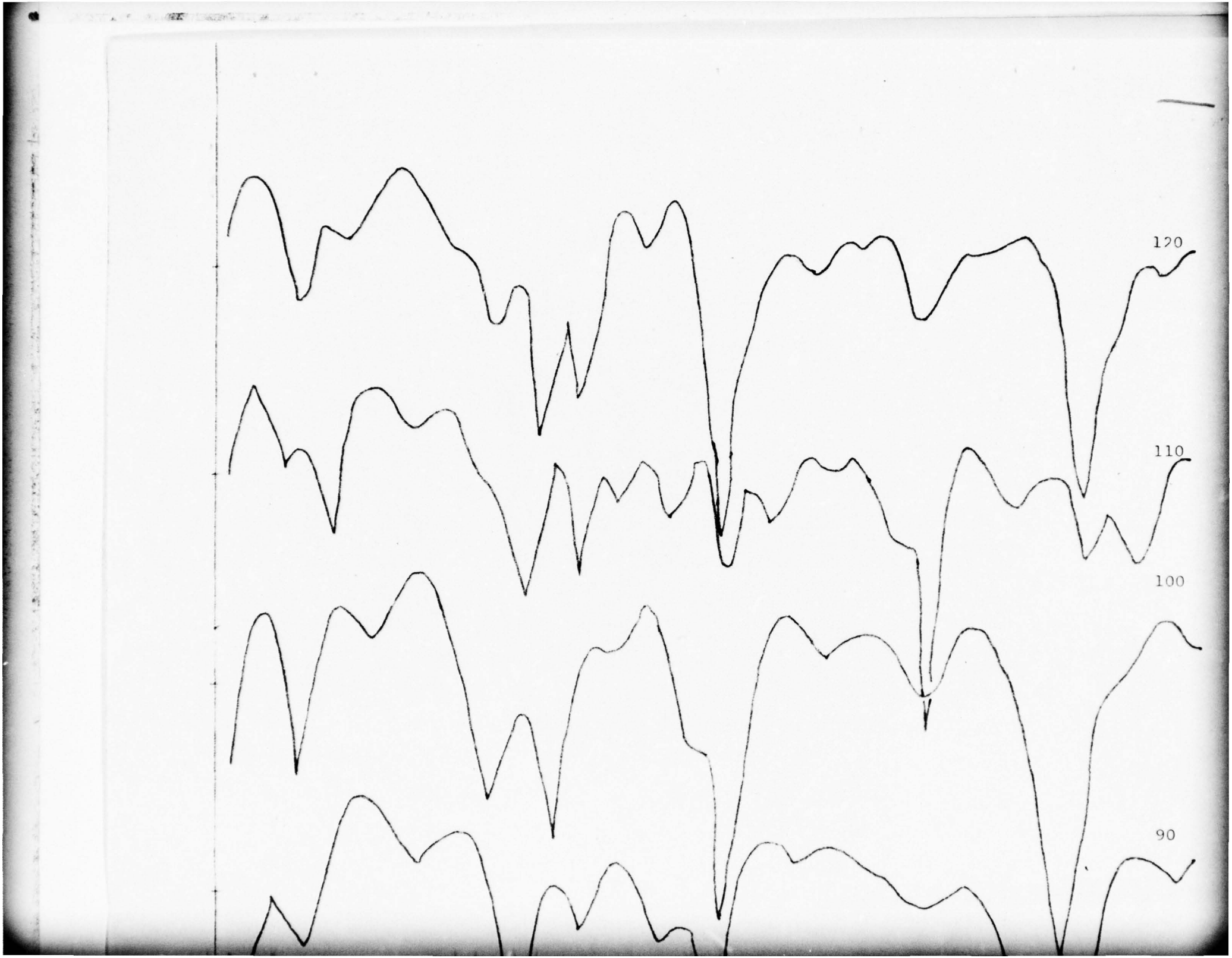
120
110
100
90

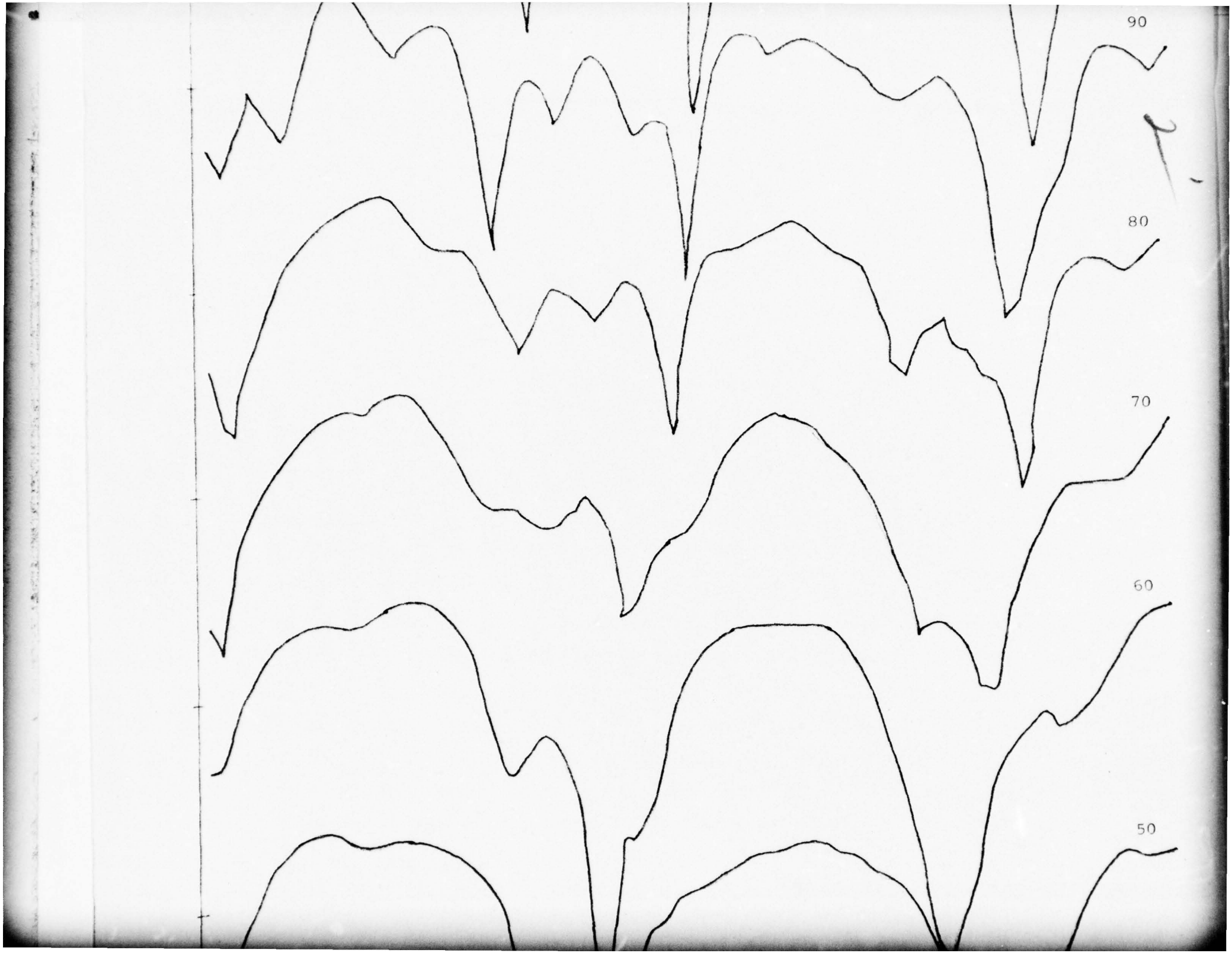
90
80
70
60
50

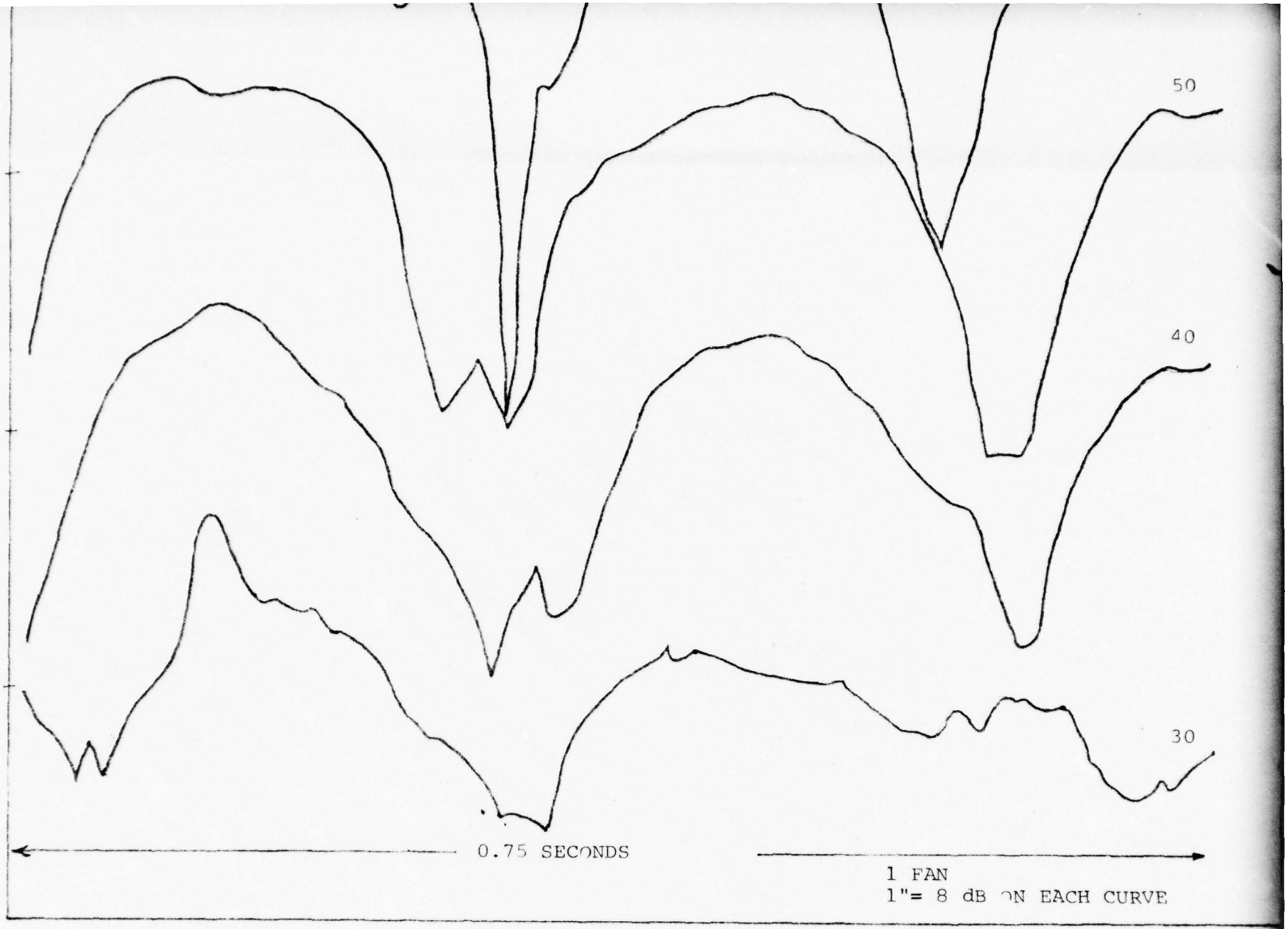

Figure 27. SPL vs Time Overlay, 1 Fan.

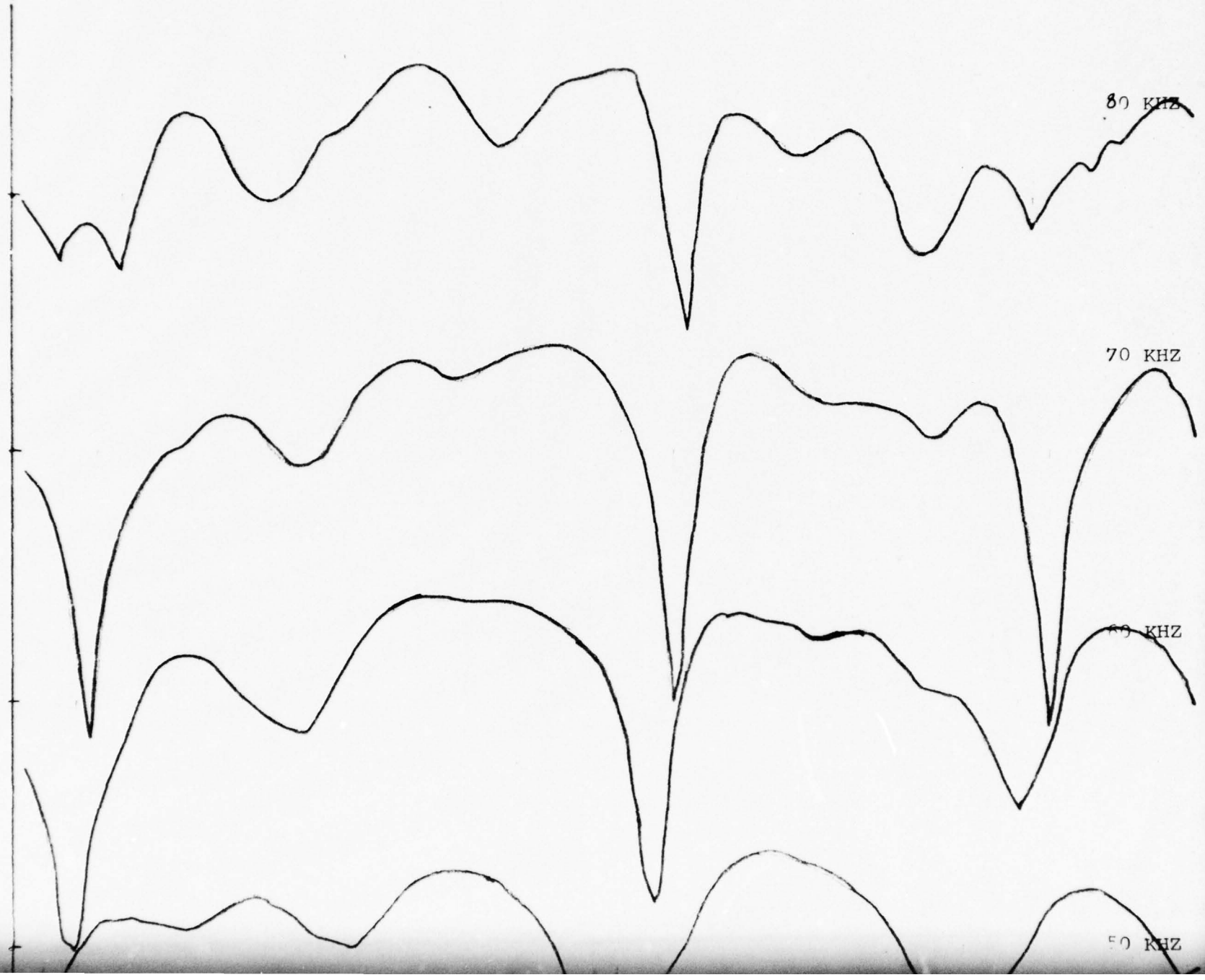
80 KHZ
70 KHZ
60 KHZ
50 KHZ

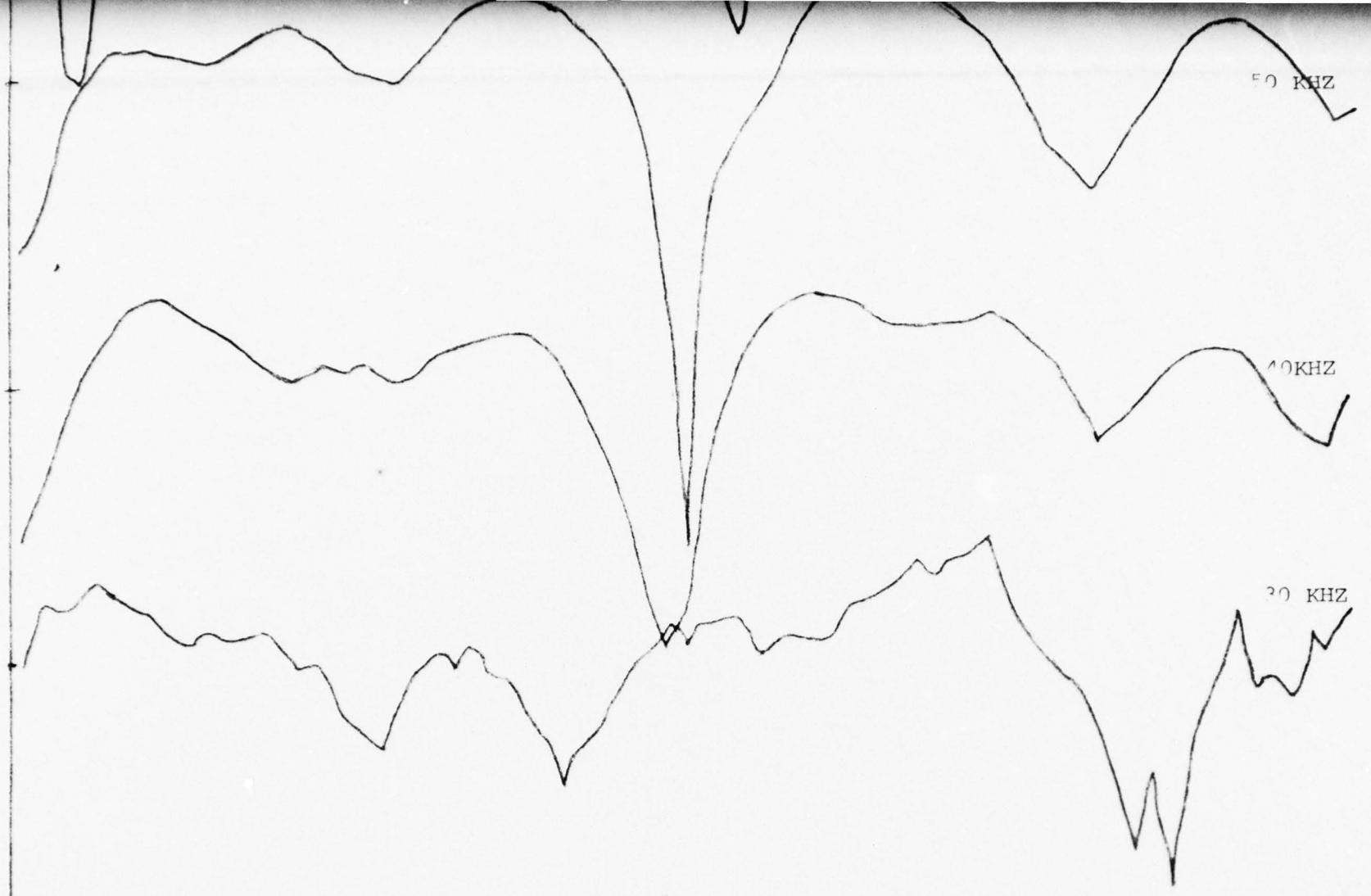

Figure 28. SPL vs Time Overlay, ? Fans.

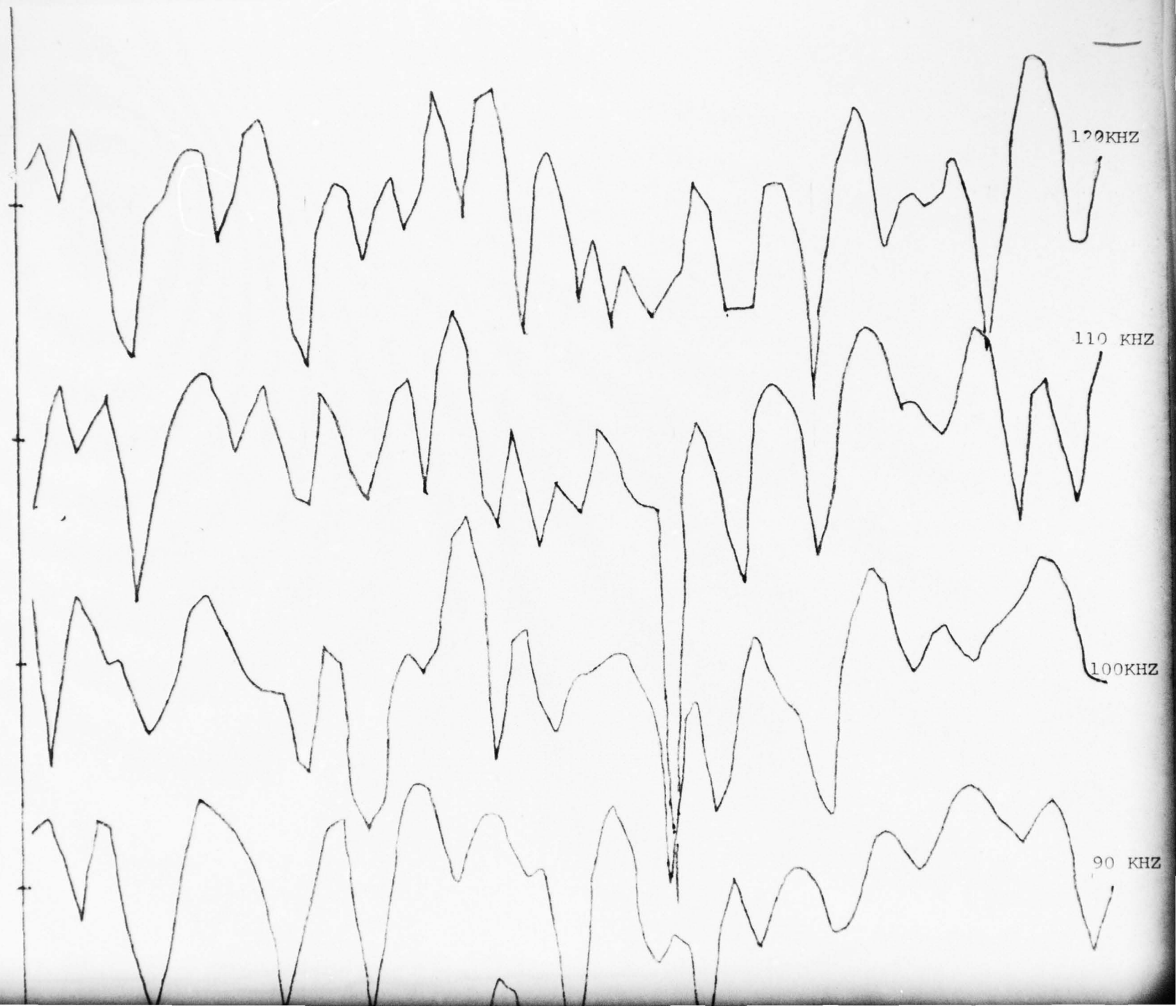
120KHZ
110 KHZ
100KHZ
90 KHZ

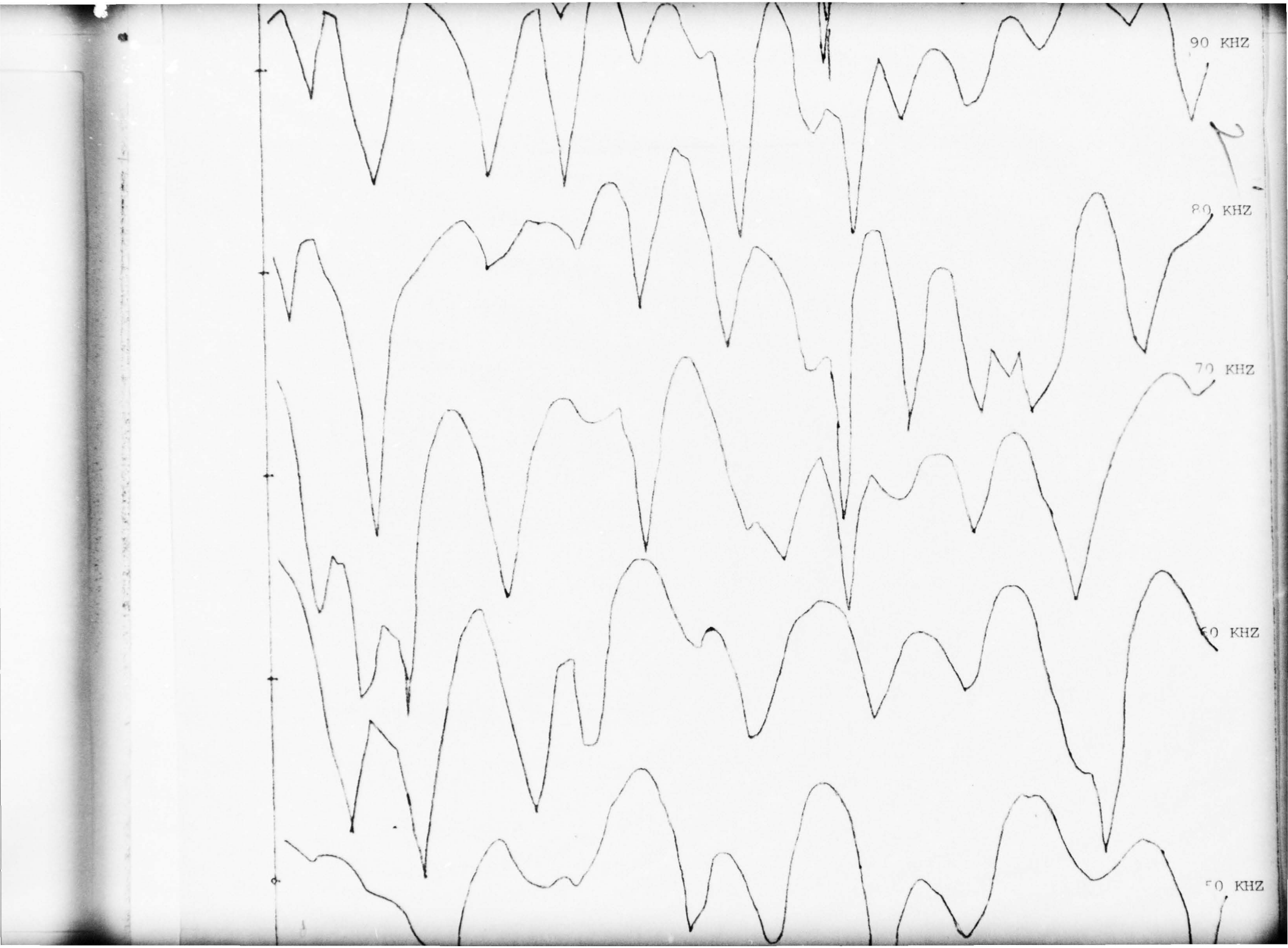
90 KHZ
80 KHZ
70 KHZ
60 KHZ
50 KHZ

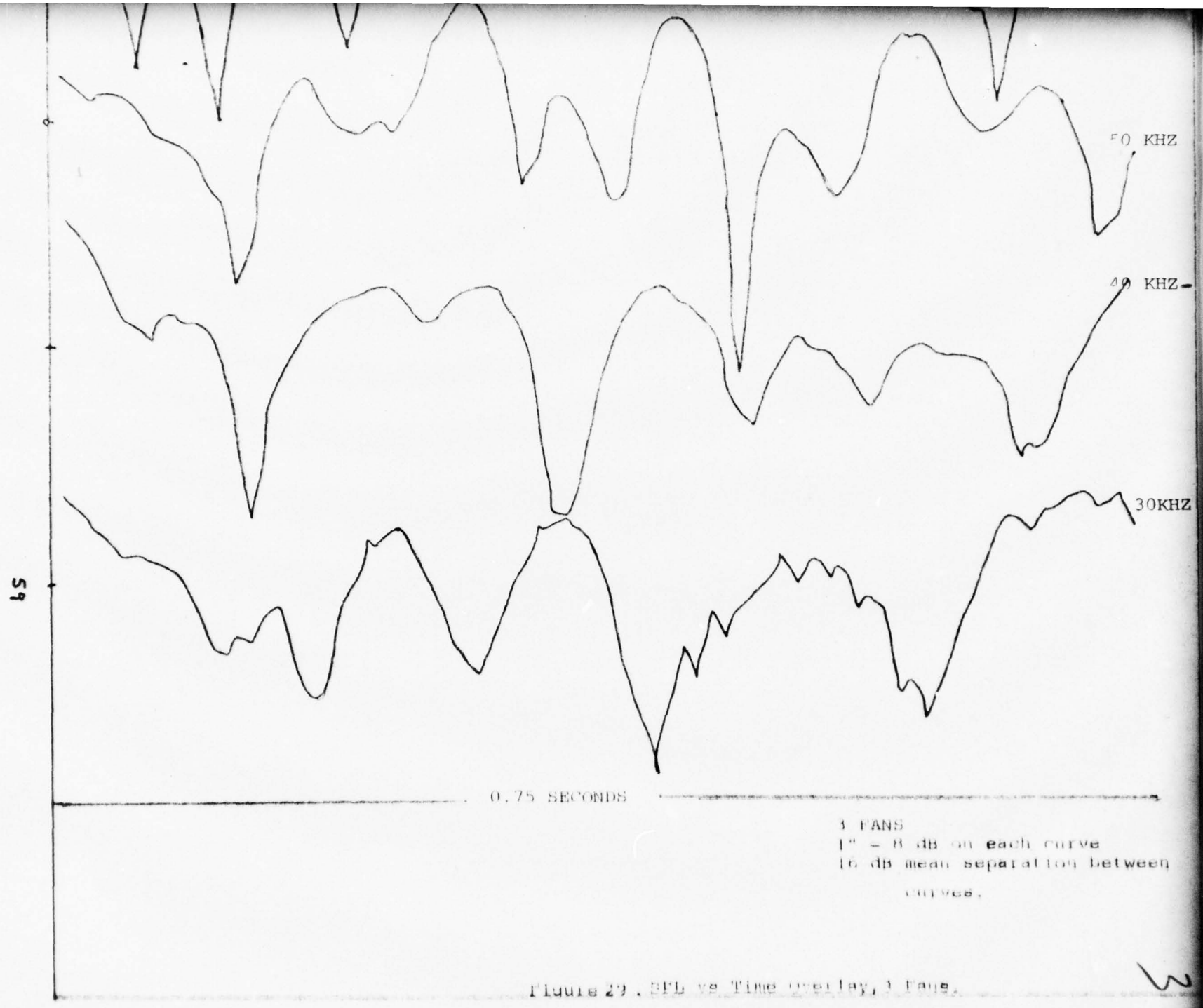

Figure 29. SPL vs Time overlay, 3 fans.

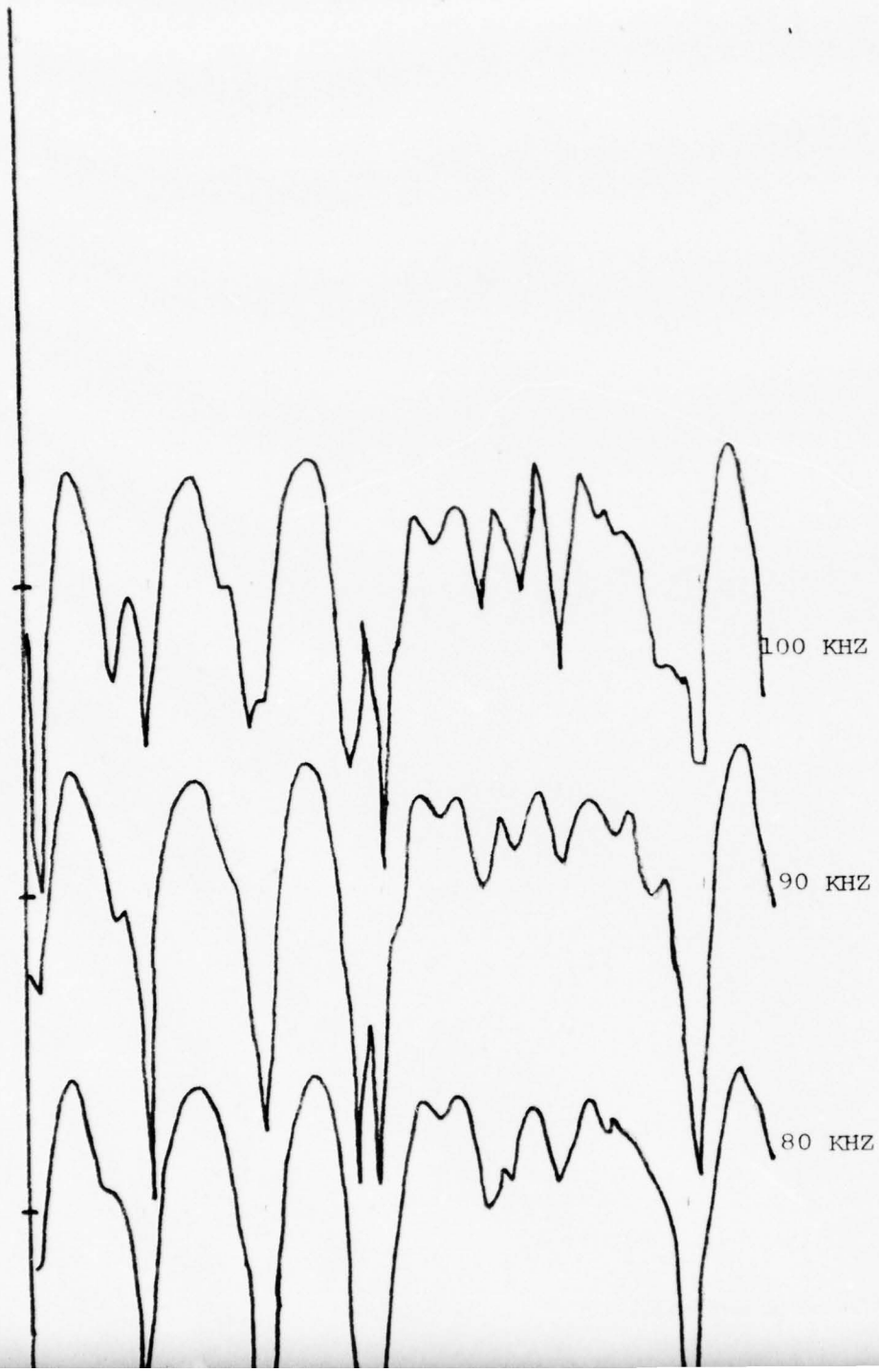
100 KHZ
90 KHZ
80 KHZ

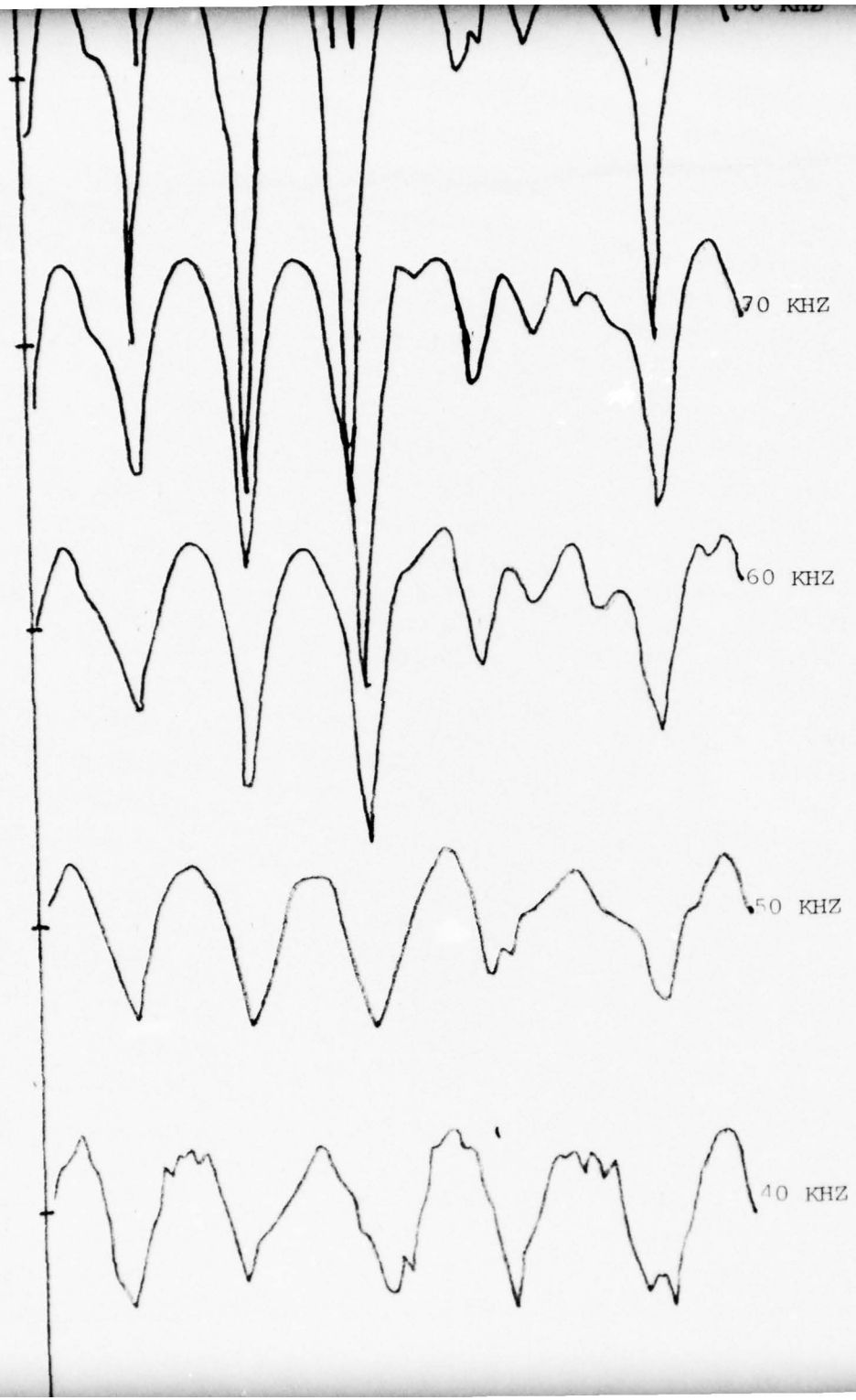
70 KHZ
60 KHZ
50 KHZ
40 KHZ

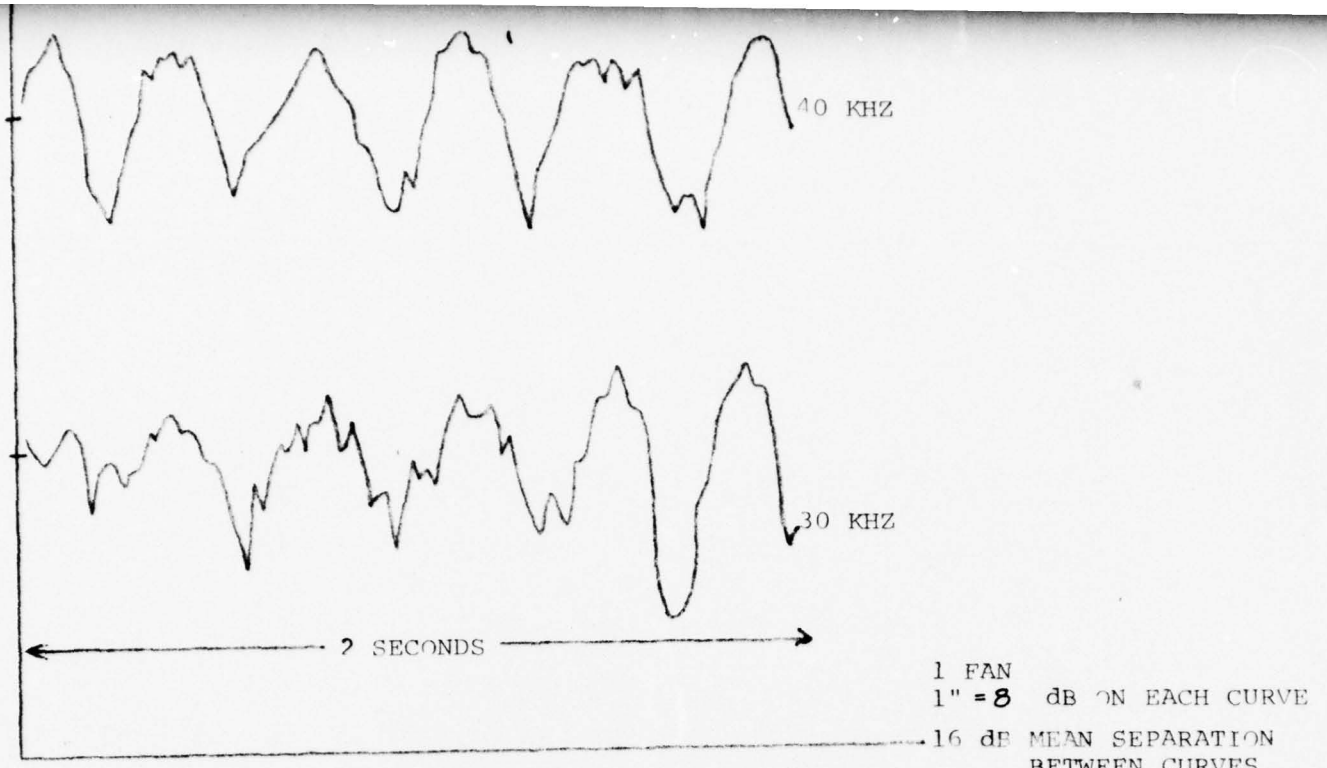

F igure 30.SPL vs Time Overlay.

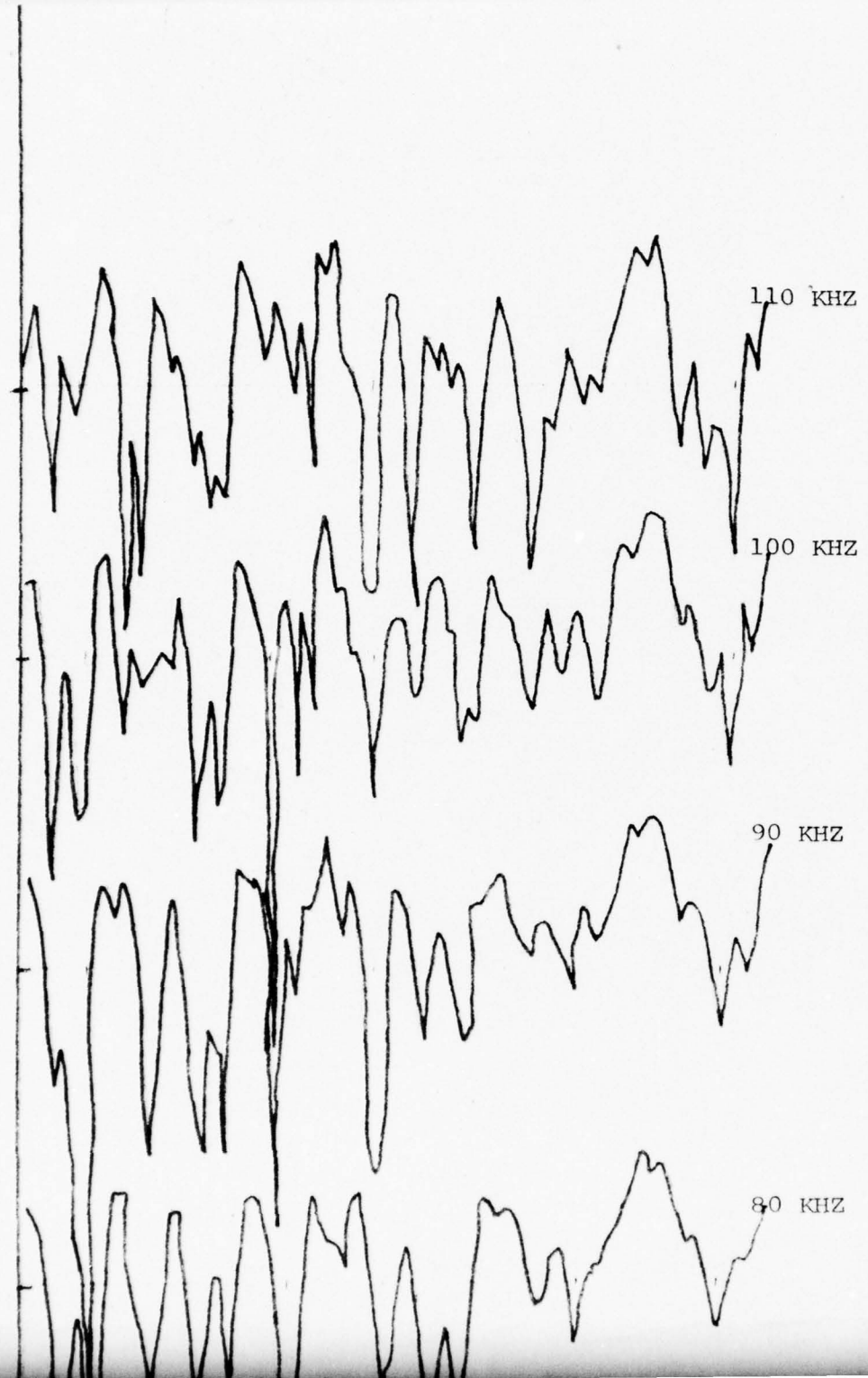
110 KHZ
100 KHZ
90 KHZ
80 KHZ

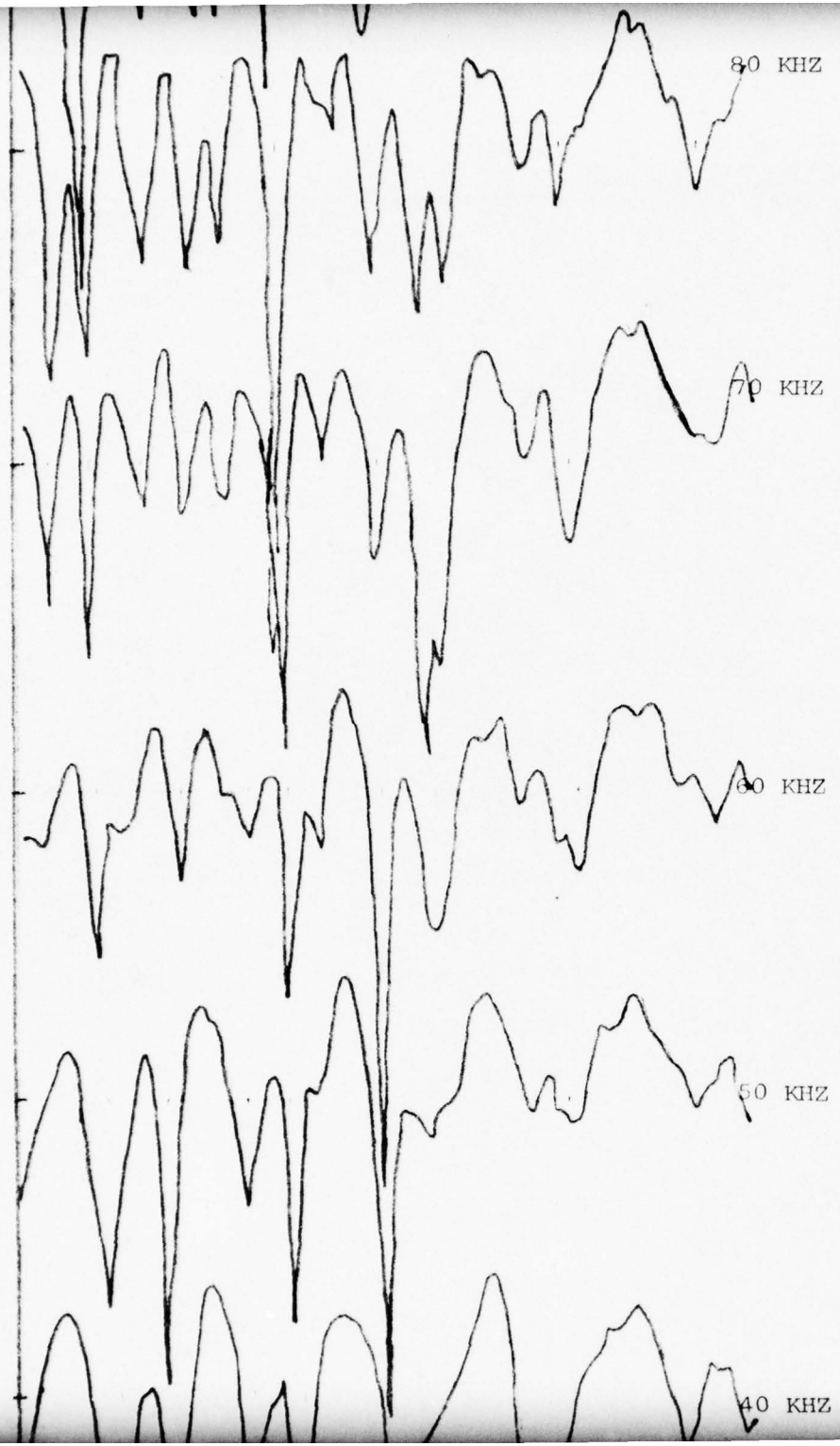
80 KHZ
70 KHZ
60 KHZ
50 KHZ
40 KHZ

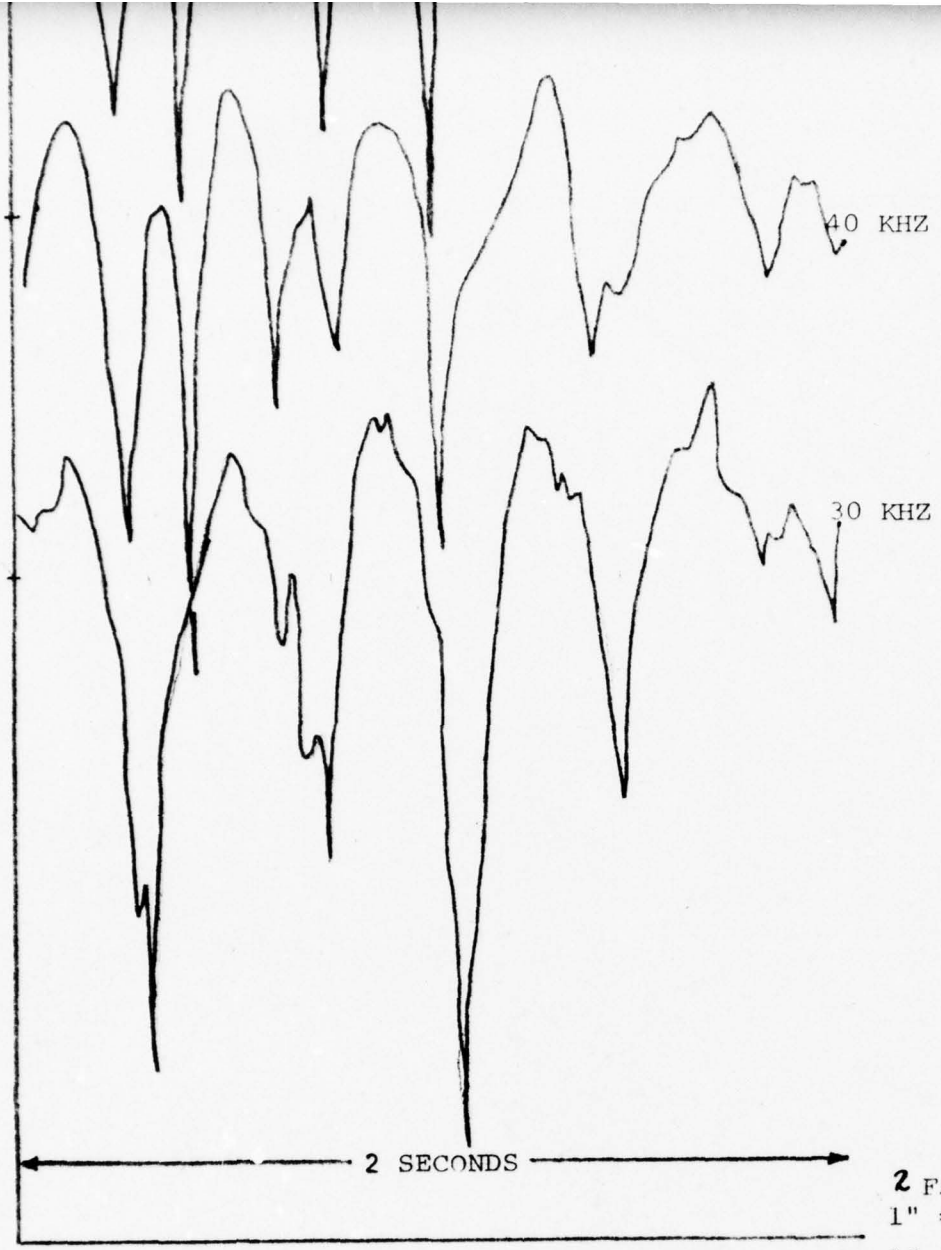

Figure 31. SPL vs Time Overlay

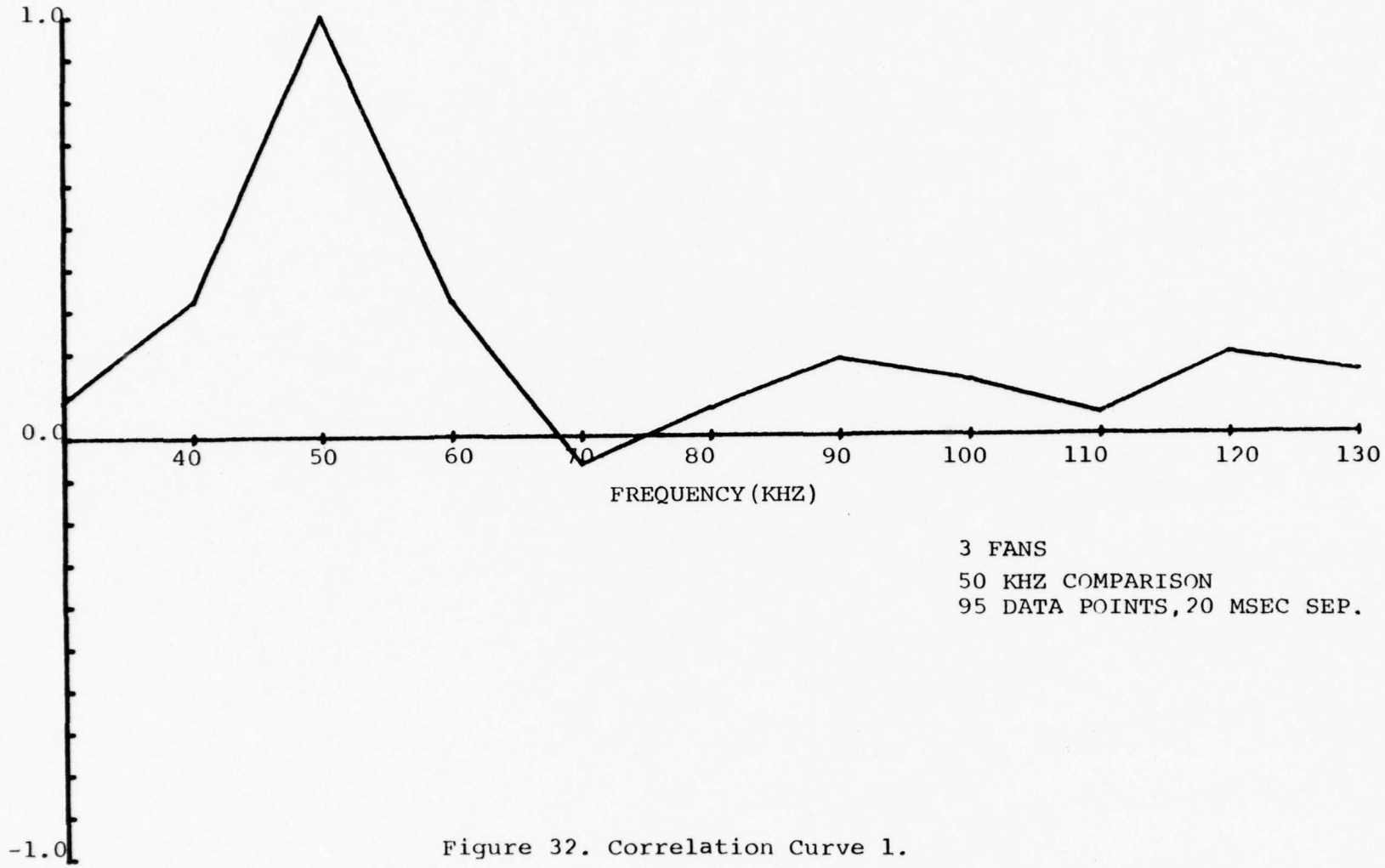

Figure 32. Correlation Curve 1.

a SPL vs. time curve at one frequency could be compared with that of another frequency and reduced to a single number representing the relative similarity of the two curves. Thus, instead of correlating in time or space, a correlation was employed using the algorithm below; it should be noted that this is a rather special type of cross-correlation wherein products of pressures at one frequency are compared with pressures at another frequency but summed over time.

$$\text{Corr}(F_1F_2) = \frac{\sum_{i=T_1}^{T_2} (P_{F_1}(i) - \mu F_1)(P_{F_2}(i) - \mu F_2)}{\left[\sum_{i=T_1}^{T_2} (P_{F_1}(i) - \mu F_1)^2 \sum_{i=T_1}^{T_2} (P_{F_2}(i) - \mu F_2)^2\right]^{\frac{1}{2}}}$$

The parameters of this algorithm are defined as follows:

F_1 = frequency for a given correlation curve

F_2 = frequency to which F_1 is being compared or correlated

$P_{F_1}(i)$ is the sound pressure (in microbars) at the ith time interval for frequency F_1

$P_{F_2}(i)$ is the sound pressure (in microbars) at the ith time interval for frequency F_2

μF_1 = mean value of P_{F_1} over the total time interval of concern

μF_2 = mean value of P_{F_2} over tht total time interval of concern

T_1 = starting point in time

T_2 = ending point in time.

Each correlation curve for a given F_1 consists of a set of 11 correlation values (30 kHz to 130 kHz, taken at 10 kHz intervals). It should be noted that the curves are normalized, i.e., when $F_1 = F_2$, $\text{Corr}(F_1F_2) = 1$.

The actual processing of the data was relatively simple since all data cards had been previously punched. A new computer program was developed for the IBM-360 to carry out the correlation algorithm and provide the appropriate output. A copy of this program is contained in Appendix A.

In addition to the correlating over the entire number of time points available, correlation was also performed over the halves or over individual fourths of some curves for comparison purposes. Table V describes those correlations which were computed and plotted. Complete presentation of all the correlation curves produced (11 curves for each case listed in Table V) is not considered feasible just from a numerical standpoint but representative results are labeled and shown in Figures 33 to 39.

5. Analysis of Results

Examination of Figures 25-31 gives insight into the qualitative aspects of the effects of frequency change on the scattering of sound. The relative periodicity, corresponding to the periodicity of the wave surface, is present for the relatively low roughness, smoother surface cases. As the frequency, and hence the roughness, increases this periodicity disappears. It is assumed that the incoherent component of the sound is growing more predominant and is responsible for this effect. Actual measurements to separate coherent and incoherent sound components were not made. For the 1 and 2 fan overlays, large peaks and valleys in the sound amplitude can be monitored as they progress up the frequency scale. For

Table V

Correlation Curves Plotted

# of Data Points	Time Separation Between Points	No. of Fans	Correlation over:
50	20 msec	4	Full curve
"	"	4	1st ½ of curves
"	"	3	Full Curve
"	"	3	1st ½ of curves*
"	"	2	Full curve
"	"	2	2nd ½ of curves
"	"	1	Full curve*
"	"	1	1st ½ of curves*
95	20 msec	3	Full curve
"	"	3	1st ½ of curves
"	"	3	2nd ½ of curves
"	"	3	1st ¼ of curves
"	"	3	2nd ¼ of curves
"	"	3	3rd ¼ of curves
"	"	3	4th ¼ of curves

*Data obtained but not plotted.

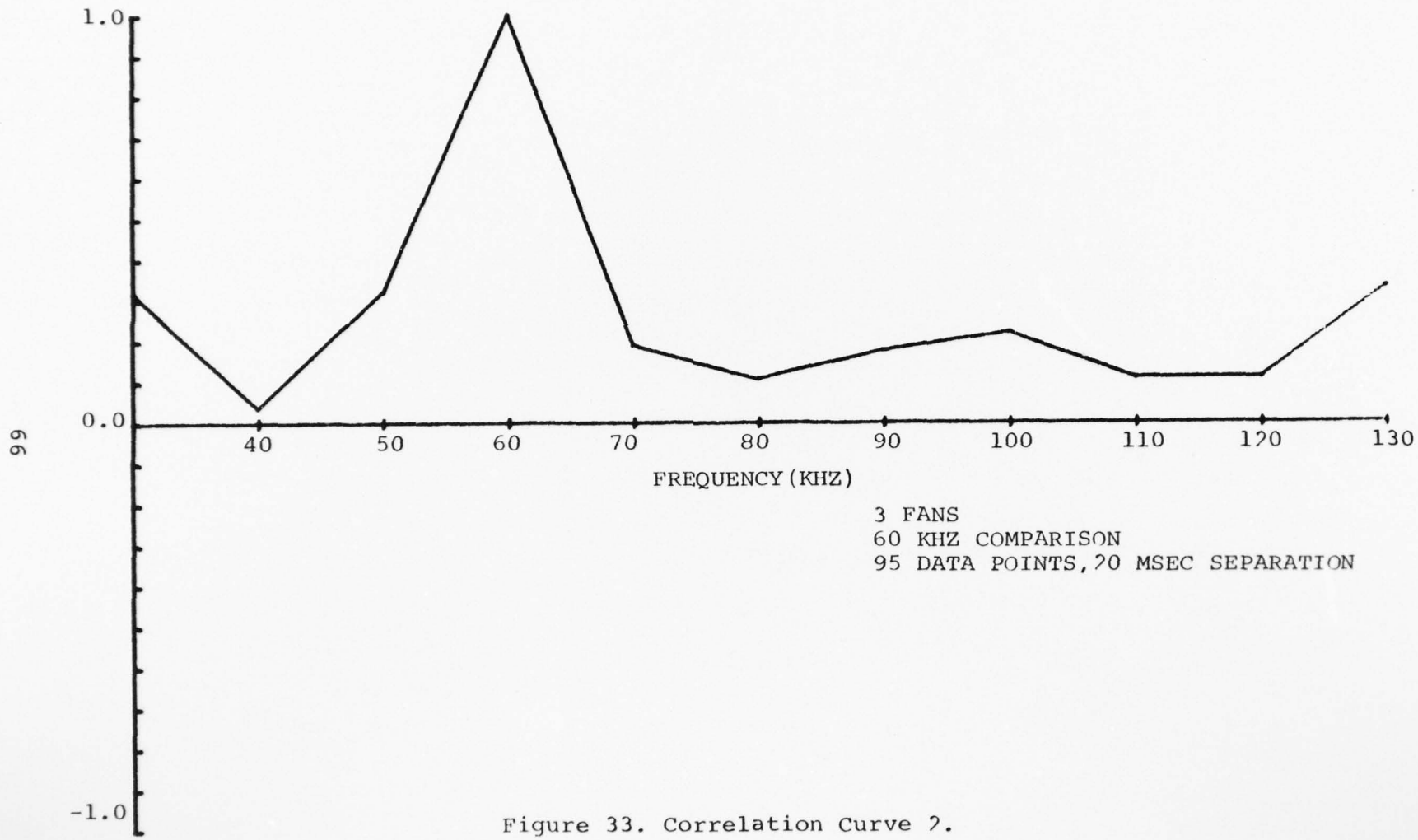

Figure 33. Correlation Curve 2.

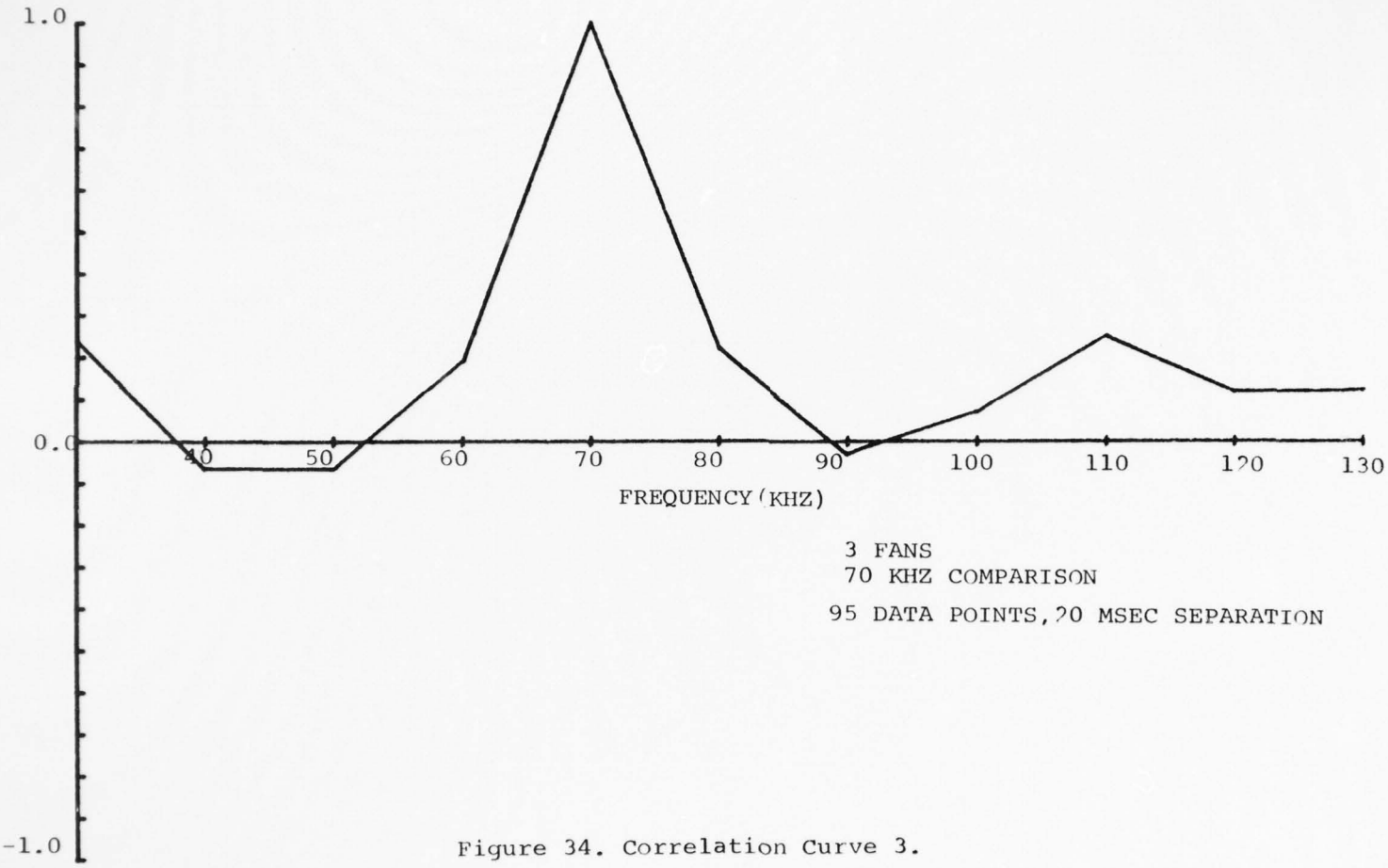

Figure 34. Correlation Curve 3.

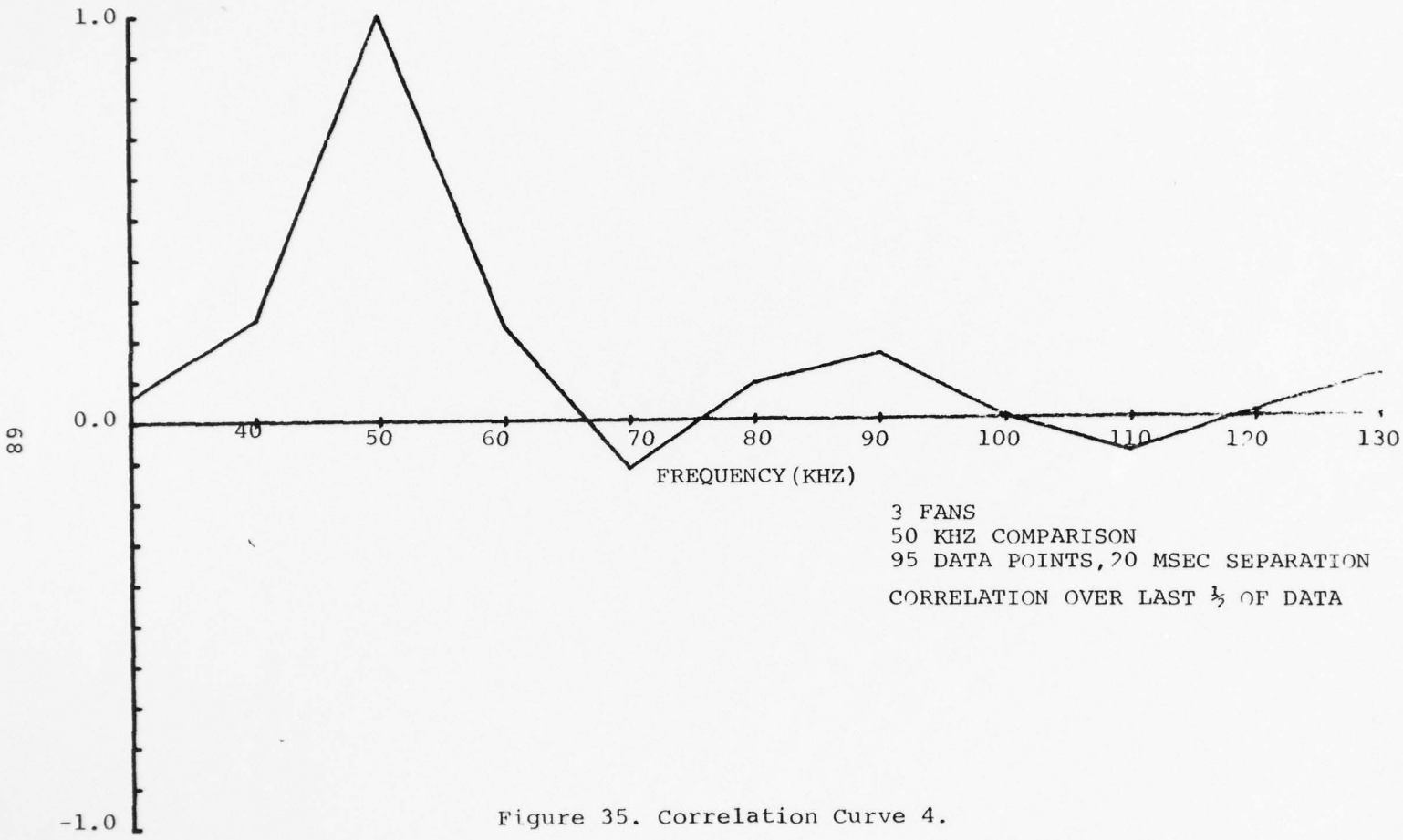

Figure 35. Correlation Curve 4.

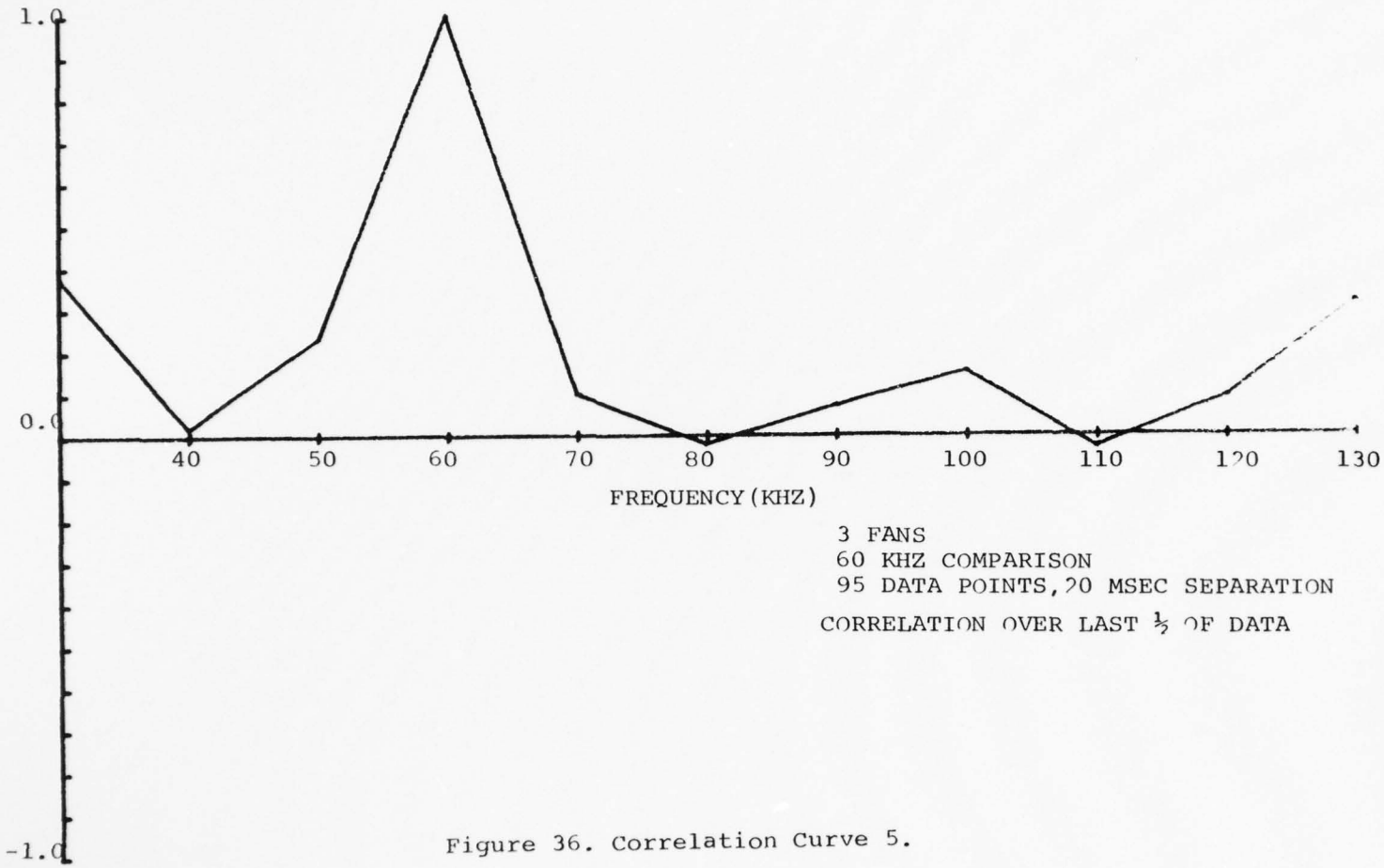

Figure 36. Correlation Curve 5.

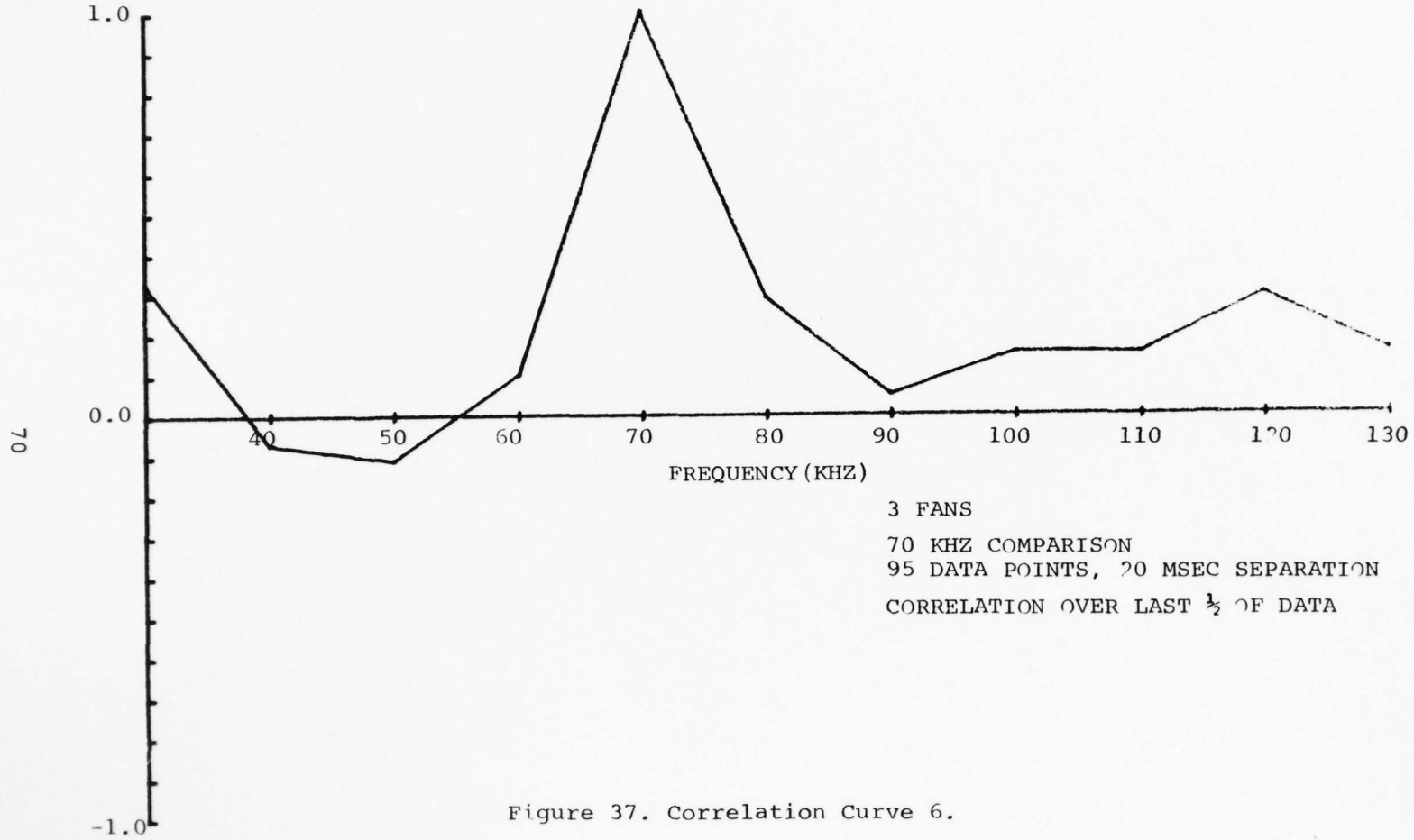

Figure 37. Correlation Curve 6.

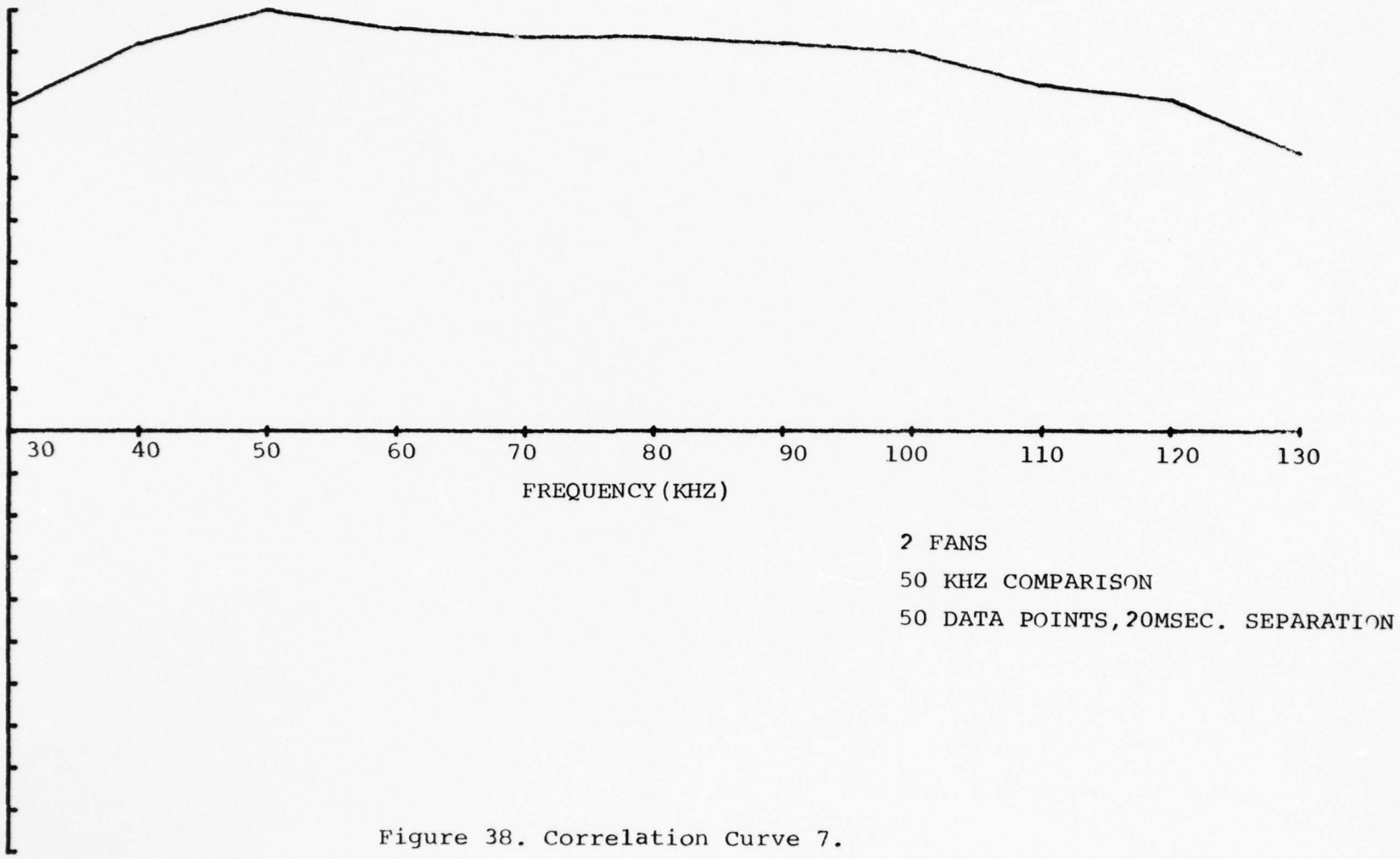

Figure 38. Correlation Curve 7.

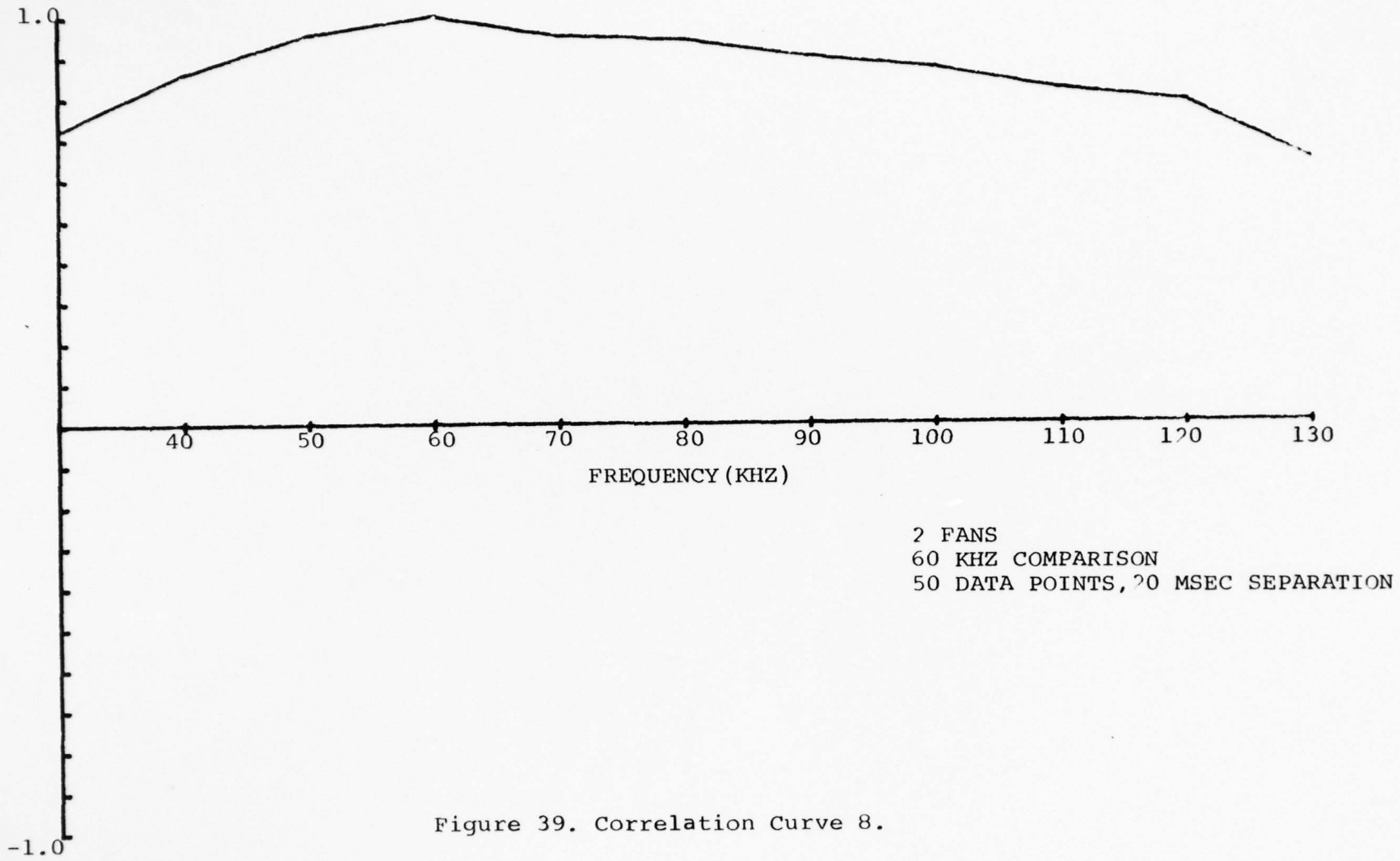

Figure 39. Correlation Curve 8.

the higher fan combinations, the incoherency is controlling, and in most instances, particular peaks and valleys cannot be followed over any appreciable frequency range.

After an exhaustive examination of the correlation curves, it was concluded that no information of a significant nature could be discerned; it is interesting to note that in the 3 fan case a rather rapid de-correlation occurs. The 2 fan case, in contrast, has a rather high correlation over the entire frequency range. This is more or less confirmed by visually correlating the curves of the overlays. It should be mentioned, that in one instance, the 1 fan combination showed slightly less correlation than that of 2 fans. Also of interest is the fact that the resulting degree of correlation is somewhat time-independent as evidenced by the large degree of similarity between the correlations over the full number of data points and the correlations over half of the data points.

In an attempt to quantify the actual effect of frequency on the scattered sound, graphs of the large, well defined minima taken from the overlays of Figures 25 to 31 vs. time were plotted. The minima values were chosen because, in general, they appeared to be more highly defined and localized than the rather broad maxima of the curves. The resultant minima plots for the various overlays appear in Figures 40 to 46 and are appropriately identified. Figure 46 illustrates how the increasing incoherency makes it impossible to trace a logical progression of features as frequency increases. By using an assumed extension of the trends developed for the 1

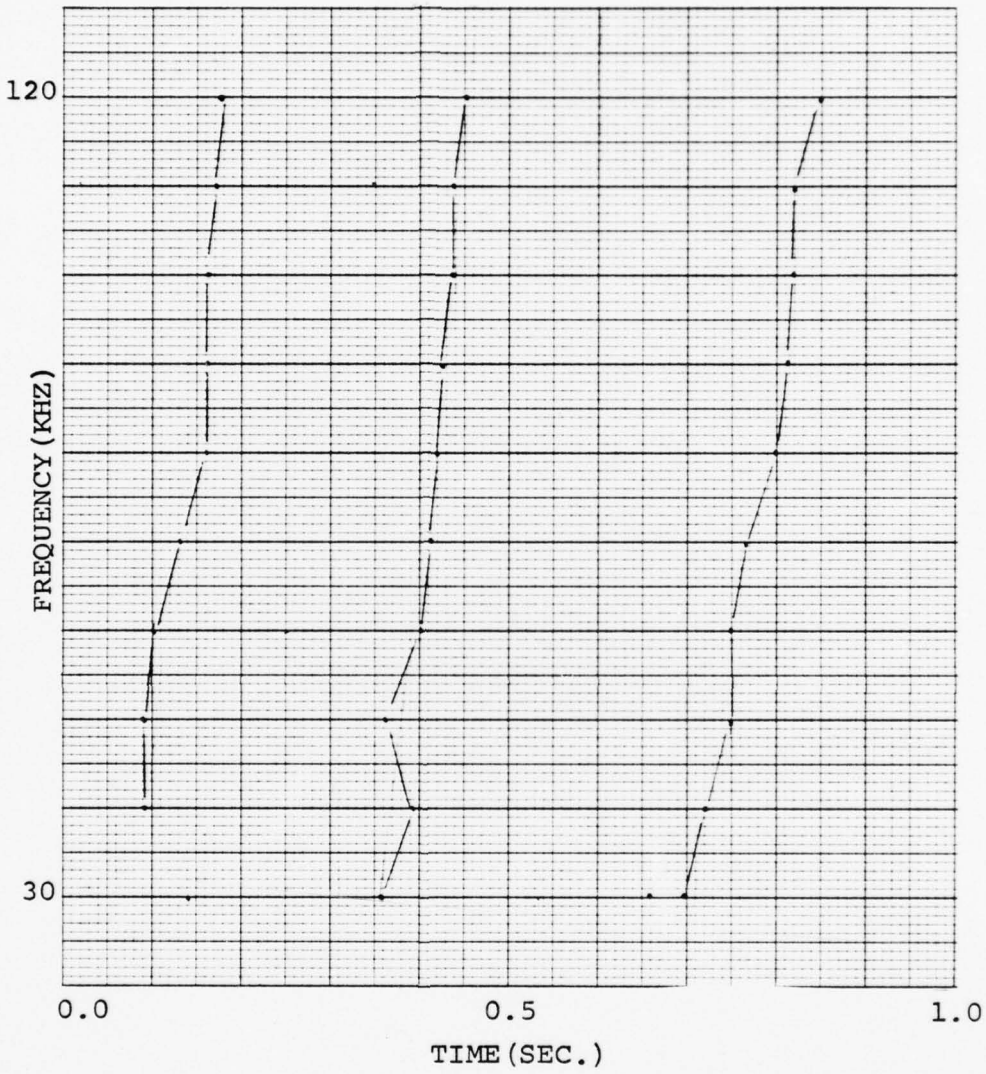

Figure 40. Minima Plot, 1 Fan, 1 Second.

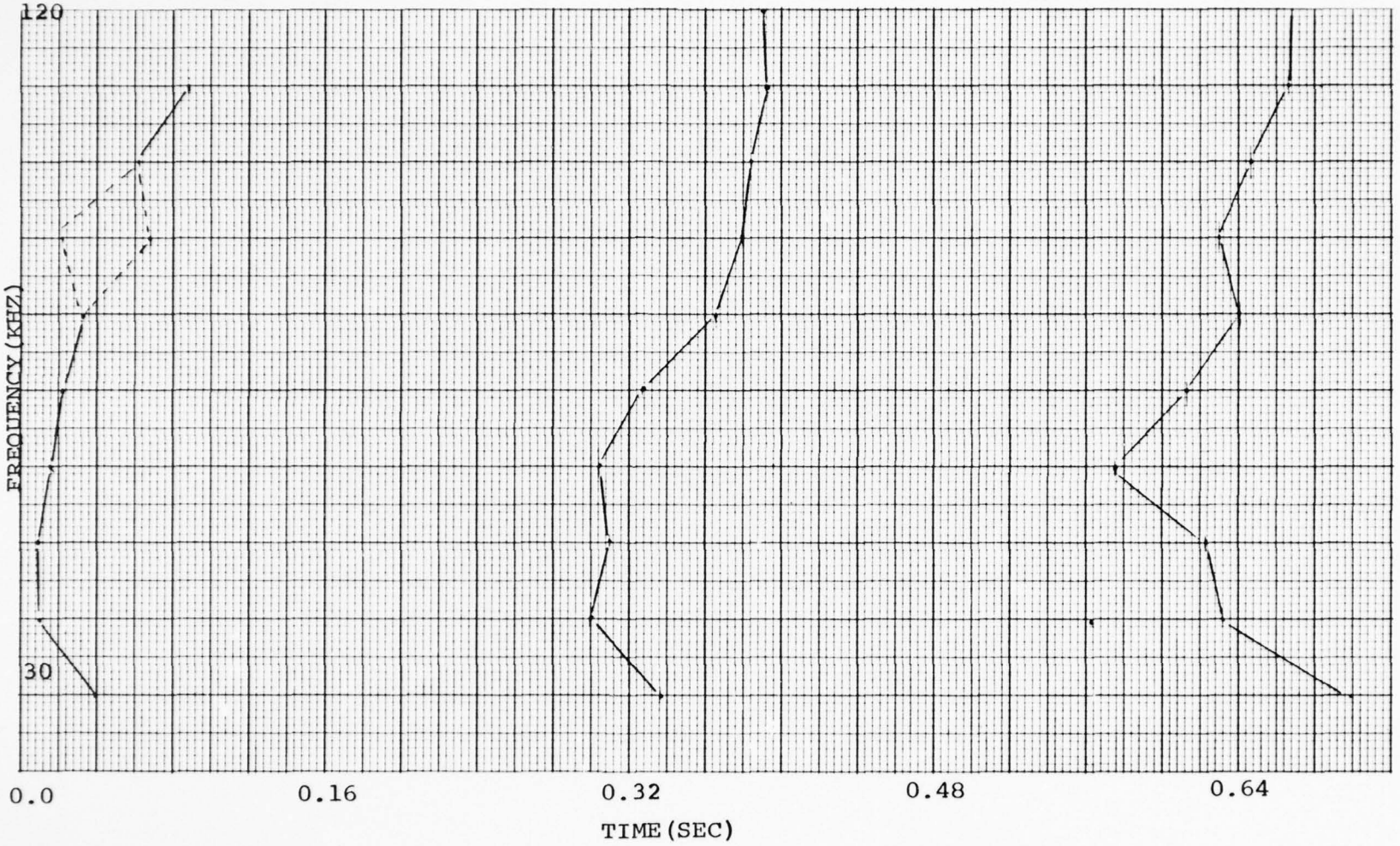

Figure 41. Minima Plot,1 Fan, 0.75 Seconds.

Figure 42. Minima Plot,1 Fan, 2 Seconds.

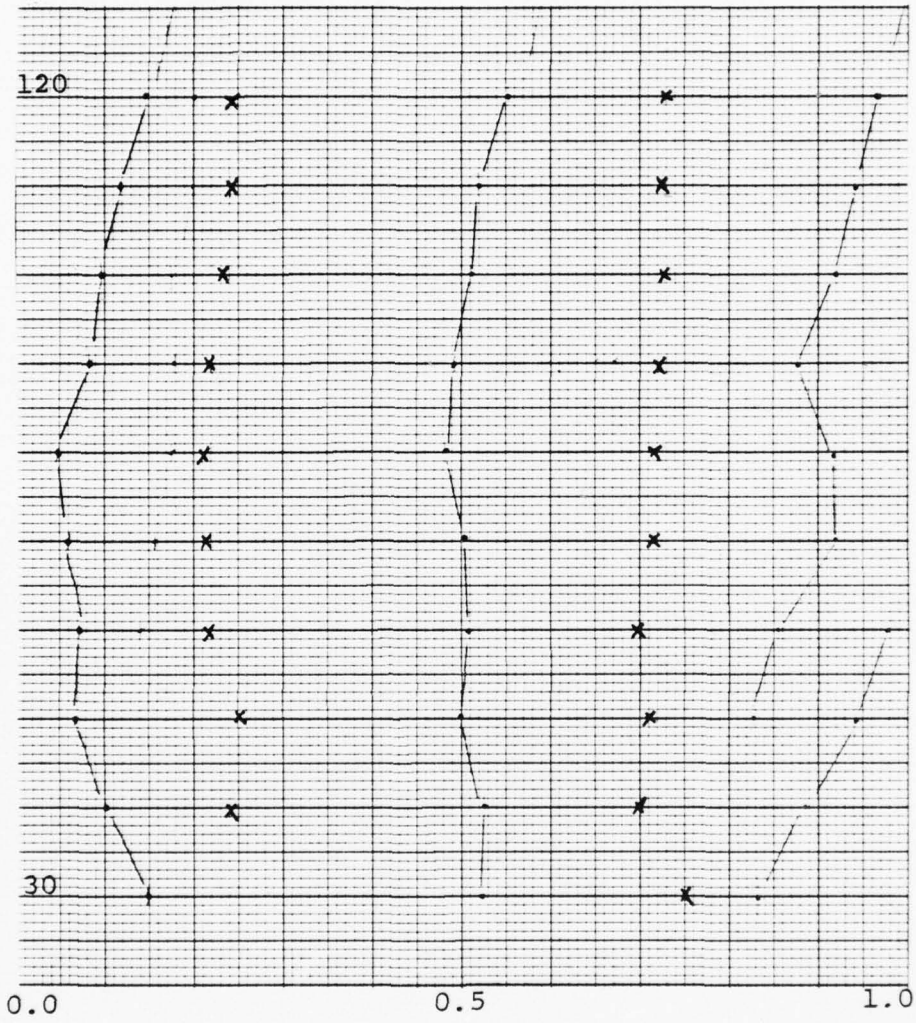

Figure 43. Minima Plot, 2 Fans, 1 Second. X's shown on the plot represent observed maxima on the graphical overlays.

Figure 44. Minima Plot, 2 Fans, 2 Seconds.

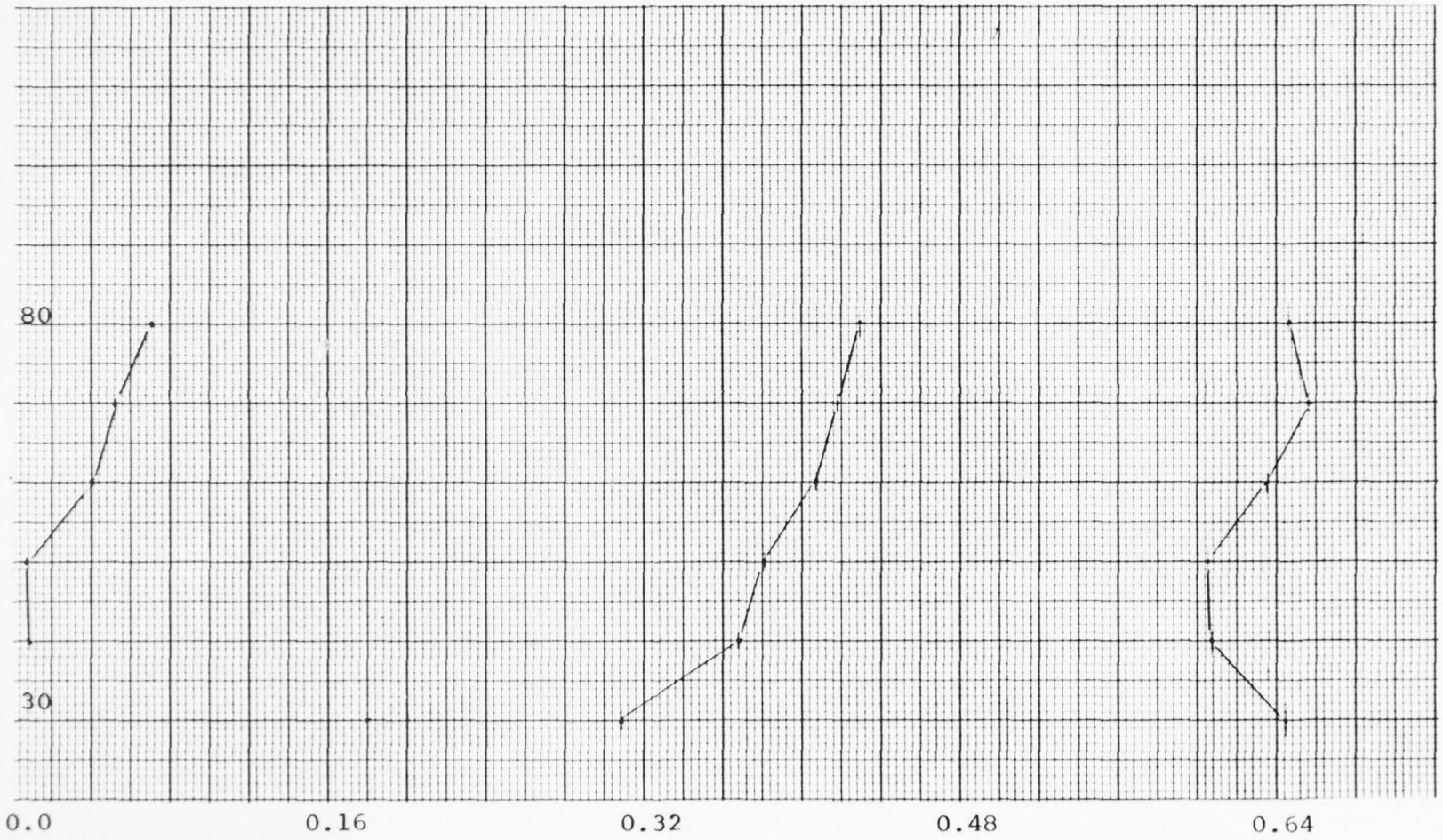

Figure 45. Minima Plot, 2 Fans,0.75 Seconds.

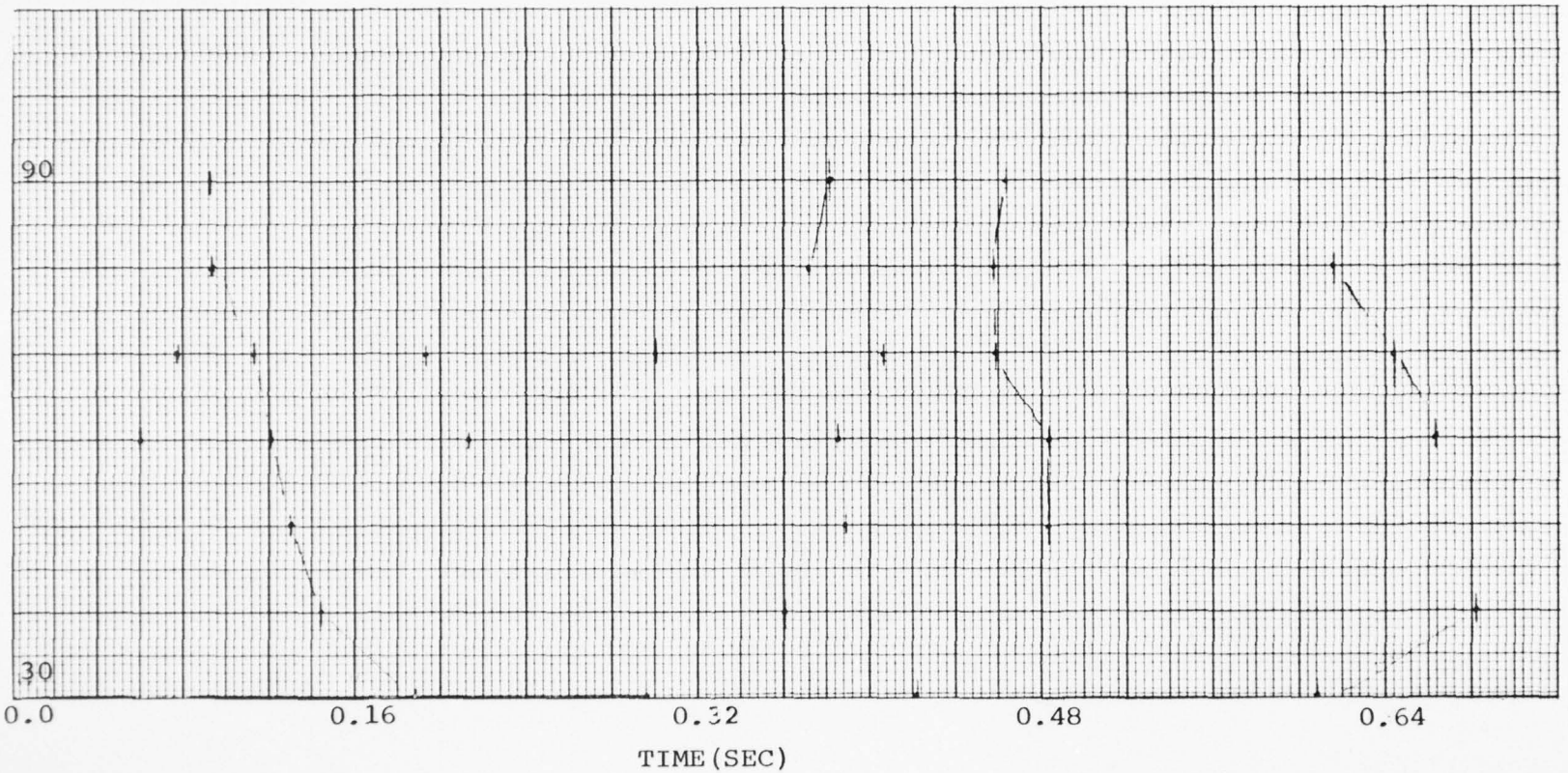

Figure 46. Minima Plot, 3 Fans.

Unconnected points represent randomly occurring minima where no logical progression from one frequency to the next could be discerned.

AD-A039 374 NAVAL POSTGRADUATE SCHOOL MONTEREY CALIF F/G 20/1
FREQUENCY-TIME CORRELATION OF SURFACE SCATTERED UNDERWATER SOUN--ETC(U)
DEC 76 M F LOOMIS

UNCLASSIFIED NL

2 OF 2
AD
A039 374

END
DATE FILMED
6-77

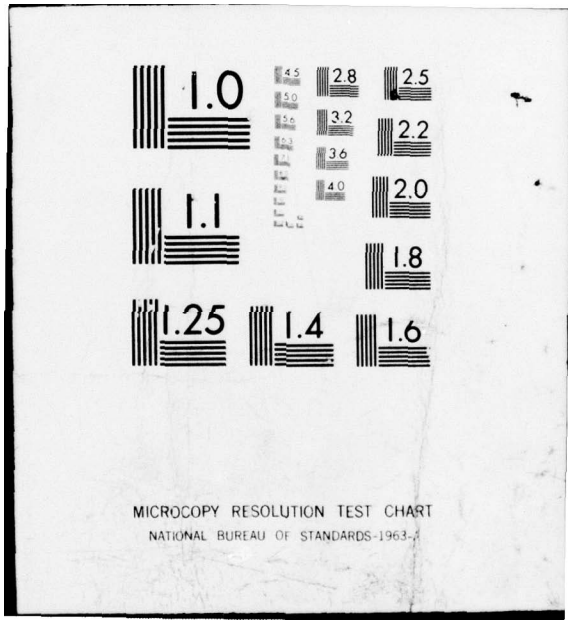
1.0
1.1
1.25
1.4
1.6
1.8
2.0
2.2
2.5
2.8
3.2
3.6
4.0
4.5
5.0
5.6
MICROCOPY RESOLUTION TEST CHART
NATIONAL BUREAU OF STANDARDS-1963-A

and 2 fan cases, and also by assuming that the maxima are, on the average, located midway between the plotted minima, it was possible to predict the change in frequency required to go from a minimum to a maximum at any given instant of time. For each of the two curves, this Δf was tabulated and averaged. For the 3 and 4 fan cases, the lack of predictability required a more numerical approach. The overlays of Figures 26 and 29 (3 fans) and the individual graphs for the 4 fan cases (not included) were examined and the average frequency change from max. to min. determined and tabulated over a number of representative cases. The results of both these methods are shown graphically in Figure 47. This curve shows the predicted change in frequency to go from a minimum to a maximum plotted against the average wave height for a given fan combination. The 1 and 2 fan frequency changes were calculated from 10 values and the 3 and 4 fan cases from 14 and 17 values respectively. Standard deviations about each of these points are also shown in Figure 47. The curve appears linear for the smoother surfaces progressing into non-linearity by the time the 4 fan surface heights are reached; however this lack of linearity of the last point may simply be due to a lack of resolution below 10 kHz increments.

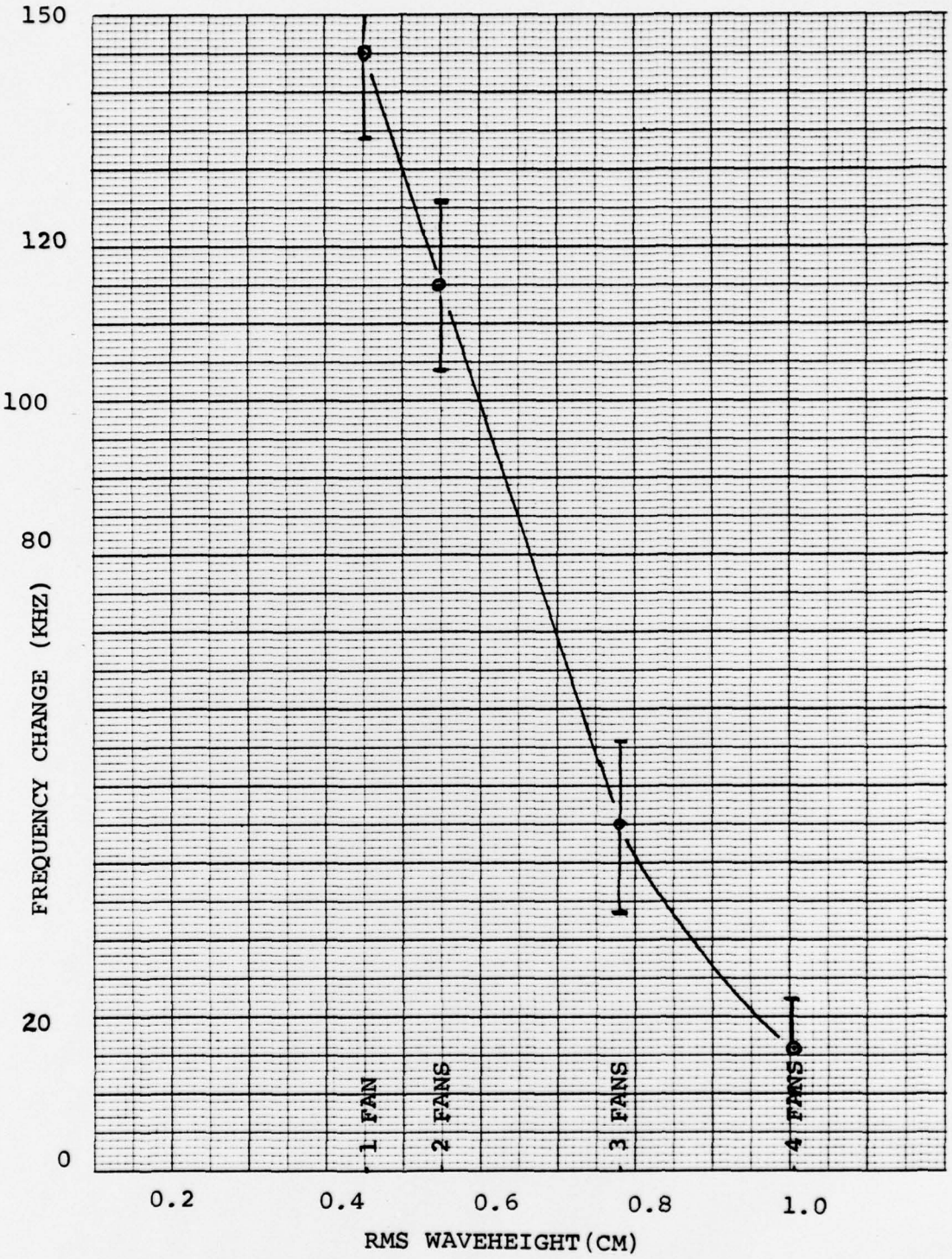

Figure 47. Frequency Change vs RMS Waveheight.

V. FUTURE RESEARCH

The author feels that the research described in the foregoing pages is a viable means for gaining new knowledge and insight into the basic process of scattering of sound off of a statistically rough surface. Further investigation should provide additional information; a number of approaches to improve the previous research are recommended below:

1. Investigation into the feasibility of using a 5 kHz base frequency, instead of the 10 kHz used herein, should be conducted. A few trials along these lines were attempted with indications that the method is feasible. The frequency resolution would then be twice that given in this paper and should be particularly valuable in giving a closer look at the 3 and 4 fan surfaces at lower roughness values. Roughness values less than 1.0 should specifically be looked at.

2. A method for separately looking at the coherent and incoherent components of the scattered sound should be developed. This appears to be capable of being accomplished using the phase information present in the FFT algorithm used in the digital computer. The SKIP-1C program has this output available. A possibility of merging the capabilities and outputs of the SKIP-1C and THCDB(1) programs should be attempted. By removing the incoherent component at the higher surface roughness values, more information can be attained from the chaos which currently presents itself.

3. Alternate means of presenting correlation data should be investigated; one possibility would be to calculate the correlation of excess pressure amplitudes relative to the mean value for a given frequency increment at a given instant in time and to display the resultant correlation values as a function of time. The advantage of this method is that it would lend further support to the hypothesis of consistent frequency separation (delta f) between relative maxima and minima discussed in section IV.B.5. It is anticipated that such curves would reveal a large negative correlation when the appropriate frequency of Figure 47 is reached. Correlation at twice this frequency increment should result in large positive correlation values once again. Analysis of existing data arrays in this manner is feasible due to the prepunched data cards available in the Ocean Physics Laboratory.

4. The effects of variation of geometry to include larger angles of incidence should be investigated.

APPENDIX A: PROGRAM DESCRIPTIONS

SKIP-1C:

Input:
1. Sample Frequency
2. Number of Sample Points per FFT
3. Number of FFT's
4. Band pass limits desired on printout

Options:
1. DC filtering
2. Triangular hanning function

Output:
1. Individual power spectral densities (PSD) for each FFT
2. Normalized average PSD vs. frequency over the stipulated bandpass
3. Average phase vs. frequency over the stipulated bandpass.
4. For each FFT, the maximum PSD and its associated frequency.

CAL-01:

Input:
1. Number of samples (maximum 8192)
2. Input reference voltage set at 1.000 volts (RMS)
3. Voltage signal from wavetank probe

Output:
1. VOUT = AC voltage of wavetank probe.

THCDB:

Input:
1. Number of sample points per FFT
2. Total number of FFT's desired (maximum of 50)
3. Conversion factor for transforming PSD to volts
4. Amplifier gain
5. Line loss
6. Hydrophone sensitivities for every 5 kHz from 0 - 160 kHz

Options:
1. SPL or VL output
   Noise run

Output:
1. Mean sound pressure level (or voltage level) vs. frequency (5 kHz increments from 0 - 160 kHz)
2. Standard deviation of SPL vs. frequency
3. Signal to noise ratio vs. frequency, if previous noise run has been performed
4. Output can be stored on a digital cassette or printed on the terminal printer

THCDB(1): Same as the previous program except the program will accept raw A/D input from a digital cassette and it can handle up to 100 FFT's as the associated output.

PERK-1A: Program to perform A/D sampling, delay a specified time and write the A/D data on a digital cassette (to be used as input for THCDB(1)).

Input:
1. Total number of A/D samples (maximum of 8200)
2. Number of samples per FFT
3. Sample frequency
4. Number of FFT's desired
5. Desired time delay between FFT's

Output:
1. Raw A/D data stored on digital cassette.

PRK-MOD: Same as previous program except total number of points has been increased to a maximum value of 13,000

SORTF: Program to take the output of THCDB(1) and sort the resulting FFT data by frequency. It can accept up to 100 blocks of FFT data with up to 75 frequency values in each block.

Output is SPL vs. time for each frequency.

```
FORTRAN IV G LEVEL 21                    MAIN                    DATE = 76293

0001                 DIMENSION SPL(33,100),PRESS(33,100),FREQ(33)
0002                 DIMENSION AVGP(33),CORR(33,33)
C
C  READ IN POINTS FOR INITIAL STARTING IN TIME AND ENDING IN TIME
C
0003                 READ(5,400)M1,M2
0004               400 FORMAT(2I2)
C
C  READ IN THE TOTAL NUMBER OF POINTS
C
0005                 READ(5,401)N
0006               401 FORMAT(I2)
0007                 WRITE(6,123)N,M1,M2
0008               123 FORMAT(//,'0','N= ',I2,2X,'M1 = ',I2,2X,'M2= ',I2,2X)
C
C  READ IN DATA FROM  PREVIOUSCARDS FROM SORTF/PLOTFRE PROGRAMS
C
0009                 DO 100 J=1,33
0010                 READ(5,500)FREQ(J)
0011               500 FORMAT(2X,F5.1)
0012                 READ(5,600)(SPL(J,K),K=1,N)
0013               600 FORMAT(5F11.3)
0014                 WRITE(6,700)FREQ(J)
0015                 WRITE(6,911)(SPL(J,K),K=1,N)
0016               911 FORMAT(2X,5F11.3)
0017               100 CONTINUE
C
C  CONVERT SPL TO PRESSURE AND FORM NEW ARRAY
C
0018                 DO 102 J=1,33
0019                 DO 103 K=1,N
0020                 PRESS(J,K) = (10.0)**(SPL(J,K)/20.0)
0021               103 CONTINUE
0022               102 CONTINUE
C
C  FORM THE TIME AVERAGED VALUE OF PRESSURE FOR EACH
C  FREQUENCY OVER THE DESIRED TIME RANGE
C
0023                 DO 104 J=1,33
0024                 SUM = 0.0
0025                 DO 105 K=M1,M2
0026                 SUM = SUM + PRESS(J,K)
0027               105 CONTINUE
0028                 AVGP(J) = SUM/FLOAT(M2-M1+1)
0029               104 CONTINUE
0030                 DO 107 J= 7,27,2
0031                 DO 108 K=7,27,2
0032                 SUM1 = 0.0
0033                 SUM2 = 0.0
0034                 DO 106 I=M1,M2
0035                 SUM1 = SUM1 + (PRESS(J,I) - AVGP(J))**2
0036                 SUM2 = SUM2 + (PRESS(K,I) - AVGP(K))**2
0037               106 CONTINUE
0038                 RMS1 = SQRT(SUM1)
0039                 RMS2 = SQRT(SUM2)
0040                 DENOM = RMS1*RMS2
0041                 UPPER = 0.0
0042                 DO 109 I=M1,M2
0043                 UPPER = UPPER+(PRESS(J,I)-AVGP(J))*(PRESS(K,I)-AVGP(K))
0044               109 CONTINUE
0045                 CORR(J,K) = UPPER/DENOM
0046               108 CONTINUE
0047               107 CONTINUE
0048                 DO 111 J = 7,27,2
0049                 WRITE(6,700)FREQ(J)
0050               700 FORMAT(////,'1',5X,'FREQUENCY = ',F12.2,'HZ')
0051                 WRITE(6,800)(CORR(J,K),K=7,27,2)
0052               800 FORMAT(6F10.6)
0053               111 CONTINUE
0054                 STOP
0055                 END
```

FORTRAN CORRELATION PROGRAM

BIBLIOGRAPHY

1. Eckart, Carl, "The Scattering of Sound from the Sea Surface," The Journal of the Acoustical Society of America, v. 25, p. 566-570, 1953.

2. Fortwin, L., "Survey of Literature on Reflection and Scattering of Sound Waves at the Sea Surface," The Journal of the Acoustical Society of America, v. 47, p. 1209-1228, 1970.

3. Medwin, H., "Specular Scattering of Underwater Sound from a Wind Driven Surface," The Journal of the Acoustical Society of America, v. 41, p. 1485-1495, 1967.

4. Horton, C. W. and Muir, T.G., "Theoretical Studies on the Scattering of Acoustic Waves from a Rough Surface," The Journal of the Acoustical Society of America, v. 41, p. 627-634, 1967.

5. Tolstoy, I., and Clay, C.S., Ocean Acoustics: Theory and Experiment in Underwater Sound, McGraw-Hill, 1966.

6. Perkins, J. B., Amplitude Modulation of Acoustic Signals by Ocean Waves and the Effect on Signal Detection, M.S. Thesis, U. S. Naval Postgraduate School, 1974.

7. Tourville, M. A., Signal Enhancement of Surface Scattered Underwater Sound, M.S. Thesis, U. S. Naval Postgraduate School, 1975.

8. Lastinger, J. L., "Acoustic Characteristics of Woods at High Hydrostatic Pressure," The Journal of the Acoustical Society of America, v. 47, p. 1209-1228, 1970.

INITIAL DISTRIBUTION LIST

		No. Copies
1.	Defense Documentation Center Cameron Station Alexandria, Virginia 22314	2
2.	Library, Code 0142 Naval Postgraduate School Monterey, California 93940	2
3.	Department Chairman, Code 61 Department of Physics and Chemistry Naval Postgraduate School Monterey, California 93940	1
4.	Professor H. Medwin, Code 61Md Department of Physics and Chemistry Naval Postgraduate School Monterey, California 93940	3
5.	LCDR Michael F. Loomis, USN 1294 Spruance Road Monterey, California 93940	1
6.	Manager, Anti-Submarine Warfare Systems Project Office Attn: CAPT D. Elliot Department of the Navy Washington, DC 20360	1
7.	Ocean Science and Technology Div. (Code 486) Office of Naval Research 800 N. Quincy Street Attn: Dr. Bazdek Arlington, Virginia 22219	1
8.	Adjunct Professor J. Novarinni (Code 61 Nq) Physics Department Naval Postgraduate School Monterey, California 93940	1